# VAPORIZATION THERMODYNAMICS OF
# SELECTED EUROPIUM(II) COMPOUNDS

Thesis for the Degree of Ph. D.
MICHIGAN STATE UNIVERSITY
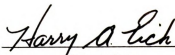ALLEPPEY V. HARIHARAN
1972

This is to certify that the

thesis entitled

VAPORIZATION THERMODYNAMICS OF
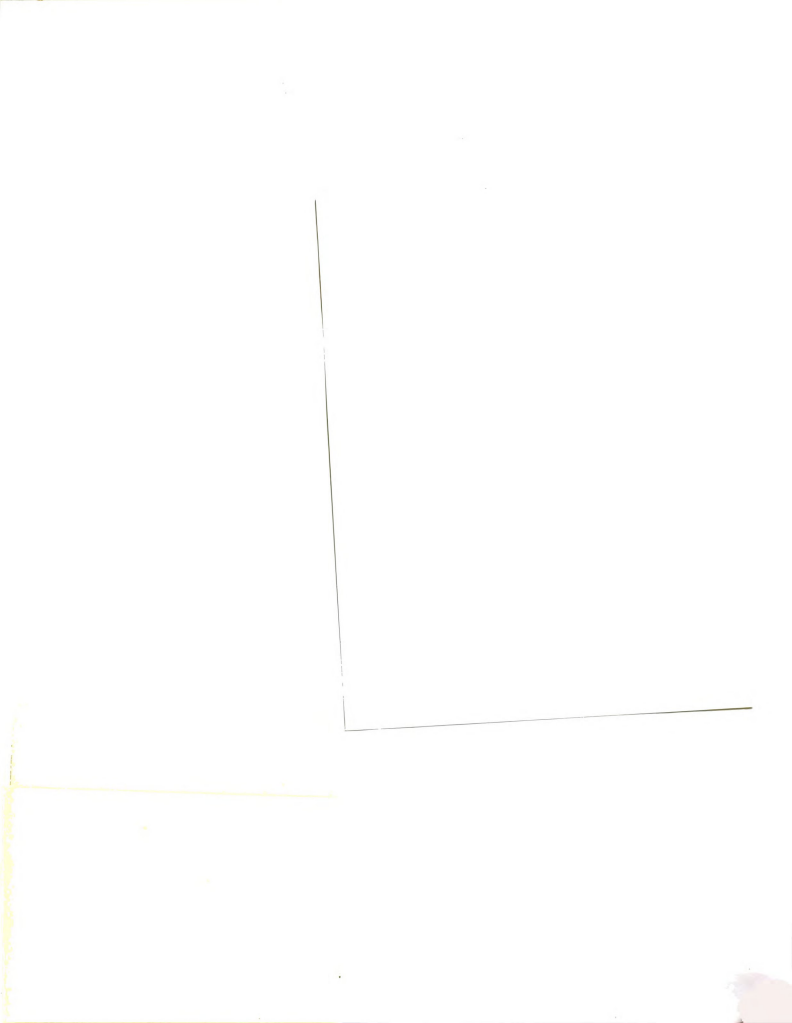SELECTED EUROPIUM(II) COMPOUNDS

presented by

Alleppey V. Hariharan

has been accepted towards fulfillment
of the requirements for

___Ph.D.___ degree in _Chemistry_

*Harry A Eick*
Major professor
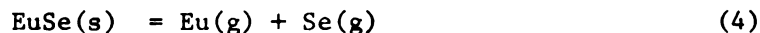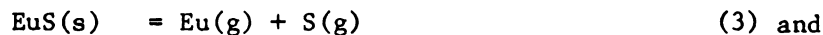
Date _November 8, 1972_

O-7639

ABSTRACT

VAPORIZATION THERMODYNAMICS OF SELECTED EUROPIUM(II) COMPOUNDS

By

Alleppey V. Hariharan

The high temperature vaporizations of selected europium(II) compounds, $EuCl_2$, $EuI_2$, EuS and EuSe, were investigated in detail. Total weight-loss, X-ray diffraction analyses and mass spectrometry were employed to characterize the vaporization mode of these compounds. The congruent vaporizations according to

$$EuCl_2(l) = EuCl_2(g) \qquad\qquad (1)$$

$$EuI_2(l) = EuI_2(g) \qquad\qquad (2)$$

$$EuS(s) = Eu(g) + S(g) \qquad\qquad (3) \text{ and}$$

$$EuSe(s) = Eu(g) + Se(g) \qquad\qquad (4)$$

were established. The appearance potentials, $EuI_2^+/EuI_2$, $EuI^+/EuI_2$, $Eu^+/EuI_2$, $Eu^+/EuS$ and $Eu^+/EuSe$, have also been determined.

A target collection Knudsen effusion technique was utilized to measure equilibrium vapor pressures in these systems. The microgram quantities of effusate on the targets were analyzed for europium by X-ray fluorescence. The temperature ranges of the vaporization studies were: $EuCl_2$ (1135-1569 K), $EuI_2$ (1086-1395 K), EuS (1801-2222 K) and EuSe(1808-2131 K).

The following second-law enthalpy and entropy changes were obtained at the median temperatures: $EuCl_2(l)$, 1352 K, $\Delta H° = 70.3_9 \pm 0.3_0$ kcal $gfw^{-1}$; $\Delta S° = 31.6_2 \pm 0.2_2$ eu; $EuI_2(l)$, 1241 K, $\Delta H° = 62.7_0 \pm 0.3_4$ kcal $gfw^{-1}$;

$\Delta S^\circ = 31.8_3 \pm 0.2_7$ eu; EuS(s), 2011 K, $\Delta H^\circ = 210._6 \pm 1._1$ kcal gfw$^{-1}$;

$\Delta S^\circ = 56.9_4 \pm 0.5_3$ eu; and EuSe(s), 1970 K, $\Delta H^\circ = 206._6 \pm 1._2$ kcal gfw$^{-1}$;

$\Delta S^\circ = 57.4_4 \pm 0.6_2$ eu. By use of available and estimated thermodynamic

functions, the experimental median temperature data were reduced to

298.15 K. The following second-law values were derived: $EuCl_2$(s),

$\Delta H^\circ_{298} = 84._9 \pm 1._1$ kcal gfw$^{-1}$; $\Delta S^\circ_{298} = 48._3 \pm 1._8$ eu; $S^\circ_{298}[EuCl_2$(s)] =

$32._9 \pm 2._4$ eu; boiling point $EuCl_2$(l), $2335 \pm 35$ K; $\Delta H^\circ_v = 58._9 \pm 1.8$

kcal gfw$^{-1}$; $\Delta S^\circ_v = 25.2 \pm 0.7$ eu; $EuI_2$(s), $\Delta H^\circ_{298} = 75._4 \pm 1._1$ kcal gfw$^{-1}$;

$\Delta S^\circ_{298} = 48._1 \pm 1._9$ eu; $S^\circ_{298}[EuI_2$(s)] = $40._4 \pm 2._6$ eu; boiling point

$EuI_2$(l), $2048 \pm 25$ K, $\Delta H^\circ_v = 53._5 \pm 1._6$ kcal gfw$^{-1}$; $\Delta S^\circ_v = 26.1 \pm 0.7$ eu;

EuS(s), $\Delta H^\circ_{298} = 215._4 \pm 1._2$ kcal gfw$^{-1}$; $\Delta S^\circ_{298} = 61.6 \pm 0.9$ eu;

$S^\circ_{298}[EuS$(s)] = $23.6 \pm 0.9$ eu; EuSe(s), $\Delta H^\circ_{298} = 211._3 \pm 1._3$ kcal gfw$^{-1}$;

$\Delta S^\circ_{298} = 62.5 \pm 0.7$ eu; $S^\circ_{298}[EuSe$(s)] = $24.8 \pm 0.7$ eu. The temperature-

independent third-law enthalpy changes for the vaporization reactions are:

$EuCl_2$(s), $\Delta H^\circ_{298} = 82._7 \pm 2._7$ kcal gfw$^{-1}$; $EuI_2$(s), $\Delta H^\circ_{298} = 73._9 \pm$

$3._1$ kcal gfw$^{-1}$; EuS(s), $\Delta H^\circ_{298} = 216._1 \pm 2._9$ kcal gfw$^{-1}$; and EuSe(s),

$\Delta H^\circ_{298} = 210._3 \pm 2._2$ kcal gfw$^{-1}$.

Additionally, the vaporization thermodynamic data were utilized to

obtain: $D^\circ_0[EuCl_2$(g)] = $209._8 \pm 1._5$ kcal gfw$^{-1}$; $D^\circ_0[EuI_2$(g)] = $156._0 \pm$

$5._0$ kcal gfw$^{-1}$; $D^\circ_0[EuS$(g)] = $79._8 \pm 4._2$ kcal gfw$^{-1}$; $D^\circ_0[EuSe$(g)] =

$61._6 \pm 5._5$ kcal gfw$^{-1}$; $\Delta H^\circ_{f,298}[EuI_2$(s)] = $-(138._9 \pm 5._0)$ kcal gfw$^{-1}$;

$\Delta H^\circ_{f,298}[EuS$(s)] = $-(106._7 \pm 1._3)$ kcal gfw$^{-1}$; and $\Delta H^\circ_{f,298}[EuSe$(s)] =

$-(112._8 \pm 1._3)$ kcal gfw$^{-1}$.

The available thermodynamic data for $EuBr_2$ and EuO were reevaluated

on the basis of the present work. The comprehensive thermochemical

values for the europium(II) halides, $EuF_2$, $EuCl_2$, $EuBr_2$ and $EuI_2$,

and monochalcogenides, EuO, EuS, EuSe and EuTe, are compared and their

similarity to the corresponding strontium(II) compounds has been brought out.

VAPORIZATION THERMODYNAMICS OF SELECTED EUROPIUM(II) COMPOUNDS

By

Alleppey V. Hariharan

A THESIS

Submitted to

Michigan State University

in partial fulfillment of the requirements

for the degree of

DOCTOR OF PHILOSOPHY

Department of Chemistry

1972

G7903360

## ACKNOWLEDGEMENTS

I wish to extend my sincere gratitude and thanks to Dr. Harry A. Eick for his guidance, understanding and encouragement throughout the course of my studies and research.  The many fruitful discussions I had with the past and present members of the high temperature research group have been of invaluable help in completing this work.  My special thanks are also due to my wife, Rajam, and my son, Suresh, for their patience and understanding.

TABLE OF CONTENTS

TABLE OF CONTENTS (Cont.)

# LIST OF TABLES

LIST OF FIGURES

## LIST OF APPENDICES

# CHAPTER 1

## INTRODUCTION

Comprehensive thermodynamic data are essential prerequisites for a meaningful analysis of the energetics and chemical bonding in simple binary compounds of a series of elements. A series particularly well suited for study is the lanthanides where, in spite of a wealth of information on the preparation and crystal structures of their compounds, accurate experimental thermodynamic data are singularly lacking. The chemical similarity among the lanthanides has led to the practice of extrapolating the few thermochemical measurements to the entire series, an extrapolation which in general follows a trend consistent with the lanthanide contraction. However, europium with its half filled 4 f electronic shell has properties significantly different from those of the other lanthanides in both the element and its compounds. For europium the divalency is more predominant, and the crystal chemistry of europium(II) compounds are strikingly similar to those of the alkaline earth, strontium.

In the research for this dissertation thermodynamic data for europium(II) halides and chalcogenides have been obtained from high temperature vaporization studies. Coupled with mass spectrometric methods, an investigation of the high temperature vaporization process is uniquely suited to establish the thermodynamic properties of the

condensed and gaseous phases. The results of these studies have been correlated and extended to provide an extensive body of information for the europium(II) compounds. These data, it is hoped, will provide a basis for the thermodynamic properties of the other definitely established divalent compounds of the lanthanides, samarium and ytterbium, and will serve to elucidate the nature of the chemical bonding in these compounds.

CHAPTER 2

SURVEY OF THE PREPARATIVE, STRUCTURAL AND THERMOCHEMICAL

ASPECTS OF THE LANTHANIDE HALIDES AND CHALCOGENIDES


This chapter is an extensive but concise survey of the pertinent

preparative, structural and thermochemical aspects of the lanthanide

halides and chalcogenides. Particular emphasis is naturally on the

divalent compounds of europium, but collateral details for the other

definitely established divalent compounds of samarium and ytterbium

are also included to provide the background and impetus for further

study. For the sake of clarity the halides and chalcogenides are

described separately, a practice followed in all subsequent sections.

2.1. Preparation of Europium(II) Compounds

   2.1.1. Europium(II) Halides

Europium forms the stoichiometric binary halides $EuF_2$, $EuCl_2$, $EuBr_2$

and $EuI_2$. Urbain and Bourion (1) reported the first preparation of a

divalent europium salt, $EuCl_2$, in 1911. However, the earliest systematic

study of these compounds was by Klemm and Döll (2), who in 1939

investigated their preparation, crystal structures and magnetic

susceptibilities. The original preparative method involved hydrogen

reduction of the anhydrous trihalides at high temperatures. Preparative

methods for the trihalides are described in some detail since they are

3
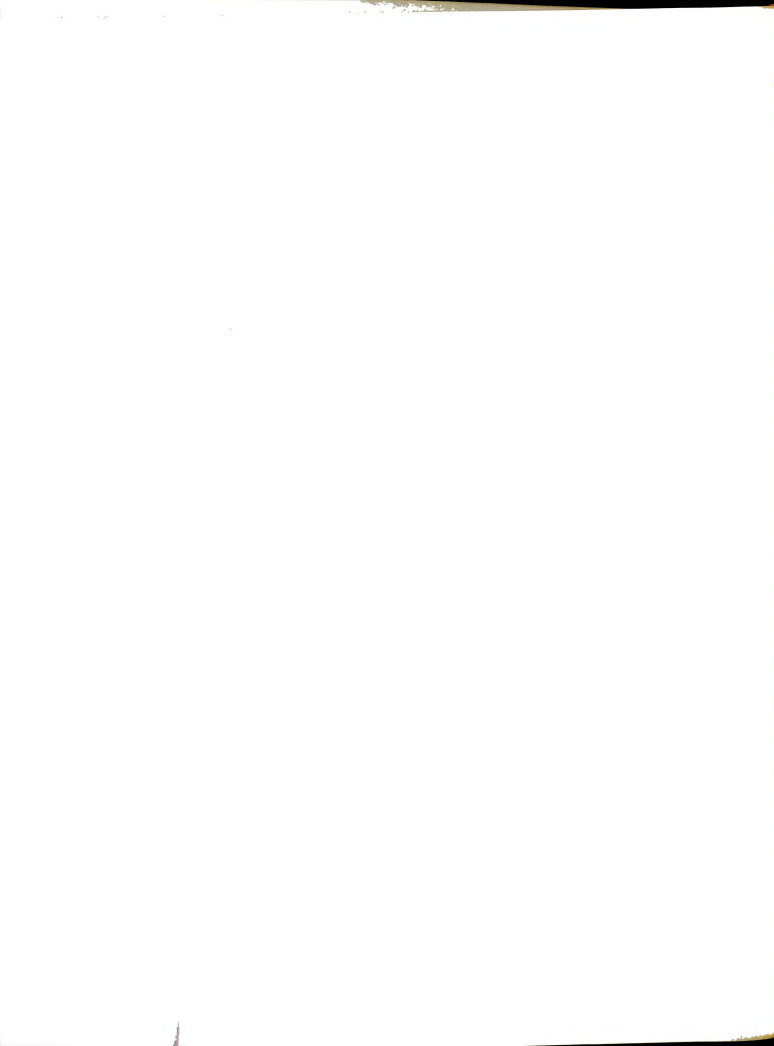
generally the source material for the preparation of the dihalides. Brown (3) has recently reviewed the halides, oxidehalides and halocomplexes of the lanthanides and actinides with particular emphasis on their crystal structures. More recent methods of preparation and practical aspects of the procedures are covered in the following sections.

### 2.1.1.1. General Methods of Preparation of Lanthanide Trihalides.

Methods of preparing anhydrous lanthanide halides have been the subject of numerous investigations if only because they are difficult to isolate in the state of high purity required for property measurements. Some of them are extremely hygroscopic and sensitive to oxygen, even at room temperature, and react according to the following equations:

$$LnX_3(s) + H_2O(g) = LnOX(s) + 2HX(g) \qquad (2-1)$$

$$2LnI_3(s) + O_2(g) = 2LnOI(s) + 2I_2(g). \qquad (2-2)$$
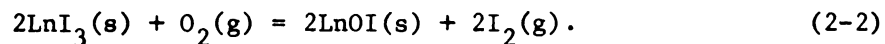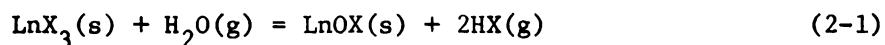
Preparative methods have been reviewed by Taylor (4), Taylor and Carter (5), and by Johnson and Mackenzie (6). In general these methods involve:

a) Direct reaction of the metal with halogen or anhydrous HX.

b) Dehydration of the hydrated trihalide formed from the oxide and aqueous hydrohalic acid with anhydrous HX or $NH_4X$. For the trichloride dehydration with $Cl_2$-$S_2Cl_2$ is also described.

c) High temperature fluorination, chlorination or bromination of the oxide or oxalate with HF, $ClF_3$, or C/CO with $Cl_2$ or $Br_2$.

d) Reaction of the oxide with $NH_4X$ at high temperatures.

e) Reaction of the oxide or oxalate with volatile chlorinating agents such as $S_2Cl_2$, $SOCl_2$, $COCl_2$ and $CCl_4$ (for chlorides only).

f) Reaction of the oxide with $AlI_3$ or an $Al-I_2$ mixture in vacuum at elevated temperatures (for iodides only).

Few of the above methods are of general applicability. However, Taylor and Carter (5) by a systematic adaptation of (b) have described a general procedure that has become widely used in the synthesis of nearly all of the lanthanide trihalides. Pure anhydrous products in fairly high yields are obtainable by this procedure.

According to Drudig and Corbett (7) only the direct synthesis, method (a), would give high purity products, but here again it is imperative to start with high purity reagents. Alternatively, sublimation or distillation of the crude product obtainable by any of the other methods (b-f) will usually compensate for the initial lack of purity and yield high purity halides.

### 2.1.1.2. Methods of Preparation of Europium(II) Halides

The europium(II) halides are almost always prepared by the reduction of the corresponding trihalide at elevated temperatures. Hydrogen or ammonia gas has been the reductant in most of the reported procedures. However, reduction with elemental europium or zinc is also possible. Polyachenok and Novikov (8) report complete reduction of $EuCl_3$ and $YbCl_3$ to the respective dichlorides by heating with zinc in an argon atmosphere at $\sim 900°C$. Complete reduction of $SmCl_3$ was not obtained. More recently DeKock and Radtke (9) described for the dichlorides of Sm, Eu and Yb a direct synthesis that involves thermally decomposing a molecularly dispersed mixture of the trichloride hydrate, $NH_4Cl$, $ZnCl_2$ and Zn at temperatures up to 550°C. This method appears adaptable to the preparation of the other divalent halides of these elements. A final vacuum distillation of the product would remove all volatile impurities.

All the dihalides of Eu and Yb, with the exception of the difluorides, have been prepared by reaction of the metals with the appropriate $NH_4X$ in liquid ammonia (10).

### 2.1.1.3. Comments on the Preparation of Europium(II) Halides.

$EuF_2$:

An apparent nonstoichiometry in $EuF_2$ was observed by Asprey, Ellinger and Staritzky (11) and Lee, Muir and Catalano (12). The so-called nominal $EuF_2$ produced by hydrogen reduction of $EuF_3$ at $\sim 1300°C$ had a composition, lattice parameter and color that seemed variable. The Eu-rich substoichiometric composition for the difluoride was placed at $EuF_{1.93}$ and $EuF_{1.82}$, respectively. However, in a detailed study of the $EuF_2$-$EuF_3$ system, Catalano et al. (13) showed that the lowest composition was exactly $EuF_{2.00}$, a phase which is face centered cubic with a = 5.840 $\overset{o}{A}$. Dehydration of the hydrated trifluoride under HF gas at $\sim 800°C$ produced $EuF_{3.00}$ which under $H_2$ at $\sim 1500°C$ in a molybdenum cell reduced to $EuF_{2.00}$. Direct reduction of $EuF_3$ with excess Eu metal in a sealed molybdenum crucible produced an inhomogeneous mixture of Eu + $EuF_{2.00}$, and thus the possibility of substoichiometry was ruled out. However non-stoichiometric compositions $EuF_{2.00}$ - $EuF_{2.25}$ and $EuF_{2.25}$ - $EuF_{2.45}$ are reported as well as an apparent two-phase region between $EuF_{2.45}$ and $EuF_{3.00}$.

$EuCl_2$:

Particular care must be exercised in the preparation of $EuCl_3$ since this compound close to its melting point (623°C) would contain $\sim 8$ mole% $EuCl_2$ (14). Nor will vacuum sublimation purify $EuCl_3$ because

of its thermal decomposition to $EuCl_2$. This characteristic of $EuCl_3$, however, will not be important in the preparation of $EuCl_2$.

## $EuBr_2$:

Haschke and Eick (15) observed that dehydration of the tribromide hydrate-$NH_4Br$ matrix always yields $EuBr_2$. Since $EuBr_3$ could not be obtained from $EuBr_2$ and 1 atm. bromine at 60°C, the preparation of $EuBr_3$ in vacuum at 350°C (5) is most unlikely. This observation has been independently corroborated by Rossmanith (16).

## $EuI_2$:

The species $EuI_2$ and $SmI_2$ are always the product of the matrix dehydration method, but preparation of $YbI_3$ by this procedure is reported (5). The method developed by Asprey and Kruse (17) for the preparation of the lanthanide and actinide iodides – reaction of the metal with mercuric iodide – was unsatisfactory for Sm, Eu and Yb. It was necessary to react the metal with elemental iodine and even here drastic reaction conditions were necessary to form $SmI_3$ (500°C: 5 atm $I_2$: 2 hr) and $YbI_3$ (500°C: 30 atm $I_2$: 16 hr). However, as expected, europium gave only the diiodide even at 600°C and 100 atm iodine pressure.

### 2.1.2. Europium(II) Chalcogenides

Compounds of europium with all the non-metals of Group VI A are considered together. Westrum (18-20) has reviewed in detail the preparation, properties and magnetism of the lanthanide oxides and binary chalcogenides through 1968. Samsonov (21) has treated the preparative and structural aspects of the sulfides of the lanthanides, while Flahaut and Laruelle (22) have discussed extensively the same aspects with regard

to the sulfides, selenides and tellurides. Non-stoichiometry in the lanthanide monosulfides is considered by Bruzzone and Olcese (LaS, CeS, PrS, NdS and GdS). Flahaut et al. (GdS through TmS) and Iandelli and Palenzona (SmS and YbS) (23). The latter authors also discuss the non-stoichiometry of SmSe, SmTe, YbS, YbSe and TmTe.

Europium forms the binary compounds EuO, EuS, EuSe, EuTe and EuPo of line-phase composition. Eick et al. (24) prepared EuO by reducing $Eu_2O_3$ with lanthanum metal at $\sim$ 1200°C. Baernighausen (25) reduced $Eu_2O_3$ and EuOX (X = halogen) with lithium hydride at $\sim$ 700°C in high vacuum. Methods generally applicable to the other chalcogenides are:

a) Direct combination of the elements in evacuated sealed tubes at 800-1000°C.

b) Reaction of the metal or the hydrided-dehydrided metal with $H_2S$, $H_2Se$ or $H_2$-Te at elevated temperatures.

c) Reaction of $EuCl_3$ or $EuCl_2$ with $H_2S$, $H_2Se$ or $H_2$-Te at $\sim$ 700°C.

d) Reaction of $Eu_2O_3$ with $H_2S$ or $H_2Se$ at 1000-1400°C.

e) Reduction of $Eu_2(SO_4)_3$ or $Eu_2(SeO_4)_3$ with aluminum (1300-1500°C) or $H_2/CO$ (800-1000°C).

Kaldis (26) reports the synthesis and vapor transport of europium chalcogenide crystals. The direct combination of Eu and S is almost complete between 90-180°C (note: initial reaction at temperatures over 90°C is explosive) and the product was annealed at 880°C in vacuum. For the preparation of EuSe and EuTe, iodine was used as the chemical transporting agent. Synthetic conditions were: EuSe, initial reaction at 185-210°C, annealing at 750°C; EuTe, initial reaction at 600-730°C, annealing at 880°C. Crystal growth was conducted in sealed evacuated molybdenum tubes.

In the only investigation of the preparation of lanthanide polonides, Kershner et al. (27) report the synthesis of several LnPo compounds by direct reaction of the metal with polonium. Europium reacted at $\sim$ 800°C for 45 min to form EuPo.

Shafer (28) prepared high purity EuS and EuSe by reaction of the elements in liquid ammonia. The product was separated by filtration and heated in vacuum at $\sim$ 600°C. There is no reason why this same method cannot be applied to the synthesis of EuTe and even EuO. In fact Fishel et al. (29) have prepared YbO using liquid ammonia as the reaction medium.

In addition to the monochalcogenides, europium forms the familiar $Eu_2O_3$ and $Eu_3O_4$ as well as $Eu_3S_4$. Attempts to prepare $Eu_2S_3$ have been unsuccessful. The compounds $Eu_3O_4$ and $Eu_3S_4$ contain both divalent and trivalent europium. A polysulfide, $EuS_{2-x}$ (tetragonal anti-$Cu_2Sb$ structure) is also known. Recently Sadovskaya et al. (30) from a thermal and X-ray analysis in the system Eu-Se reported both $Eu_2Se_3$ and $Eu_4Se_7$ in addition to EuSe.

Samarium and ytterbium form the higher chalcogenides $M_2X_3$, $M_3X_4$ and $MX_{2-x}$. All these compounds decompose to the nonstoichiometric monochalcogenides at high temperatures in vacuum.

## 2.2. Crystal Structures of Europium(II) Compounds

The crystal chemistry of divalent europium halides and chalcogenides and their crystallographic relationships with the corresponding alkaline earth compounds were first reported in 1939 by Döll and Klemm (2) and Klemm and Senff (31). The crystal radius of $Eu^{2+}$ (1.12 Å; Ref. 69) is so similar to that of $Sr^{2+}$ (1.13 Å; Ref. 69) that structural similarity between their compounds is very nearly the rule.

### 2.2.1. Europium(II) Halides

Powder diffraction results for $EuF_2$ (13) and single crystal data for $EuCl_2$, $EuBr_2$ and $EuI_2$ have been surveyed by Baernighausen et al. (32). In addition to the nominally observed structures, a high pressure form of $EuF_2$ and an $SrI_2$-type, $\gamma$-$EuI_2$, are known. Pertinent data on these structures are summarized in Table 1. The $\gamma$-$EuI_2$-type can be related to the monoclinic form of $EuI_2$ by assuming an intracellular twinning of the latter.

### 2.2.2. Europium(II) Chalcogenides

Europium(II) monoxide and monochalcogenides all have the cubic rocksalt structure. The lattice parameter increases systematically from the oxide to the polonide (Table 2).

## 2.3. Thermochemical Measurements on Europium(II) Compounds

Direct calorimetric data on the enthalpies of formation and heat capacities of lanthanide compounds are singularly lacking. Available data on $Ln_2O_3$ and $LnCl_3$ compounds have been reviewed extensively (35,36). Enthalpies of formation of most of the other lanthanide compounds are derived from high temperature equilibrium measurements and because of the large number of data reduction steps have large errors associated with them. When the divalent compounds of Sm, Eu and Yb are excluded, these values correlate well with the trends generally observed in the lanthanide series.

### 2.3.1. Halides

Brewer et al. (37,38) estimated comprehensive thermodynamic data such as the enthalpies of fusion, vaporization and formation, heat

Table 1.  <u>Crystal Structures of Europium(II) Halides.</u>[a]

| $EuX_2$ | Structure Type | Space Group and No. | a | b | c |
|---|---|---|---|---|---|
| $EuF_2$ | Cubic $CaF_2$ | Fm3m, 225 | 5.840 | | |
| | | | 5.839(3) | | |
| $EuF_2$[*] | Orthorhombic $PbCl_2$ | Pbnm, 62 | 7.435(4) | 6.324(4) | 3.803(2) |
| $EuCl_2$ | Orthorhombic $PbCl_2$ | Pbnm, 62 | 8.93 | 7.51 | 4.50 |
| | | | 8.958(6) | 7.534(5) | 4.504(3) |
| $EuBr_2$ | Tetragonal $SrBr_2$ | P4/n, 85 | 11.574(6) | | 7.098(5) |
| | | | 11.567(7) | | 7.094(5) |
| $EuI_2$ (m) | Monoclinic | $P2_1/c$, 14 | 7.64(2) | 8.26(2) | 7.88(2) |
| | | | | ($\beta = 98.0 \pm 0.5°$) | |
| $EuI_2$[#] ($\gamma$) | Orthorhombic $SrI_2$ | Pbca, 61 | 15.12(3) | 8.18(2) | 7.83(2) |

[a] Reference 32

[*] Reference 33

[#] Reference 34

Table 2.   Lattice Parameters of Europium(II) Chalcogenides.

Structure Type:  FCC  NaCl Type

Space Group:  Fm3m,  No. 225

| EuX | Lattice Parameter, ($\pm$ 0.001)$\overset{\circ}{\text{A}}$ | Ref. |
|------|-----------------------------|---------|
| EuO  | 5.144, 5.143, 5.142         | 24, 25  |
| EuS  | 5.969, 5.968, 5.970         | 22      |
| EuSe | 6.185, 6.190, 6.197         | 22      |
| EuTe | 6.585, 6.603, 6.594         | 22      |
| EuPo | 6.720(5)                    | 27      |

capacities and other thermal functions for the lanthanide trihalides and the dihalides of Sm, Eu and Yb. Since then these extensive tables have formed a veritable source book for the thermochemical properties of these compounds. Although the estimates appear internally consistent, there have been few experimental verifications, and in these cases agreement has only been marginal. Feber (39) in 1965 reevaluated the then available experimental values based on more consistent heat capacity estimates and calculated the dissociation energies of the $LnX_3$ and $LnX_2$ gaseous molecules. Thermochemical data for the divalent halides and the stabilities of the dichlorides have also been assessed by Novikov and Polyachenok (40) and by Johnson (36).

### 2.3.1.1. Calorimetric Studies

Charlu et al. (41) determined the high temperature enthalpy increments for $CeF_3$, $PrF_3$, $NdF_3$, $GdF_3$ and $YbF_3$. Heat capacities and enthalpy changes in fusion and transition for selected lanthanide(III) chlorides, bromides and iodides were determined by Dworkin and Bredig (42-44). However, no data are available for the corresponding compounds of divalent Sm, Eu and Yb. The enthalpies of formation of $EuCl_2$ (45) and $YbCl_2$ (46) have also been measured.

### 2.3.1.2. High Temperature Sublimation and Vaporization Studies

Since 1966 there have been extensive studies on the sublimation of lanthanide trifluorides by torsion-effusion and mass spectrometric methods. Vapor pressure values and sublimation thermodynamics for $LaF_3$, $CeF_3$ and $PrF_3$ (47-49) and $ScF_3$, $YF_3$, $LaF_3$, $NdF_3$, $DyF_3$, $HoF_3$, $ErF_3$, $TmF_3$, $YbF_3$ and $LuF_3$ (50-53) have been reported. Mass spectrometric data on the bond dissociation energies and stabilities of the mono- and difluorides,

including those of Sm and Eu, have been presented (54,55). An interesting result of such studies is the observation of gaseous $La_2F_6$ and the determination of its stability (56).

During the course of this thesis work, Petzel and Greis measured the sublimation pressure of $EuF_2$ by a mass effusion method (57).

Vapor pressures of selected lanthanide trichlorides and tribromides have been measured by Harrison (58), Shimazaki and Niwa (59), Moriarty (60), Polyachenok and Novikov (61) and Weigel and Trinkl (62) with only very limited accuracy and consistency. No sublimation or vaporization studies of lanthanide triiodides are reported, but recently Hirayama and Camp (63) have examined $NdI_3$ and $SmI_3$. Polyachenok and Novikov (8) reported for $SmCl_2$, $EuCl_2$ and $YbCl_2$ limited data on vapor pressure measurements effected by the "boiling point" method, but admit a lack of sufficient accuracy in the derived thermodynamic data. However, their measurement of the dissociation pressure of $EuCl_3$ (14) appears satisfactory and provides a reasonably accurate value for the enthalpy of formation of $EuCl_2$ if the currently available data for $EuCl_3$ (36) are utilized. Haschke and Eick studied the vaporization thermodynamics of $EuBr_2$ (64), and their data will be considered in detail in Chapter 6. Hastie et al. (65) studied the vapor composition over $LaCl_3$, $EuCl_3$, $LuCl_3$, and mixtures of these phases and observed the dimeric species $La_2Cl_6$, $Lu_2Cl_6$ and $EuLuCl_6$ in the gas phase. During their investigation, mass spectrometric data on the vaporization of $EuCl_2$ were also obtained.

### 2.3.2. Chalcogenides

The preparation, properties and crystal chemistry of the lanthanide monoxides and monochalcogenides have been the subject of numerous reviews

(sec. 2.1.2.). However, comprehensive treatment of their thermodynamic properties has not been possible due to a dearth of experimental data.

### 2.3.2.1. Calorimetric Studies

Montgomery (66) measured the enthalpies of formation of LaS and CeS by solution calorimetry. Burnett and Cunningham (67) and Huber and Holley (68) determined the enthalpy of formation of what was nominally assessed as $EuO_{1.02}$. Haschke and Eick (69) confirmed their value through a vaporization study. Heat capacity measurements for the europium chalcogenides are limited to very small ranges in the low temperature region (18-20) except for EuO where measurements extend from 15-280 K.

### 2.3.2.2. High Temperature Vaporization Studies

White et al. (70) and Ames et al. (71) carried out extensive studies on the vaporization of $Ln_2O_3$ at high temperatures and derived the enthalpies of formation and dissociation energies of the monoxides. The latter values were in turn confirmed by isomolecular oxygen exchange reactions in the gas phase and typically for EuO consisted of reaction (2-3):

$$Eu(g) + SmO(g) = EuO(g) + Sm(g) \qquad (2-3)$$
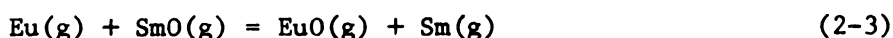
The comparatively low thermal stability of the gaseous monoxide molecules EuO and YbO (and to some extent SmO) was confirmed by Panish (72).

The sublimation thermodynamics and dissociation energies of LaS (73,74), CeS (75), PrS (76), GdS (77), ScS and YS (78) have been determined from effusion and mass spectrometric methods. Subsequently the dissociation energies of selected lanthanide monochalcogenides were measured from mass spectrometric isomolecular exchange reactions (79-81). Recently Gordienko et al. (82) examined the high temperature vaporization of LaS,

NdS, GdS, NdSe, SmSe and EuSe mass spectrometrically. Pertinent to this dissertation are the observations that the intensity ratio $I_{Eu^+}/I_{EuX^+}$ at $\sim$ 2000 K are > 1000 for both EuS (77) and EuSe (82), both of which were reported after the present work was completed and are in good agreement with it.

A cursory mass spectrometric study of the thermal stability of LaPo, NdPo, GdPo and DyPo has been reported by Steiger and Miles (83).

## 2.4. Molecular Geometry and Infra-red Spectra of Lanthanide Compounds

Considerable effort has recently been devoted to the study of the molecular geometry and spectra of gaseous lanthanide compounds to provide, hopefully, a basis for understanding their structure and bonding. The techniques that are in current use involve:

  a)  Electron diffraction of molecular beams.

  b)  Infra-red spectra of the gaseous molecules isolated at low temperatures in inert gas matrices.

  c)  Electric quadrupole deflection of molecular beams in inhomogeneous electric fields.

Although the complementary results of such studies have not always provided positive answers to the molecular properties of the lanthanide compounds and in some cases conflicting results arise, the information has, overall, been of invaluable use in thermodynamic studies of these compounds.

### 2.4.1. Halides

Results of the three types of measurements on the molecular geometry of $LnF_3$ gaseous species are presented in Table 3. As mentioned in section 2.4, the data are not unequivocal between planar and pyramidal

Table 3.  Molecular Geometry of Gaseous Lanthanide Trifluorides.

| MF$_3$/M: | Sc | Y | La | Ce | Pr | Nd | Pm | Sm | Eu | Gd | Tb | Dy | Ho | Er | Tm | Yb | Lu | Ref. |
|---|---|---|---|---|---|---|---|---|---|---|---|---|---|---|---|---|---|---|
| | D | D | D | | | D | | | | | | | | | | | | 84 |
| | D | C | C | C | C | C | | | C | C | C | | C | | | C | C | 85 |
| | | | D | D | C | C/D | | D | D | C | | | D | | D | | | 86 |
| | C | C | C | C | D | D | | D | D | C | D | D | D | C | C | D | C | 87 |

C: C$_{3v}$

D: D$_{3h}$

Ref. 84, Electron diffraction

Ref. 85, Matrix isolation infrared

Ref. 86, Matrix isolation infrared

Ref. 87, Electric deflection

geometry for most of the trifluorides. However, it appears that any distortion of the $MF_3$ molecules from the planar configuration is quite small, but changes in the geometry of the molecules across the lanthanide series seem definitely established. Correlation of the molecular structure and polarity with the electronic configuration of the central $Ln^{3+}$ ion is also not clear.

Matrix-isolation IR and electric deflection experiments concur on the geometry of the definitely established difluorides of Sm, Eu and Yb (87-89). These molecules in the vapor phase have the polar bent structure with F-M-F angle of $110 \pm 15°$ for $SmF_2$ and $EuF_2$ and $140 \pm 15°$ for $YbF_2$. Gas phase vibrational frequencies have also been established reasonably accurately.

The only molecular data available for the other gaseous lanthanide trihalide molecules are the bond distances in the Y, La and Nd species (84). Among the dihalides the matrix infra-red data have provided only the bond angles, $130 \pm 10°$ for $SmCl_2$ and $EuCl_2$ and $140 \pm 10°$ for $YbCl_2$, and their vibrational frequencies.

### 2.4.2. Chalcogenides

Spectroscopic studies of the lanthanide oxides and chalcogenides are relatively in a retarded state compared to those of the halides. DeKock and Weltner studied the gas phase IR and electronic spectra of the lanthanide monoxides and the dioxides of Ce, Pr and Tb (90). The monoxide molecules of all the lanthanides, except EuO and YbO, have ground state vibrational frequencies between 808 and 832 $cm^{-1}$. The assumption of the same vibrational frequency for EuO in particular (71) is thus clearly in error. The impact of this error in the thermodynamic
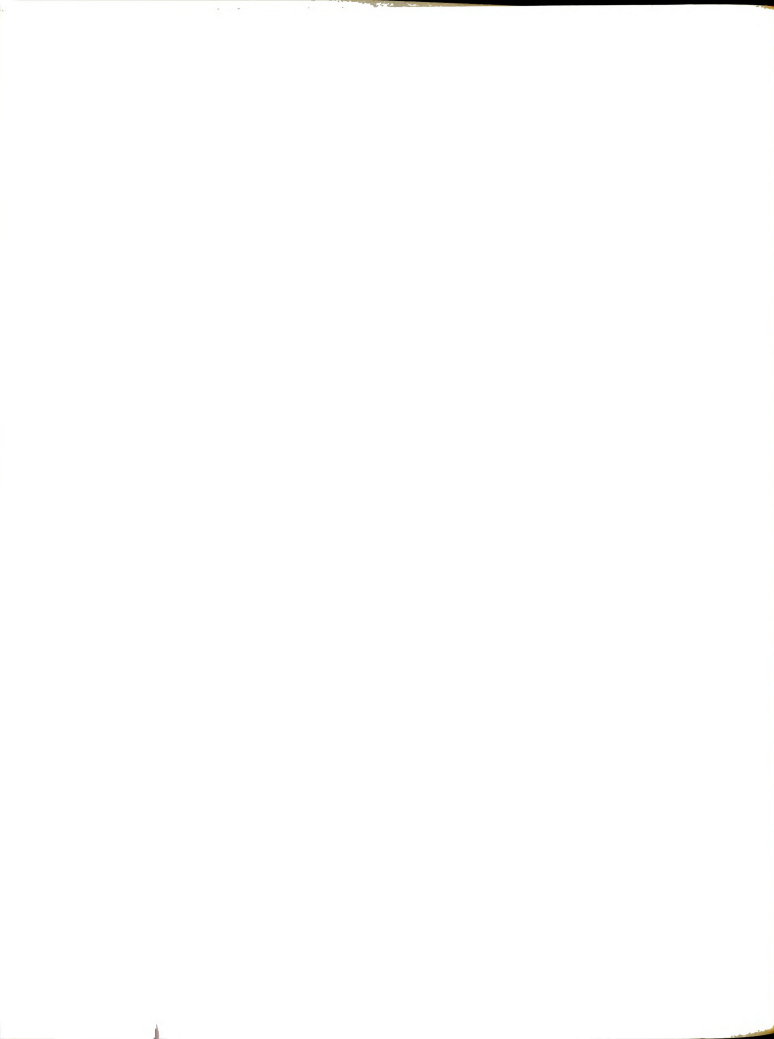
properties of EuO will be considered in Chapter 6. Gaseous $CeO_2$ and $PrO_2$ are reported nearly linear, but $TbO_2$ is definitely bent. Here again the results of electric deflection experiments (91) on $CeO_2$ are in conflict since they indicate a polar bent molecule.

Bond distances and vibrational frequencies of all the lanthanide chalcogenides have only been estimated (79-81).

## 2.5. Electronic Structure of the Gaseous Lanthanide Compounds

The problem of adequately considering the electronic ground state of the gaseous molecules of the lanthanide compounds has been an extremely difficult task in the absence of a reasonable amount of experimental knowledge about them. Brewer and Rosenblatt (92) in a compilation of the dissociation energies of the metal dioxides suggested that the electronic portion of the free energy functions for the transition metal compounds may be obtained from that of the free ion. Brewer and Mastick (93) showed that for metal monoxides an $M^+O^-$ model appeared more reasonable than the $M^{2+}O^{2-}$ model and that for the dihalides the doubly charged cation should be a reasonable model. Uncertainties in such approximations in free energy calculations have been significant in a variety of cases.

The electronic ground states of ScO (94,95), YO (94,96), LaO (94,97,98), ScS and YS (99) have now been well established as $^2\Sigma^+$, in agreement with a Hartree-Fock SCF calculation in the case of ScO (100).

Smoes et al. (80), in light of the known electronic states of TiO, VO and CeO, suggest that in the gaseous lanthanide monoxides and monochalcogenides the ground electronic state is given by the electronic structure of the singly ionized $(M-1)^+$ ion in statistical mechanical

calculation of the partition functions. Use of this approximation in this thesis work, as discussed later, entails an uncertainty of a factor of two in the ground state statistical weight (product of the multiplicity and the degeneracy of the state) for europium monoxide and monochalcogenides. The corresponding uncertainty in the entropy and the free energy functions is thus $R\ln 2$ ($\equiv 1.377$ eu). Nevertheless, contrary to Brewer and Mastick's (93) suggestion, I have used this approximation also for the europium(II) halides, and have admitted the cited uncertainty of 1.377 eu in the statistical mechanically calculated entropy and free energy functions.

CHAPTER 3

THEORETICAL CONSIDERATIONS

## 3.1.  Nature of the Evaporation Process

Evaporation processes may be classified as congruent or incongruent according to the nature of the net chemical reaction.  In congruent vaporization the vapor phase has the same composition as the condensed phase from which it arises.  The system is thus univariant and fixing the temperature uniquely determines the fugacity of the single component in the condensed and vapor phases.  In an incongruent process the vapor phase has a composition different from that of the condensed phase or phases.  Such a process may be univariant or bivariant depending on phase considerations applicable to the system.

This dissertation is concerned with only the congruent type of evaporation processes; e.g.,

$$AB(s) \text{ or } (1) = AB(g) \tag{3-1}$$

$$AB(s) \text{ or } (1) = A(g) + B(g) . \tag{3-2}$$
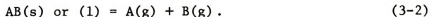
Although the system is in principle two-component, the singularity of the stoichiometric composition at AB requires it to be regarded as one-component and thus univariant.

## 3.2.  Free Energy Changes in the Vaporization Process

The primary consideration in a vaporization study is thermodynamic; i.e., the goals are (1) to determine the free energy changes in the

21

evaporation process and (2) to derive all other pertinent thermochemical data. When the condensed and vapor phases in a congruent system are in thermodynamic equilibrium at a specified temperature, the activities of the component in the two phases are determined by the equilibrium constants. If the condensed phase is pure (and thus at unit activity) and the vapor phase is dilute, the equilibrium constants for reactions (3-1) and (3-2) are represented by (3-3) and (3-4), respectively.

$$K_1 = P_{AB(g)} \qquad (3-3)$$

$$K_2 = P_{A(g)} \cdot P_{B(g)} \qquad (3-4)$$

where the activity (or fugacity) of the vapor is considered equal to its partial pressure. Such an assumption is valid in the low pressure ranges ($10^{-7} - 10^{-3}$ atm) encountered in high temperature vaporization of refractory substances. The standard free energy change for the evaporation process is related to the equilibrium constant according to

$$\Delta G^{\circ}_T = -RT \ln K_T. \qquad (3-5)$$

Determination of the equilibrium constants and their variation with temperature allows calculation of a variety of thermochemical data for the process. The study therefore resorts to the measurement of the vapor pressures in the equilibrium system.

## 3.3. Measurement of the Vapor Pressures

There are several methods of measuring the vapor pressures of substances. Of these the most common ones are the static, boiling point, transpiration, Langmuir free evaporation, Knudsen effusion and torsion effusion methods. The theoretical and experimental aspects of these methods have been described by Margrave in some detail (101). For

refractory substances at high temperatures the Langmuir free evaporation, Knudsen, and torsion effusion techniques are widely used to measure vapor pressure in the range $10^{-10}$ to $10^{-3}$ atm. This research has utilized the Knudsen effusion method to determine the vapor pressures of $EuCl_2$, $EuI_2$, EuS and EuSe.

### 3.3.1. Theory of Knudsen Effusion Method

Thermodynamically, vapor pressure is defined as that pressure obtained when a condensed phase and its vapor are in equilibrium at a constant temperature. The Knudsen effusion technique is an attempt to approximate these conditions well enough so that a valid experimental determination of the equilibrium pressure can be made.

In the Knudsen method the saturated vapor in equilibrium with the condensed phase in an enclosure called the Knudsen cell effuses through an ideal aperture into a space where the pressure of the vapor is negligible. For the ideal orifice in a Knudsen cell the kinetic theory of dilute gases provides the theoretical prediction of the angular number distribution and the total number of molecules effusing from the cell through the orifice. The angular number distribution, $dn(\theta)$, which represents the number of molecules effusing at an angle $\theta$ normal to the plane of the orifice into a solid angle $d\omega$, is given by

$$dn(\theta) = \frac{n\bar{c}}{4\pi} \cos\theta \, dA_o \, d\omega, \tag{3-6}$$

where n is the number density (number of molecules per cc) in the gas, $dA_o$ the element of area of the orifice and $\bar{c}$ the average molecular velocity. Equation (3-6) is the kinetic theory expression for the cosine distribution. The total number of molecules effusing per second from an orifice, area $A_o$, or the effusion flux J, is obtained from (3-6) by integration:

$$J = 1/4 \ n\bar{c}A_o. \tag{3-7}$$

By combining (3-7) with the ideal gas law and $\bar{c} = [\frac{8kT}{\pi m}]^{1/2}$, where k is

the Boltzmann constant, one derives the Hertz-Knudsen equation (3-8)

(102,103) which relates the vapor pressure p, in dynes $cm^{-2}$, to the mass

w, in grams, of the material which effuses during t seconds at a fixed

temperature T.

$$p = \frac{w}{A_o t} [\frac{2\pi kT}{m}]^{1/2} \tag{3-8}$$

### 3.3.2. Target Collection Technique

In the target collection vaporization method only a small fraction

of the effusate from the orifice is collected on a condensation target

located in an evacuated space directly above the orifice. If the orifice

and target are circular, parallel and coaxial, and the orifice radius,

$R_o$, relatively small compared to both the target-orifice distance, C,

and the target radius, R, application of equation (3-6) provides the

exact expression to the collection efficiency, F:

$$F = R^2/C^2 + R^2. \tag{3-9}$$

By combining (3-8) and (3-9) and substituting the known constants, one

obtains equation (3-10) which relates the vapor pressure, P (atm),

with experimentally determinable quantities and the molecular weight

of the effusing species, M, in amu.

$$P_{atm} = \frac{w}{44.33 \ A_o t} [\frac{T}{M}]^{1/2} \frac{1}{F} \tag{3-10}$$

### 3.3.3. Assumptions in the Derivation of Knudsen Effusion Equations

Several assumptions were incorporated in the derivation of the

expressions for molecular effusion, some of which are implicit in the

kinetic theory of dilute gases.  These are:

a)  The system comprising the cell and its contents is isothermal.

b)  The molecules are identical point masses.

c)  Isotropy of the gas exists inside the Knudsen cell.

d)  The molecular velocity distribution is Maxwellian.

e)  Molecular interactions are absent in the gas phase.

f)  The orifice walls do not intercept and return to the cell any appreciable fraction of the molecular current leaving the cell.

g)  Molecules are not returned to the cell once they have passed through the orifice.

h)  Loss of effusate must occur only by vapor transport through the orifice.

i)  Equilibrium pressure of the effusing vapor is maintained inside the Knudsen cell and is not affected by molecular losses through the small effusion orifice.

j)  There are no molecular collisions in the vapor phase within the orifice.

In an ideal Knudsen effusion all of the above assumptions are valid in strict detail.  However in practice the effusion orifice will be (1) almost ideal or knife-edged, that is, a small hole in an infinitely thin sheet with $L_o/R_o \sim 0$, where $L_o$ is the length of the orifice and $R_o$ its radius; or (2) non-ideal, e.g., a hole located in a thick sheet so that $L_o/R_o > 0$.  The design of the non-ideal orifice may take several shapes such as right circular cylindrical, conical, spherical, or truncated right circular cone and its inverse.  This aspect and the assumptions f-j will be considered in greater detail.

### 3.3.4. The Clausing Transmission Factor

Clausing considered vapor transport through right circular cylindrical channels (104). In his development of a theory for the angular number distribution and the total flow, he assumed a linear pressure gradient in the orifice channel and a random restitution of the gas molecules to the vapor phase from the orifice wall according to the cosine distribution law. Along with the assumption that molecules that do not strike the channel wall obeyed equations valid for the ideal orifice, Clausing derived

$$dn(\theta) = \frac{n\bar{c}}{4\pi} T \cos\theta \, dA_o \, d\omega \qquad (3-11)$$

$$J = \frac{n\bar{c}}{4} A_o W, \qquad (3-12)$$

where $T = T(\theta, L_o, R_o)$ and $W$ is the Clausing transmission probability. On the basis of these equations Clausing predicted that some of the gas molecules which enter the channel are returned to the cell interior by diffuse reflection, and a focussing of the effusion flux results in marked deviations from the cosine distribution law for real channels of finite length, especially at higher angles to the orifice normal. The Clausing factor for an ideal orifice would necessarily be unity. Similar corrective factors for other orifice shapes, based on Clausing's assumptions, have also been obtained (105-111); in all these treatments $W$ is purely a geometrical parameter of the orifice.

Winterbottom, Hirth and Ruth (108,112-114) however emphasized the importance of surface diffusion to the spatial distribution and total flow of effusing molecules. They postulated that a gas molecule incident on the orifice wall has a high probability of being adsorbed and that reevaporation of the molecule may occur from a site removed

from the point of impingement. Except for absorption and surface
diffusion, no other interaction of the molecules with the orifice wall
was invoked. The derived expressions for the surface diffusion contribution
to the angular number distribution and total flow are functions of the
orifice factors $(L_o/R_o)$, cell temperature (and pressure), the nature of
the cell material, the effusing species and the surface diffusion
coefficients. The effect of surface diffusion contribution appears to
be greatest at decreased $L_o$ and $R_o$ - in other words as the orifice tends
to be ideal.

Wang and Wahlbeck (115) studied angular number distributions of CsCl
molecules effusing from a near-ideal orifice $(L_o/R_o \sim 0.05)$ under
molecular flow conditions (sec. 3.3.6). Their results are in good
agreement with the cosine distribution law and they concluded that for
ideal and near-ideal orifices kinetic theory accurately predicts the
angular number distribution and total flow.

### 3.3.5. Vapor Saturation in the Knudsen Cell

The assumption that the vapor entering the effusion orifice is
effectively at the equilibrium vapor pressure of the condensed material
has been discussed extensively. In a completely enclosed isothermal
cell (with no orifice) the gross evaporation flux must equal the gross
condensation flux on the surface of the condensed material in equilibrium
with the vapor at the surface temperature. In other words the
evaporation coefficient, $\alpha_v$ defined as the rate of vaporization compared
to the equilibrium rate, and the condensation coefficient, $\alpha_c$ defined
as the fraction of impinging vapor molecules that condense, must be
equal. However with a finite orifice in the cell, continuous material
loss occurs by effusion through it and a steady state situation may
arise. The measured pressure, $P_m$, based on the steady state effusion
rate will not be equal to the equilibrium vapor pressure, $P_e$. Whitman (116),

Motzfeldt (117) and Balson (106) have derived expressions that relate $P_m$ to $P_e$ with two major assumptions: (1) the evaporation and condensation coefficients of the vapor at the surface are equal under steady state conditions, and (2) there is a linear pressure gradient in the cell body itself of the type assumed by Clausing for the orifice channel. Expression (3-13) derived by Motzfeldt has been used widely in vapor pressure studies.

$$P_e = P_m [1 + f(\frac{1}{\alpha} + \frac{1}{W_a} - 2)] \qquad (3-13)$$

In this equation $f = W_b A_o/A$ with $A_o$ and $A$ the orifice and sample surface area respectively, $W_b$ and $W_a$ the Clausing transmission factors for the orifice and cell body, and $\alpha = \alpha_v = \alpha_c$. For Knudsen cells with length to diameter ratios of $\sim 1$ as are commonly used in vaporization studies, $W_a$ is $\sim 0.5$. Pressure measurements, $P_m$, made with different sized effusion orifices may be plotted against the quantity, $P_m f$, and from the resulting straight line the values of $P_e$ and $\alpha$ are computed. It is also evident that with knife-edge orifices and $A_o/A \leq 0.01$, $P_m \stackrel{\sim}{\sim} P_e$, provided that $\alpha$, the coefficient of evaporation (or condensation) does not differ significantly from unity.

Carlson (118) has reexamined the question of vapor saturation and included, in addition to the earlier assumptions, the radial dependence of the vapor pressure inside the Knudsen cell. If $\alpha = 1$, his more exact but cumbersome equations reduce to the same form as (3-13).

Hirth and Pound (119) point out that the complete evaporation and condensation coefficients may be multiples of several specific constraints and are in general not equal. In addition, these constraints are functions of temperature, pressure and other surface properties that cannot always be clearly delineated, and may even change during the course of an experiment. A recent discussion of these coefficients and

the state of the art of their determination is provided by Work (120)

and Pound (121). But even if one separates the evaporation and

condensation coefficients, as was done by Paule and Margrave (122), the

resulting expression

$$P_e = P_m \frac{\alpha_c}{\alpha_v}[1 + f(\frac{1}{\alpha_c} + \frac{1}{W_a} - 2)] \qquad (3\text{-}14)$$

indicates that, with $W_a \sim 0.5$, $P_m$ is not significantly different from

$P_e$. Carlson's data (118) on the vapor pressure of mercury indicate that

the vapor within the cell can be considered saturated to within 2%,

and even this latter figure is based entirely on the overall accuracy of

his measurements and does not preclude 100% vapor saturation.

### 3.3.6. Knudsen Molecular Flow Conditions and Pressure Limits

Effusion studies are considered reliable and accurate only if they

are specifically restricted to the region of "molecular flow" where the

pressure of the gas is very low and gas molecules rarely or never collide

with one another in the region of the orifice. Early experiments by

Knudsen (123) and Knauer and Stern (124) showed that when the mean free

path, $\lambda$, of the gas molecule was decreased (by an increase of pressure)

in comparison to the diameter of the effusion orifice, deviations from

the cosine distribution and total flow equations, (3-6) and (3-7),

occurred. The term "molecular flow" has since been used to denote

rarified gas flow in which $\lambda$ is large compared to the orifice diameter.

Thus there appears to be an upper pressure limit (or lower $\lambda$ limit) for

molecular flow; Knudsen, on the basis of his experiments, set this value

at $\lambda/2R_o > 10$. Above this pressure limit effusion traverses a little

understood transition region before reaching the hydrodynamic stage.

It is interesting to note that neither Knudsen nor any other researcher

has delineated a low pressure limit to molecular flow conditions.

### 3.3.6.1. Upper Pressure Limit

The upper pressure limit to molecular flow has been studied since

the early work of Knudsen by several investigators (see Wang and Wahlbeck,

Ref. 115). The exact reason for the onset of hydrodynamic flow is

however barely understood, except that it appears to relate to the

absence of isotropicity of the gas at all points in the Knudsen cell.

There is also no consensus as to the limit of the "Knudsen number",

$\kappa = \lambda/2R_o$, at which the molecular flow equations of the kinetic theory

fail. Estimates of these limits have varied from $\kappa = 0.05$ to $10$

(123,125-128) for ideal and near-ideal effusion orifices. Schulz and

Searcy (129) noticed a dependence of $\kappa$ on the orifice parameters, $L_o/R_o$,

for short channels, with molecular flow prevailing even at $\kappa = 0.3$ for

$L_o/R_o \sim 1$.

### 3.3.6.2. Lower Pressure Limit

In principle there does not seem to be a low pressure limit for

molecular flow, and utilization of the effusion equations (3-6) and (3-7)

to determine the vapor pressures is limited only by the sensitivity of

the equipment detecting the effusing vapor. However Ward et al. (130,131),

using experimental and computer simulation of molecular effusion,

observed that deviations occur from the kinetic theory expressions at

extremely low pressures. They demonstrated that gas-solid interactions

between the effusing gas and the cell material can have important effects

on the angular number distribution and at low pressures even very small

"wall losses" would significantly affect molecular effusion. These authors

however did not specify any low pressure limit.

### 3.3.7. Accuracy of the Knudsen Effusion Method

In spite of the various considerations discussed above, the Knudsen effusion method of determining equilibrium vapor pressures of condensed material at high temperatures appears valid and accurate. Such a conclusion is based on detailed investigation of the various parameters in the method and the excellent correspondence of the pressure measurements effected by the effusion technique and the more direct static and transpiration methods. The important points that now seem well established are:

a) For ideal and near-ideal orifices angular number distribution and total flow are accurately described by the kinetic theory equations (3-6) and (3-7).

b) Use of effusion orifice areas of $\sim 10^{-3}$ cm$^2$ reduces the possibility of kinetic diminution of equilibrium vapor pressure inside the Knudsen cell.

c) Evaporation and condensation coefficients of most metals and liquid halides are approximately unity.

d) Provided significant "wall losses" are absent, target collection techniques, where the target subtends only a small solid angle at the effusion orifice, and which measure the sample emission, will be most accurate.

e) High temperatures tend to reduce any effect of small "wall losses" and angular number distribution of the vapor becomes very nearly cosine.

f) Pressures in the range $10^{-10}$ to $10^{-3}$ atm appear to be safely in the molecular flow region, and at these pressures the effects of "wall losses" and mean free path are negligible.

g) In the molecular flow region mixed species behave completely independently of each other, and their behavior is a separate function of the kinds of interactions they make with the various surfaces within the Knudsen cell.

## 3.4. Temperature Measurements

### 3.4.1. Optical Pyrometry

Temperatures above 1000°C are measured conveniently with the disappearing filament optical pyrometer. The theory and principles of such units are adequately discussed by Margrave (132) and Corruccini (133). The device consists of an electrically heated filament located at the focal plane of the objective. Temperature readings are obtained from a calibration of the filament voltage when the brightness of the filament matches, or "disappears" against, the background of the luminous source whose temperature is desired. With careful technique disappearing filament optical pyrometers have proved accurate to about 1°C at or near the standard gold point (1063°C). However uncertainties of over 1°C arise at lower and higher temperatures. The lower limit of the optical pyrometer is about 800°C, while in principle there is no upper limit; the highest temperatures can always be attenuated through proper optics to the operating range of the instrument.

### 3.4.2. Wien's Law Correction Factor

In practice measurement of the temperature of a Knudsen cell inside a vacuum enclosure is effected by sighting into the blackbody hole in the cell through a set of optical elements. The latter in the experimental set up has consisted of a Pyrex window integral to the apparatus and an external Pyrex prism. Correction factors for the overall attenuation

of the radiation from the blackbody hole through the optical elements are obtained from measurements of the temperatures of a constant radiation tungsten strip lamp with and without the optical constraints. By use of Planck's exact radiation law (132,133) the brightness temperature, $T_b$, can be related to the apparent temperature, $T_a$, read with the optical elements in the radiation path according to

$$[\frac{1}{T_a} - \frac{1}{T_b}] = \frac{\lambda}{C_2} \ln [\frac{W_b}{W_a}] , \qquad (3\text{-}15)$$

where $W_b$ and $W_a$ are the energy density per unit wavelength interval in a blackbody cavity at $T_b$ and $T_a$, respectively, and $C_2$ is the second radiation constant (1.438 cm K). If the radiating source is not truely blackbody, then a further correction for the emissivity of the source must be made:

$$[\frac{1}{T_t} - \frac{1}{T_b}] = \frac{\lambda}{C_2} \ln \epsilon_\lambda , \qquad (3\text{-}16)$$

where $\epsilon_\lambda$ is the emissivity for radiation at the wavelength $\lambda$ and $T_t$ is the true temperature.

In an optical pyrometer which utilizes a band of wavelengths, the cut-off on the short wave side is provided by a red filter and on the long wave side by the insensitivity of the human eye to infrared radiation. Thus the effective pass band in an optical pyrometer is fairly narrow and the instrument senses essentially "monochromatic" radiation of wavelength $\lambda_e$ which is only weakly temperature dependent. The value of $\lambda_e$ is $\sim$ 650 nm. Equations (3-15) and (3-16) may thus be reduced to

$$\Delta = [\frac{1}{T_t} - \frac{1}{T_a}] = \frac{\lambda_e}{C_2} [\ln \epsilon_{\lambda_e} - \ln \frac{W_b}{W_a}] = \frac{\lambda_e}{C_2} \ln \epsilon_{\lambda_e} \tau_{\lambda_e} , \qquad (3\text{-}17)$$

where $\tau_{\lambda_e}$ is the transmittance of the optical elements. In the range of measurement of the pyrometer the term $\Delta$, commonly called the Wien's Law correction factor, is essentially constant and independent of temperature.

### 3.4.3. Temperature Scale

All temperature measurements in this thesis are based on the International Practical Temperature Scale of 1948 and consequently the derived thermochemical values also refer to the same scale. A more recent scale, IPTS-1968, became effective on January 1, 1969 (134). Douglas (135) provides equations for the conversion of existing thermochemical data to the IPTS-1968 basis. However no attempt has been made in this thesis to effect such a conversion.

### 3.5. Mass Spectrometry

In recent years high temperature mass spectrometry has become an important tool in the study of gas-solid and gas-liquid equilibrium reactions. Excellent review articles on the subject have appeared (136,137) and it is a continuing theme in the series on Advances in Mass Spectrometry. The principal applications of such investigations are in the identification of the equilibrium gaseous species and determination of their bond dissociation or atomization energies. Mass spectrometric methods have, additionally, been utilized in studies of the mechanisms and kinetics of vaporization and condensation processes.

Pertinent to this work is the use of the mass spectrometer to investigate the molecular beam which effuses from a Knudsen cell in a typical vaporization experiment. The necessity and importance of such a study parallel to the regular vaporization study (sec. 3.3) cannot be overemphasized, for the mass spectrometer is unique in establishing the

where $\tau_{\lambda_e}$ is the transmittance of the optical elements. In the range of measurement of the pyrometer the term $\Delta$, commonly called the Wien's Law correction factor, is essentially constant and independent of temperature.

### 3.4.3. Temperature Scale

All temperature measurements in this thesis are based on the International Practical Temperature Scale of 1948 and consequently the derived thermochemical values also refer to the same scale. A more recent scale, IPTS-1968, became effective on January 1, 1969 (134). Douglas (135) provides equations for the conversion of existing thermochemical data to the IPTS-1968 basis. However no attempt has been made in this thesis to effect such a conversion.

### 3.5. Mass Spectrometry

In recent years high temperature mass spectrometry has become an important tool in the study of gas-solid and gas-liquid equilibrium reactions. Excellent review articles on the subject have appeared (136,137) and it is a continuing theme in the series on Advances in Mass Spectrometry. The principal applications of such investigations are in the identification of the equilibrium gaseous species and determination of their bond dissociation or atomization energies. Mass spectrometric methods have, additionally, been utilized in studies of the mechanisms and kinetics of vaporization and condensation processes.

Pertinent to this work is the use of the mass spectrometer to investigate the molecular beam which effuses from a Knudsen cell in a typical vaporization experiment. The necessity and importance of such a study parallel to the regular vaporization study (sec. 3.3) cannot be overemphasized, for the mass spectrometer is unique in establishing the

composition of the vapor species, which may be extremely complex. In a
high temperature mass spectrometric study the following steps must be
effected: (a) a representative sample of the molecular beam must be
isolated from the Knudsen cell, (b) the various neutral species present
in the beam must be ionized, (c) the mass of the ions must be determined
and the individual ion intensities recorded, (d) the neutral precursor
species of the ions must be determined, (e) the flux of neutral vapor
species effusing from the cell must be calculated from the ion intensity
data, and finally (f) the thermodynamics of the various equilibrium
processes which occur inside the cell must be derived.

### 3.5.1. Mass Spectrometer

Grimely has discussed the various types of mass spectrometers that
are equipped with high temperature Knudsen cell inlets (137). In this
study a Time-of-Flight instrument, manufactured by the Bendix Corporation,
Cincinnati, Ohio, was utilized. This instrument is non-magnetic; ion
separation is based on velocity selection of ions of given energy in a
field-free flight region. Configurationally the molecular, electron and
ion beams are mutually perpendicular in the instrument. Ion detection
is through use of a gated magnetic electron multiplier.

### 3.5.2. Determination of the Appearance Potentials

In most commercial mass spectrometers the molecular beam is ionized
by electron impact and the positive ions identified. The subsequent
goal of identifying the precursor species is frequently achieved by
obtaining ionization efficiency curves and determining from them the
ionization or appearance potentials of the various species. A variety
of techniques are available to determine the latter quantities (138).
The usual methods utilized in high temperature mass spectrometry are:

(a) vanishing current; (b) extrapolated voltage difference; (c) linear extrapolation; (d) semi-log; and (e) retarding potential difference. Of these the linear extrapolation technique is the least accurate and results obtained by its use have always been 0.1-0.3 eV too high. Simultaneous monitoring and extrapolation of the ionization efficiency curves of standard reference masses, $H_2O^+$, $N_2^+$ and $Hg^+$, tend to reduce the uncertainties. In spite of its disadvantages, the linear extrapolation method was utilized in this research.

### 3.5.3. Conversion of Ion Intensities to Absolute Pressures

Determination of the absolute pressure of a species in a Knudsen cell when its ion intensity has been measured in the mass spectrometer is a most difficult task that has never been resolved satisfactorily. Expressions which relate the observed ion intensity, $I^+_i$, to the molecular density and pressure, $p_i$, of the gaseous precursor inside the Knudsen cell have been derived (136,137). The simplified equation is

$$I^+_i \, T = p_i \sigma_i \gamma_i A, \qquad (3-18)$$

where $\sigma_i$ is the ionization cross section for the process considered at the electron energy, $\gamma_i$ is the detector multiplier gain and $A$ is a function related to a composite of the source configuration, ionizing electron energy and transmission factors. Most ionization cross sections have been based either on those of Otvos and Stevenson (139) and on their additivity principle, or on the calculations of Mann (140). The instrumental factors may be established either through use of a calibrant such as silver or by computation. In many systems that vaporize without complications, a simultaneous determination of the total weight-loss at a fixed temperature serves to calibrate internally all the factors involved in (3-18).

### 3.5.4. Derived Thermochemical Quantities

Once the vapor species in the equilibrium system has been established and the appearance potentials of the various fragments and their parent molecule have been determined, the individual ion intensity data as a function of temperature may be utilized to derive pertinent thermochemical values for the process.

The relative or absolute ion intensity-temperature data may be combined to give, from a graph of log $I_i^+$ T $\underline{vs}$ 1/T, the enthalpy, $\Delta H^\circ_T$, for the process (e.g., reaction (3-1)). If the mass spectrometer has not been calibrated absolutely for pressures the entropy change, $\Delta S^\circ_T$, cannot be determined.

One of the most subtle uses of the ionization and appearance potential data is in establishing bond dissociation and atomization energies. Apart from their practical uses, such data are becoming increasingly important in the theoretical treatment of the bonding involved in the molecules and molecule ions. There has also been some correlation of the fragmentation pattern and appearance potentials with regard to open shell or closed shell electronic configuration of molecules (141,142). The pertinent equations follow directly from thermochemical cycles:

$$D^\circ_0 (MX)^+ = D^\circ_0 (MX) + IP (M) - IP (MX) \qquad (3-19)$$

$$D^\circ_0 (MX_2) = AP (M^+/MX_2) - IP (M) \qquad (3-20)$$

$$D^\circ_0 (XM-X) = AP (MX^+/MX_2) - IP (MX) \qquad (3-21)$$

$$D^\circ_0 (XM-X)^+ = D^\circ_0 (XM-X) + IP (MX) - IP (MX_2). \qquad (3-22)$$

However positive errors in many appearance potential values and the fact that the fragment ions in certain instances are formed with appreciable kinetic energies tend to make the derived thermochemical values higher than the

calorimetric and equilibrium data. Errors of the order of 0.1 to 0.2 eV might also arise in using the "vertical" ionization potential instead of the spectroscopic "adiabatic" ionization potential.

## 3.6. X-Ray Fluorescence Analysis

Characteristic radiations in the electromagnetic region of the spectrum arise from energy transfers involved in the rearrangements of orbital electrons of an element excited by a primary radiation. When the primary excitation is caused by high energy photons, fluorescent radiations characteristic of the element result. Fluorescence X-ray spectrometry involves measurement of the wavelength and intensity of these characteristic radiations. The method has proved to be a particularly simple and non-destructive analytical technique applicable to low concentration ranges.

### 3.6.1. Geometry of Fluorescent X-Ray Spectrometers

The spectrometer consists basically of a primary source of X-radiation, a system of collimators, the analyzing crystal, and the detector. The specimen to be analyzed is interposed between the primary beam and the analyzing crystal.

In wavelength dispersive analysis, the nearly parallel beam of fluorescent radiation from the sample is analyzed through use of the well-known Bragg equation

$$n\lambda = 2d \sin\theta, \qquad (3-23)$$

where n is the order of diffraction (usually n = 1), $\lambda$ is the wavelength of the characteristic radiation in $\overset{\circ}{A}$, d is the interplanar spacing of the analyzing crystal in $\overset{\circ}{A}$ and $\theta$ is the angle of incidence. The diffracted beam is analyzed with a detector placed at $2\theta$ with respect to the incident beam.

Two conventional geometries of the analyzing crystal are the flat- and curved-crystal arrangements. A variety of analyzer crystals are in use (143,144); the choice of a crystal depends on the wavelength to be analyzed and the resolution desired. The more common crystals are LiF (2d = 4.028 Å; 200 plane), Graphite (2d = 6.708 Å; 002 plane) and EDDT (2d = 8.808 Å; 020 plane). The large spacing crystals can diffract both short and long wavelengths, but the dispersion ($\Delta\theta/\Delta\lambda$) is poorer than that achieved with low spacing crystals. However in many cases the divergence established by the collimators is the limiting factor in resolution rather than the analyzing crystal. The three common types of detectors used in fluorescence spectrometry are the proportional counter (sealed or flow type), the scintillation counter and the solid-state counter. Selection of a detector depends, among other things, on resolution, counting efficiency and optimum peak-to-background ratios. These aspects and electronic pulse height analysis are considered in detail by Jenkins and DeVries (143). Energy analysis of the fluorescent radiation via the proportional response of such detectors is the basis of the energy dispersive fluorescence methods, which, in contrast to the wavelength dispersive procedure, eliminates both the spectrometer and the analyzing crystal.

### 3.6.2. Fluorescent Yield

The ratio of the useful X-ray photons arising from a certain electronic shell to the total number of primary photons absorbed in the same shell is denoted as the fluorescent yield, $\omega$. The value of $\omega$ is necessarily less than unity due to the Auger effect (the fluorescent X-radiation which causes ejection of one or more electrons from the outer shell of the atom) and decreases markedly with the atomic number of the

element.  In general L-fluorescent yields are less than K-fluorescent

yields.  For europium approximate values of $\omega_K$ and $\omega_L$ are 0.9 and 0.2,

respectively, within their uncertainties of 10-20%.

### 3.6.3.  Matrix Effects

The fluorescent X-ray intensity of an element depends on the

absorption coefficients (for the particular radiation) of other elements

present in the sample.  A more important effect of the matrix is

enhancement, wherein the characteristic radiation of a component in the

matrix, excited along with the element under analysis, has enough

energy to excite the characteristic radiation of that element.  The

enhancement effect can at times be advantageous.  It is the combination

of these two matrix effects that in reality controls the shapes of the

calibration curves.  For example copper $K\alpha$-radiation enhances the

L-radiations from europium, and thus advantageously increases the intensity

of the latter.

## 3.7.  Thermodynamic Treatment of Vaporization Data

Vapor pressure data determined from a set of experiments over a

temperature range of 300-400°C are customarily analyzed by two procedures

to derive the enthalpy, entropy and free energy changes for reactions

of type (3-1) and (3-2).  These procedures are the second-law (or

average slope) and third-law methods.

### 3.7.1.  The Second-Law Method

The second-law method of treatment of vapor pressure data for a

typical reaction (3-1) utilizes equation (3-5) in the form

$$\ln P_{(atm)} = -\frac{\Delta H^{\circ}_T}{RT} + \frac{\Delta S^{\circ}_T}{R}. \qquad (3-24)$$

For this treatment a linear least squares fit of the experimental vapor pressure-temperature values is made. One obtains the enthalpy and entropy changes for the reaction (3-1) at a temperature T from the slope and intercept of the least squares straight line. Inherent in equation (3-24) is the assumption that the vapor pressure is sufficiently low for the gas to be considered ideal (cf. sec. 3-2). In addition, since the heat capacity change, $\Delta C^{\circ}_{p}$, for the reaction (3-1) is normally not zero, $\Delta H^{\circ}$ and $\Delta S^{\circ}$ are correspondingly slowly varying functions of temperature and a slight curvature in the $\ln P_{(atm)}$ vs $1/T$ plot would be expected. Equation (3-24) is strictly valid at any specified temperature, T, for which the corresponding vapor pressure, $P_{T}$, is known. However the linear equation is usable without serious error over a small temperature range closely related to the measurement region since the $\Delta C^{\circ}_{p}$ correction is insignificant in most cases of practical interest. The method in essence therefore calculates an "average slope" and an "average intercept" to correspond to a specified temperature, T (145). But there is ambiguity as to the value of the specific temperature. Horton (146) in a statistical treatment of the second-law procedure points out that the average slope thus derived does not represent unambiguously the enthalpy change at any recognizable temperature within the range of the experiment. He states that the usual choice of T as median of T or 1/T, or averages of all the experimental temperatures introduces definite bias in the second-law enthalpy, but a bias which is quite small and well within the currently attainable precision of most methods now used for measuring vapor pressures at high temperatures. In this thesis the linear least squares data are referred to the median of the experimental range of temperatures.

The enthalpy and entropy changes derived for reaction (3-1) from equation (3-24) may be reduced to the reference temperature (298.15 K in this thesis and referenced as 298) by use of three different procedures which take into account the heat capacity change in the reaction.

### 3.7.1.1. General Treatment

The enthalpy and entropy changes for reactions (3-1) and (3-2) are calculated from the exact thermodynamic relations

$$\Delta H^\circ_{298} = \Delta H^\circ_T + \int_T^{298} \Delta C^\circ_p \, dT \qquad (3\text{-}25)$$

$$\Delta S^\circ_{298} = \Delta S^\circ_T + \int_T^{298} \frac{\Delta C^\circ_p}{T} \, dT. \qquad (3\text{-}26)$$

If the change in the heat capacities, $\Delta C^\circ_p$, for the reactions may be expressed in either of the analytical forms

$$\Delta C^\circ_p = \Delta a + \Delta bT \qquad (3\text{-}27)$$

$$\Delta C^\circ_p = \Delta a + \Delta bT + \Delta cT^{-2}, \qquad (3\text{-}28)$$

this may be utilized directly in equations (3-25) and (3-26) to derive the enthalpy and entropy values at 298.15 K. On the other hand, if the heat capacities of the reactants and products of reactions (3-1) and (3-2) are known or may be estimated, then the thermal functions, $(H^\circ_T - H^\circ_{298})$ and $(S^\circ_T - S^\circ_{298})$, may be utilized directly to reduce the experimental data from the median temperature. This latter procedure is generally utilized in this work since the heat capacities of the condensed and vapor phases had to be estimated (sec. 3.8.1). A more accurate data reduction may be effected later if experimental heat capacity values become available without any loss of the information content of the present experimental work. This procedure also permits a more realistic

error estimate in the derived data than if estimated heat capacity changes for broad classes of reactions (147) had been used.

### 3.7.1.2. $\Sigma$-Treatment

The $\Sigma$-method due to Kelley (148) utilizes analytical expressions (3-27) and (3-28) for measured or estimated heat capacity changes in combination with individual experimental vapor pressure-temperature values. From the thermodynamic expressions

$$\Delta H^{\circ}_{T} = \Delta H_1 + \int \Delta C^{\circ}_{p} \, dT = \Delta H_1 + A(T) \tag{3-29}$$

$$\Delta G^{\circ}_{T}/T = -R \, \ell n \, K = -\int \Delta H^{\circ}_{T}/T^2 \, dT$$

$$= \Delta H_1/T - \int A(T)/T^2 \, dT + I$$

$$= \Delta H_1/T - B(T) + I, \tag{3-30}$$

where the integrations are performed without limits and $\Delta H_1$ and I are the respective integration constants, Kelley defines $\Sigma$ according to

$$\Sigma = -R \, \ell n \, K + B(T) = \Delta H_1/T + I. \tag{3-31}$$

A plot of $\Sigma$ vs $1/T$ should theoretically be linear with slope $\Delta H_1$ and intercept I. The enthalpy and entropy changes at any temperature, including the reference temperature, 298.15 K, may be evaluated according to (3-32) and (3-33):

$$\Delta H^{\circ}_{T} = \Delta H_1 + A(T) \tag{3-32}$$

$$\Delta S^{\circ}_{T} = -I + A(T)/T + B(T). \tag{3-33}$$

### 3.7.1.3. $\Sigma'$-Treatment

The $\Sigma'$-method due to Cubicciotti (149) utilizes the free energy functions (sec. 3.7.2) or the analytical expressions for the heat capacities of the reactants and products with each vapor pressure-temperature data point. The term $\Sigma'$ is defined according to

$$\Sigma' = -R \ln K + \Delta FEF_{298} - \Delta FEF_T$$

$$= -R \ln K - \Delta(H°_T - H°_{298})/T + \Delta(S°_T - S°_{298})$$

$$= \Delta H°_{298}/T - \Delta S°_{298}. \qquad (3-34)$$

A plot of $\Sigma'$ $\underline{vs}$ $1/T$ should be linear with slope and intercept that give directly the enthalpy and entropy changes at 298.15 K. The $\Delta$'s in equation (3-34) refer to the appropriate thermodynamic functions of the products minus those of the reactants.

It may be pointed out that while all three treatments are exact thermodynamic relationships, approximations are introduced to the extent that heat capacities, or changes thereof, are expressed in the analytical forms (3-27) and (3-28). It is important to note that many high temperature systems lack experimentally established heat capacity data and recourse must be made to estimates. Both the $\Sigma$ and $\Sigma'$ treatments lose the original vapor pressure-temperature or equilibrium constant-temperature data in their quest to provide single numbers, $\Delta H_1$ and I or $\Delta H°_{298}$ and $\Delta S°_{298}$, respectively.

### 3.7.2. The Third-law Method

The third-law method of treating vapor pressure-temperature data follows directly from the definitions of the free energy function according to

$$FEF = (G°_T - H°_{298})/T \qquad (3-35)$$

$$FEF = (H°_T - H°_{298})/T - S°_T. \qquad (3-36)$$

Calculations of the free energy functions are based on a knowledge of the absolute entropy, $S°_{298}$ (measured or estimated), and analytical expressions for the heat capacity, $C°_p$. For a reaction of the type (3-1),

$$\Delta FEF_T = \Delta(G°_T - H°_{298})/T = -R \ln P_T - \Delta H°_{298}/T \qquad (3-37)$$

Combination of each experimental pressure value with the change in free energy function for the reaction at the temperature of the measurement, T, provides individual $\Delta H°_{298}$ values directly for each data point according to

$$\Delta H°_{298} = T(-\Delta FEF - R \ln P_T) \qquad (3-38)$$

The individual $\Delta H°_{298}$ may then be averaged to provide the statistically best value for the enthalpy change. The uncertainty assigned to an enthalpy calculated by this method should include the uncertainty in $\ln P$ and must include that in the free energy functions.

The individual enthalpy values obtained by the third-law procedure are more amenable to an analysis of systematic errors in the experimental pressure and temperature data than is the one value obtained by the second-law, $\Sigma$ or $\Sigma'$ procedure.

### 3.7.3. Comparison of Second- and Third-Law Methods

It is a common practice among high temperature thermochemists to compare the enthalpy and entropy changes derived through use of the second-law and third-law methods, but to place more reliance on the latter values. If measured free energy functions are available, the

third-law method, by its very nature of analyzing individual experimental data, appears to be more reliable in that grossly erratic data points can be located easily and eliminated. However when estimated free energy functions must be used, lack of a temperature or pressure dependent trend in the third-law enthalpies is only an internal check of the consistency of the estimates with the measured temperature and pressure values. Under the same circumstances if the experimental data are correct, the second- and third-law derived values should agree within their respective uncertainties. Lack of agreement would point to systematic errors in the experiment, incorrect formulation of the vaporization reaction, non-equilibrium conditions and/or incorrect thermodynamic functions, especially $S°_{298}$ and $C°_p$.

McCreary and Thorn (150) in a statistical analysis of the two procedures point out that the informational content of the third-law enthalpies with respect to errors and reproducibility among sets of experiments is nearly the same as that contained in the second-law enthalpies of the same sets. In essence the two procedures differ only in the kind of statistical analysis performed on a given set of experimental data. Thorn (151) argues that comparison of the entropy of vaporization derived from the $\ln P$ vs $1/T$ graph ($\Delta S°$, second-law) with that obtained from the absolute entropies ($\Delta S°$, third-law) is a more meaningful measure of the consistency of the data than is the regularly applied check of the enthalpies. However if there is strict correspondence between the two entropy changes, the second- and third-law treatments for the enthalpy are also identical. This statement may be verified by recasting equation (3-24) into the following forms

$$-R \ln P = \Delta H^\circ_{298}(2)/T + \Delta(H^\circ_T - H^\circ_{298})/T$$
$$-\Delta S^\circ_{298}(2) - \Delta(S^\circ_T - S^\circ_{298}) \qquad (3\text{-}39)$$

$$= \Delta H^\circ_{298}(2)/T + \Delta(G^\circ_T - H^\circ_{298})/T$$
$$+\Delta S^\circ_{298}(3) - \Delta S^\circ_{298}(2) \qquad (3\text{-}40)$$

$$-R \ln P - \Delta FEF = \Delta H^\circ_{298}(3)/T$$

$$= \Delta H^\circ_{298}(2)/T + \Delta S^\circ_{298}(3) - \Delta S^\circ_{298}(2), \qquad (3\text{-}41)$$

where the numbers in parentheses refer to the second- and third-law treatments.

It has also become a practice to fit the experimental data according to equation (3-41) to derive the second-law enthalpy change while maintaining the intercept $\Delta S^\circ_{298}(3) - \Delta S^\circ_{298}(2)$ to accomodate errors (152).

## 3.8. Estimation of Thermochemical Data

The collection and evaluation of thermochemical data for material systems requires the availability of considerable calorimetric information that must be correlated to provide the tabulated properties over an extended temperature range. However for many systems of interest some of the required thermal data are imperfectly known or even completely unknown. It then becomes essential to estimate the missing data with reasonable accuracy. Such estimative techniques have become a science in themselves and are discussed in great detail by Kubaschewski and Evans (147) and Stull and Prophet (153). Although the validity of estimative methods in thermodynamics has been abundantly established, the accuracy of the derived values can only be judged on the basis of overall internal consistency.

### 3.8.1. Heat Capacities

#### 3.8.1.1. Solids

The heat capacity at constant pressure, $C^\circ_p$, is the quantity that is ordinarily needed for calculations of thermochemical equilibria over wide ranges of temperatures. It is related to the heat capacity at constant volume, $C^\circ_v$, by the well-known thermodynamic relationship

$$C^\circ_p = C^\circ_v + \alpha^2 \, \bar{V} \, T/\beta, \qquad (3-42)$$

where $\alpha$ is the volume thermal expansivity $[\frac{1}{\bar{V}}(\frac{\partial \bar{V}}{\partial T})_P]$, $\bar{V}$ is the molar volume and $\beta$ is the isothermal compressibility $[-\frac{1}{\bar{V}}(\frac{\partial \bar{V}}{\partial P})_T]$. The quantity $\alpha^2 \, \bar{V} \, T/\beta$ is known as the dilation term. For a solid $C^\circ_v$ may be represented in general as the contributions of several factors according to

$$C^\circ_v = C_1 + C_a + C_e + C_d, \qquad (3-43)$$

where $C_1$ is the contribution of harmonic lattice vibrations and constitutes the main factor, $C_a$ is a term that accounts for anharmonicity, $C_e$ the heat capacity of the conduction, d or f electrons and $C_d$ that due to lattice defects. These various heat capacity factors cannot usually be adequately obtained from experimental or theoretical methods. Empirical procedures have been attempted in a few classes of compounds with partial success.

For solids that form a coordination lattice, $C^\circ_v$ at 298.15 K is approximately 6 cal deg$^{-1}$/g atom when the lattice is in a state of complete oscillation. The dilation term at room temperature is $\sim$ 3-8%, but accounts for $\sim$ 15-20% of the lattice contribution near the melting point of the solid. On this basis, Kubaschewski approximates (147) that

close to the transition point, $C^\circ_p$ for a solid is $\sim$ 7 to 7.25 cal/deg$^{-1}$/g atom.

Where heat capacity measurements are available for an isostructural compound, the Neumann-Kopp rule may be employed

$$C^\circ_p \ (MX_2) = C^\circ_p \ (M'X_2) - C^\circ_p \ (M') + C^\circ_p \ (M). \tag{3-44}$$

Since heat capacities of most metals are known accurately, data derived through use of equation (3-44) have in many cases been found to be extremely accurate.

Recently Kellogg (154) suggested an estimative procedure for heat capacities of solids at 298.15 K based on the contributions of the cationic and anionic constituents of solid inorganic compounds. The method parallels Latimer's method of entropy estimations closely (sec. 3.8.2.1) and the author cites accuracies within 0.1-0.2 cal deg$^{-1}$/g atom for a variety of systems.

### 3.8.1.2. Liquids

The heat capacity, $C^\circ_p$, of a liquid is a more difficult number to estimate. From limited experimental numbers available, it is suggested for inorganic liquids that $C^\circ_p$ is $\sim$ 8 to 8.75 cal deg$^{-1}$/g atom or for $MX_2(\ell)$, $C^\circ_p \sim$ 24-26.25 eu. Very little is known about the temperature dependency of the heat capacity of liquid inorganic substances, and it has been a common practice to assume a constant value over the entire liquid range.

### 3.8.1.3. Gases

The heat capacities of vapor phases have been estimated somewhat successfully by correlation with similarly structured species (155).

However ideal gas statistical calculations are preferred even when the pertinent molecular data need to be estimated. In such procedures a consistent set of thermodynamic functions, and in particular the entropy of the gas, is realized. Aspects of such calculations are considered in Section 3.9.

### 3.8.2. Standard Entropies

#### 3.8.2.1. Solids

The standard entropy, $S^\circ_{298}$, of predominantly ionic solid inorganic compounds may be estimated by Latimer's additivity method (156). In this method the entropy contributions of the cationic and anionic constituents are added. By use of these empirical numbers, which take into account the effects of ionic mass, size and charge, entropy values accurate to within 2 to 4 eu for a variety of inorganic compounds are realized. More recently Gronvold and Westrum (157) and Kelley (in Ref. 153) have revised Latimer's estimates to provide standard entropies accurate to within 1 to 2 eu. In addition Westrum (158) has considered the magnetic contribution of the lanthanide metal to the entropy of the solids.

Pitzer and Brewer (148) suggest a relationship that appears particularly applicable to a series of compounds of an element.

$$S^\circ_{298} (MX_n) = S^\circ_{298} (MY_n) + \frac{3}{2} n R \ln \frac{M_x}{M_y} \qquad (3\text{-}44)$$

In (3-44) $M_x$ and $M_y$ are the atomic weights of the anionic constituents X and Y respectively. However significant changes in the structures of the solids, $MX_n$ and $MY_n$, would affect the validity of such relationships.

### 3.8.2.2. Liquids

The standard entropy of a liquid inorganic compound is not normally needed in the thermodynamic calculations. However, such quantities may be estimated or obtained from the standard entropy of the solid by adding the entropy of fusion or from that of the gas by subtracting the entropy of vaporization.

### 3.8.2.3. Gases

From certain empirical regularities in the standard entropies of monatomic, diatomic and polyatomic gases in relation to only the molecular weight, Kubaschewski and Evans (147) have derived very approximate relationships that might find use in estimating $S^\circ_{298}$ values for gases. However it is probably more prudent to resort to statistical methods as for the heat capacity. The pertinent details are considered in Section 3.9.

### 3.8.3. Entropies of Transitions

#### 3.8.3.1. Entropy of Fusion

The regularity in entropies of fusion of metals is expressed by Richards' rule which states that $\Delta S^\circ_{fus} \sim 2.2$ eu/g atom (147). The entropies of fusion of inorganic compounds with a coordination lattice range from 2 to 3.5 eu/g atom, but the entropies of fusion of substances that have distinct molecular units in the solid and liquid tend to be lower.

#### 3.8.3.2. Entropy of Vaporization

The regularity in entropies of vaporization is evidenced in the widely known Trouton's rule that $\Delta S^\circ_v$ at the normal boiling point is

$\sim$ 22 eu (147). Entropies of vaporization of liquids with boiling points near and below room temperature tend to be lower than the Trouton value; those of liquids with boiling points higher than room temperature tend to be higher. Gschneidner recommends a value of 25.5 eu for the latter class of substances (159).

## 3.9. Ideal Gas Statistical Calculations of Thermodynamic Functions

For atoms, diatomic molecules and simple polyatomic molecules, statistical-mechanical calculations, if they are based on detailed spectroscopic data of rotational, vibrational and electronic states, permit evaluation of accurate thermodynamic functions for ideal gases. The theory and methods of calculations are available in standard texts on Statistical Thermodynamics (e.g., Hill, Ref. 160) and have been discussed more concisely by Stull and Prophet (153). This section deals with the essentials of such statistical calculations as applied to the diatomic and triatomic gas molecules encountered in this work.

For a system of N identical indistinguishable and non-interacting molecules satisfying the condition that the number of available molecular states is much greater than N, the system partition function, Q, is expressed in terms of the molecular partition function, q, according to equation

$$Q = q^N/N! .\qquad\qquad(3\text{-}45)$$

For gas molecules the contributions of the translational, rotational, vibrational and electronic terms in the partition function are often nearly independent and the product of these independent terms gives the total molecular partition function according to (3-46):

$$q(V,T) = q_t(V,T) \cdot q_r(T) \cdot q_v(T) \cdot q_e(T). \tag{3-46}$$

The translational partition function is given by the Sackur-Tetrode equation

$$q_t = (2\pi m k T/h^2)^{3/2} V, \tag{3-47}$$

where V is the volume, m the molecular mass and k and h the Boltzmann and Planck constants, respectively. The partition functions for a two-dimensional and three-dimensional rigid rotator are given by

$$q_r \ (2\text{-}D) = (8\pi^2 I k T/h^2)/\sigma \tag{3-48}$$

$$q_r \ (3\text{-}D) = (\pi^{1/2}/\sigma) \cdot (8\pi^2 k T/h^2)^{3/2} \cdot (I_x \cdot I_y \cdot I_z)^{1/2}, \tag{3-49}$$

where I is the moment of inertia of a diatomic or linear polyatomic molecule and $I_x$, $I_y$ and $I_z$ are the three principal moments of inertia for a non-linear molecule. The term $\sigma$ is the symmetry number, and is unity for an unsymmetric molecule and two for a symmetric molecule. The vibrational partition function for each degree of freedom is given by

$$q_v = \exp \ (-h\nu/2kT) \cdot (1 - \exp \ (-h\nu/kT))^{-1}, \tag{3-50}$$

where $\nu$ is the frequency (expressed as $c\omega$ with $\omega$ in $cm^{-1}$) of each normal vibrational mode of the molecule. The electronic partition function can be calculated from a detailed knowledge of the electronic spectrum of the gas molecule. For the types of molecules encountered in this work, electronic states other than the ground state usually have no significant population except at very high temperatures (160). Hence the degeneracy of the ground state, $g_o$, is normally accepted as a satisfactory approximation for the electronic partition function (cf. Sec. 2.5).

The derived thermodynamic functions for one mole of an ideal gas on the rigid-rotator harmonic-oscillator model, excluding nuclear energy states and internal rotations, are given by

(a) Diatomic and Linear Triatomic Molecules

$$C^\circ_p = \frac{7}{2} R + \sum_{i=1}^{3n-5} R(\frac{\theta\omega_i}{T}) \, e^{\theta\omega_i/T} (e^{\theta\omega_i/T} - 1)^{-2} \tag{3-51}$$

$$H^\circ_T - H^\circ_0 = \frac{7}{2} RT + \sum_{i=1}^{3n-5} Nhc\omega_i \, (e^{\theta\omega_i/T} - 1) \tag{3-52}$$

$$S^\circ_T = \frac{3}{2} R \ln M + \frac{7}{2} R \ln T - R \ln P + R \ln I$$

$$-R \ln \sigma + R \sum_{i=1}^{3n-5} [\frac{\theta\omega_i}{T}(e^{\theta\omega_i/T} - 1)^{-1} - \ln (1 - e^{-\theta\omega_i/T})]$$

$$+S^\circ_e + 175.362 \tag{3-53}$$

(b) Non-Linear Triatomic Molecules

$$C^\circ_p = 4 R + \sum_{i=1}^{3n-6} R(\frac{\theta\omega_i}{T})^2 \, e^{\theta\omega_i/T}(e^{\theta\omega_i/T} - 1)^{-2} \tag{3-54}$$

$$H^\circ_T - H^\circ_0 = 4 RT + \sum_{i=1}^{3n-6} Nhc\omega_i \, (e^{\theta\omega_i/T} - 1)^{-1} \tag{3-55}$$

$$S^\circ_T = \frac{3}{2} R \ln M + 4 R \ln T - R \ln P + \frac{1}{2} R \ln I_x \cdot I_y \cdot I_z$$

$$-R \ln \sigma + R \sum_{i=1}^{3n-6} [\frac{\theta\omega_i}{T}(e^{\theta\omega_i/T} - 1)^{-1} - \ln (1 - e^{-\theta\omega_i/T})]$$

$$+S^\circ_e + 265.338. \tag{3-56}$$

In these equations, (3-51) to (3-56), M is expressed in amu, P in atm, the moments of inertia in cgs units and $S^\circ_e = R \ln g_o$. The values of the other constants used in this work are R = 1.98726 eu, $hc/k = \theta = 1.4386$ cm K, Nhc = 2.8589 cal cm/mole and $N = 6.0238 \cdot 10^{23}$/mole. For

an ideal gas in the standard state (1 atm), the term involving pressure is zero.

## 3.10. Error Analysis

A true uncertainty in the type of thermodynamic data encountered in this work is difficult to assign satisfactorily. The primary enthalpy and entropy values were derived from linear least squares fits of the experimental data. However errors in temperature measurement and calibration, vapor pressure equipment constants, Knudsen cell orifice area and the X-ray fluorescence analytical scheme could not be apportioned systematically as to their effect on the overall data. To that extent the error values of the least squares fits must be considered conservative.

Overall uncertainties in derived thermochemical values have been computed on the basis of additivity of variances, equation (3-57), on the assumption of independence in the errors of the various contributing thermodynamic functions.

$$\text{var(over all)} = \sum_{i=1}^{n} (\text{var})_i \qquad (3\text{-}57)$$

In the reduction of the second-law enthalpy and entropy data from the median temperature values to 298.15 K uncertainties in the heat capacities and thermal values for transitions are included. Errors in the third-law enthalpies are the composite of the standard deviation in the individual third-law data and the uncertainty in the free energy functions. The contribution due to the latter has been computed according to $\pm\Delta\text{FEF}$ multiplied by the median temperature of the vaporization experiment.

CHAPTER 4

EXPERIMENTAL MATERIALS, EQUIPMENTS AND PROCEDURES

## 4.1. Chemicals

(a) Europium oxide, 99.9%, American Potash and Chemical Corp., West Chicago, IL; Michigan Chemical Corp., St. Louis, MI; (b) helium, Air Reduction Co. Inc., New York, NY; (c) ultra high purity hydrogen (99.999%), Matheson Gas Products, Joliet, IL; (d) hydrogen sulfide, 99.5+%, Matheson Gas Products, East Rutherford, NJ; (e) hydrogen selenide, 98+%, Matheson Gas Products, East Rutherford, NJ; (f) ammonium chloride, reagent; (g) ammonium iodide, reagent; (h) hydrochloric acid, reagent; (i) hydriodic acid, reagent; (j) nitric acid, reagent; (k) silver nitrate, reagent; (l) palladous chloride, reagent; (m) barium chloride, reagent; (n) bromine, reagent; (o) potassium bromide, reagent; (p) sodium metabisulfite, reagent; (q) hydroxylamine hydrochloride, reagent; (r) ammonium hydroxide, reagent; (s) ammonium nitrate, reagent; (t) phosphorus pentoxide, reagent; (u) Molecular Sieve, Activated Linde Type 5A, 1/8", Matheson Coleman Bell, Norwood, OH; (v) Catalyst R 3-11, Badische Anilin Soda Fabrik, AG, Ludwigschafen am Rhein, W. Germany; (w) silver wire, reagent.

## 4.2. Materials

(a) Graphite stock, Becker Brothers Carbon Co., Cicero, IL; (b) molybdenum rod, tungsten rod, tungsten-molybdenum stock, Kulite

Tungsten Corp., Ridgefield, NJ; (c) platinum, J. Bishop and Co., Malvern, PA; (d) copper stock, McMaster Carr Supply Co., Chicago, IL; (e) vitreous carbon boats and crucibles, Beckwith Carbon Corp., Van Nuys, CA; (f) quartz, Thermal Syndicate Ltd., England (boats); Engelhard Industries, Inc., Hillside, NJ (tubings).

## 4.3. Recirculating Argon-Atmosphere Glove Box

All storage and handling of air- and moisture-sensitive materials such as $EuCl_2$, $EuI_2$ and the chalcogenides were made in the recirculating argon-atmosphere glove box described previously (161). However a number of modifications were made to ensure that the atmosphere was routinely dry and inert. The entire gas purification train and recirculation line were changed to all metal construction. The glove box atmosphere was circulated by a SPRAYIT model 906 CA-20 diaphragm pump (Thomas Industries Inc., Sheboygan, WI) through the purification manifold. This manifold had a series of two 30 cm long, 3.8 cm nominal bore brass towers, one filled with Linde Molecular Sieve pellets to remove moisture and the other filled with BASF catalytic oxygen remover R 3-11. A second Molecular Sieve drier served as a stand-by parallel to the main tower. All coupling lines were built of 0.95 cm nominal bore copper tubing with Hoke needle valves which were hard-soldered together. The manifold carried a purge argon inlet and Bourdon gage to monitor for excess pressure. The Molecular Sieve driers were alternated to permit regeneration of the dessicant by in-line heating to $\sim$ 200°C in vacuum.

Although no monitoring of the continuously circulated glove box atmosphere for $H_2O$ and $O_2$ was possible, the quality of the atmosphere in the box was judged from an open tray of phosphorus pentoxide. The

dessicant remained very dry and non-flaky while the glove box was
purified routinely by circulation.

The box is nominally kept at $\sim$ +2.5 cm water gage with respect to
the external atmosphere. This pressure was monitored by an oil manometer,
which also served as an emergency blow-off line. The glove box was
entered through a vacuum lock which had a separate cylinder argon inlet,
and routine entries were minimized to ensure a high degree of purity
inside.

## 4.4. Preparative

Gas-solid reactions of the type used in the preparations of air-
and moisture-sensitive europium compounds were performed in an experimental
set up depicted in Figure 1. The apparatus consisted of a 75 cm long,
3 cm i.d. quartz/Vycor reaction tube (A) in a standard 30 cm laboratory
Hevi-Duty tube furnace (B). The inlet end of the reaction tube was
connected to a 3 cm i.d. Pyrex isolator section with a vacuum stop-cock
(C) through which the reactant and sweep gases entered the system. The
exit side was equipped with a safety trap, a gas bubbler and disposal
sections (D). A gas-handling manifold with a phosphorus pentoxide drier
(E) and/or a liquid nitrogen trap (F) and an auxiliary inlet line completed
the experimental set up. Reaction temperatures were monitored with a
chromel-alumel thermocouple and Sym-Ply-Trol millivolt meter.

At the conclusion of the reaction, the boat containing the product
was slid into the isolator section which was then capped as a high flow
of dry helium passed through it. The isolator section was then evacuated
before transfer into the glove box.
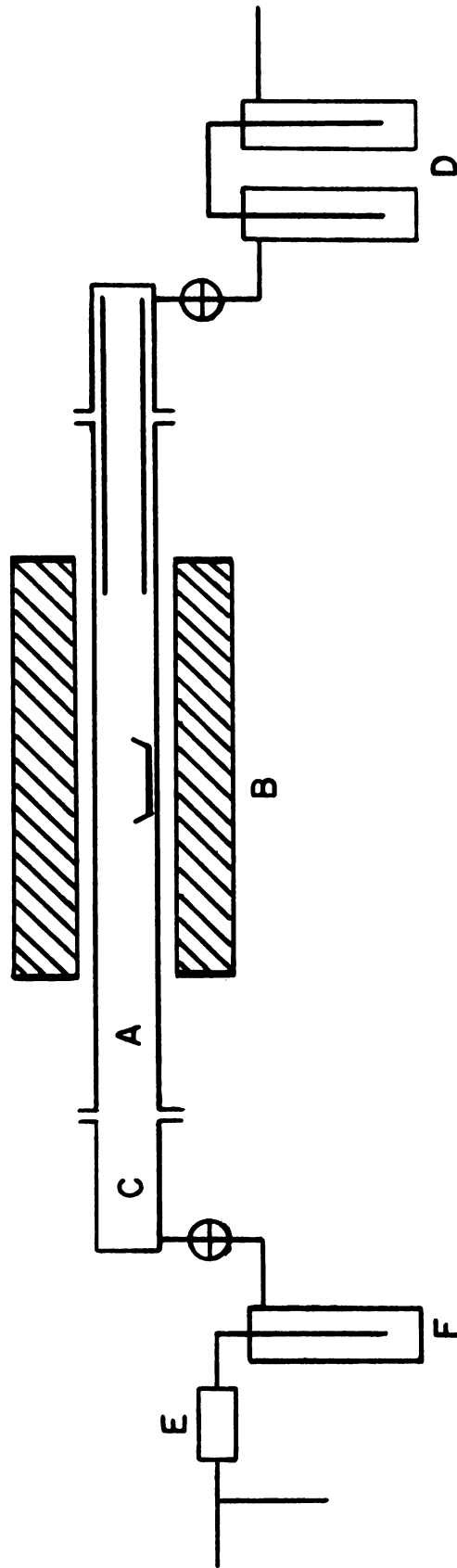
Figure 1.  Experimental Arrangement for Gas-Solid Reactions

Experimental details on the preparation of the various europium

compounds are described in the following sections.

### 4.4.1.  $EuCl_2$

Europium(II) chloride was prepared by hydrogen reduction of anhydrous

europium(III) chloride.  The latter was prepared from 99.9% pure $Eu_2O_3$

by the method of Taylor and Carter (5).  The trichloride, contained in

a vitreous carbon boat, was reduced _in situ_ at temperatures up to 750°C

with a stream of dry hydrogen.  The product was cooled under hydrogen

and isolated into the argon-filled glove box where all further handlings

were made.

The crude $EuCl_2$ was subsequently distilled in an out-gassed high

density graphite assembly (Figure 2).  Distillation was effected by

inductive heating to $\sim$ 1400°C in high vacuum (< $10^{-5}$ torr).  The

distilled $EuCl_2$ collected on the sides and lid of the secondary graphite

cell; no obvious residue remained in the primary vitreous carbon container.

The distillation assembly was removed into the glove box for subsequent

storage of the pure product.

### 4.4.2.  $EuI_2$

Anhydrous europium(II) iodide was prepared by a modification of the

method of Taylor and Carter (5).  The molecularly dispersed mixture of

hydrated $EuI_3$ and $NH_4I$ was dried over conc. $H_2SO_4$ in a vacuum dessicator.

The dried cake, contained in a vitreous carbon boat and situated in the

Vycor flow apparatus, was heated slowly to $\sim$ 650°C in a stream of

helium dried by passage through traps of $P_2O_5$ and liquid nitrogen.  A

final heating at this temperature for about 4 hours yielded a greenish

colored melted product in the carbon boat.
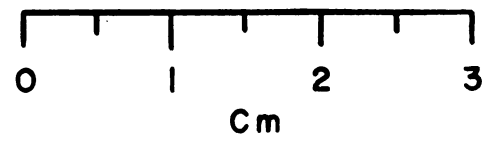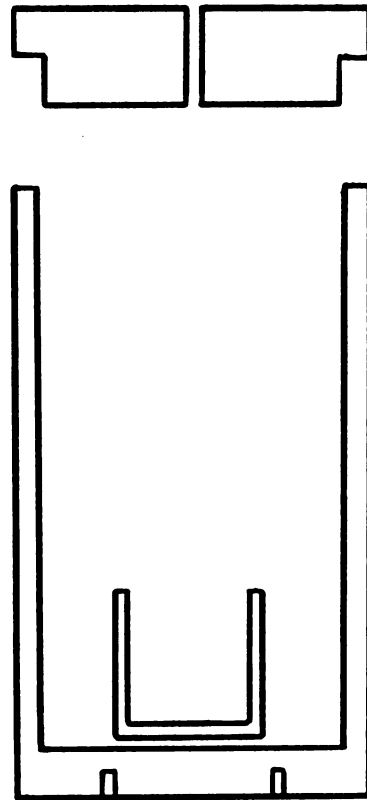
Figure 2.   Graphite Distillation Assembly for $EuCl_2$ and $EuI_2$

Distillation of the impure product was carried out as described for EuCl$_2$ at $\sim$ 1200°C.

### 4.4.3. EuS

Europium monosulfide was prepared by direct reaction of Eu$_2$O$_3$, confined in a quartz boat, with gaseous H$_2$S at $\sim$ 1200°C/8 hours. The product was cooled under the H$_2$S stream and later annealed at $\sim$ 500°C in a 10$^{-6}$ torr vacuum to remove adsorbed gases.

### 4.4.4. EuSe

Europium monoselenide was prepared by the reaction of anhydrous europium(III) chloride with H$_2$Se. EuCl$_3$ prepared as described in Sec. 4.4.1 was reacted in situ with dry H$_2$Se at $\sim$ 750°C/2 hours. There was appreciable deposition of elemental selenium on the inside of the reaction tube. At the end of the reaction period the product was cooled under a stream of H$_2$Se-He and later out-gassed at $\sim$ 800°C in a 10$^{-6}$ torr vacuum to remove adsorbed H$_2$Se and Se.

### 4.5. X-Ray Powder Diffraction Analysis

Powder diffraction patterns of as-prepared samples of EuCl$_2$, EuI$_2$, EuS and EuSe, and residues from the vaporization and weight-loss experiments were routinely obtained with a Haegg Type Guinier forward-focussing camera (radius 80 mm) and Cu K$\alpha_1$ radiation, $\lambda\alpha_1$ = 1.54051 Å, t = 24 $\pm$ 1°C. The X-radiation source was a fine focus X-ray tube powered by a Picker 809 B generator.

Sample preparation, film measurement and Guinier techniques have been reported elsewhere (161,162). Hygroscopic materials such as EuCl$_2$ were protected by a thin film of sodium-dried paraffin oil. Extremely

moisture-sensitive samples such as $EuI_2$ were totally sealed in a 2-mil thick PVC bag. Platinum powder served as an internal standard ($a_o$ = 3.9238 ± 0.0003 $\overset{o}{A}$) and permitted correction for film shrinkage and other experimental characteristics.

## 4.6. Analytical

As-prepared samples of $EuCl_2$, $EuI_2$, EuS and EuSe were analyzed for europium and the respective anion contents by conventional analytical methods. Since all the binary compounds used in this work were purified materials, the more direct hydroxide precipitation method for europium assay was utilized instead of the oxalate method. Except in the case of $EuI_2$, the europium and anion contents were analyzed in separately weighed samples. All analytical samples were weighed inside the argon-filled glove box.

### 4.6.1. Europium

The hydroxide precipitation method and assay as $Eu_2O_3$ (163) was utilized to estimate the europium content of the samples. The acid solution of the europium compound ($HNO_3$ or HCl) containing $\sim$ 100 mg Eu in $\sim$ 100 ml was heated to near boiling. Carbonate-free ammonium hydroxide (1:1 v/v) was added dropwise until precipitation was complete. Concentrated $NH_4OH$ was then added to $\sim$ 10% of the solution volume. The gelatinous precipitate was digested for $\sim$ 1 hour at near boiling until the precipitate flocked and settled. It was then cooled, filtered, washed 10X with a solution containing 2 w/v percent $NH_4Cl$ and 10 v/v percent $NH_4OH$. The filter paper and precipitate were dried and ignited to constant weight at $\sim$ 900°C in a platinum crucible.

Samples of EuS and EuSe in acid solutions were repeatedly evaporated to low bulk to remove the possibly interfering $H_2S$ or $H_2Se$ before analysis for europium began. A few drops of nitric acid in the dissolution medium ensured complete oxidation of Eu(II) to Eu(III).

### 4.6.2. Chloride

Chloride contents of $EuCl_2$ samples were analyzed by the gravimetric AgCl method (164,165). To the cold dilute nitric acid solution of $EuCl_2$ an excess of 0.5 M silver nitrate solution was added slowly with stirring. After complete precipitation, the slurry was heated until the precipitate coagulated. It was then settled overnight, filtered through a weighed Pyrex sintered glass crucible, washed with dilute $HNO_3$ until free of $Ag^+$, dried at 140-150°C and weighed.

### 4.6.3. Iodide

The $EuI_2$ samples were dissolved in a cold 1 v/v percent HCl medium. Iodide was determined in the filtrate from the europium analysis by the palladous iodide method (164,165). After excess ammonia had been removed, the solution was neutralized with HCl until an excess of 1% by volume was present. A solution of $PdCl_2$ was then added until precipitation was complete. After the slurry had settled for 48 hours, it was filtered on a weighed Pyrex sintered glass crucible, washed repeatedly with hot water and finally once with alcohol, dried at 90°C and weighed as $PdI_2$.

### 4.6.4. Sulfur

The sulfur content of europium monosulfide samples was determined by wet oxidation to sulfate and assay as $BaSO_4$ (164). A 100-150 mg EuS sample was dissolved in ice-cold 10-30 ml $Br_2$-KBr solution (prepared by dissolving 160 g KBr in minimum distilled water, adding 100 ml $Br_2$ and

diluting to 1000 ml with distilled water). After about 10 min, 10-25 ml conc. $HNO_3$ was added and the solution cleared. It was then heated to near dryness, extracted with 3 M HCl, and the sulfate in solution was precipitated by the "reverse precipitation" method with a 3 M HCl solution of barium chloride. After precipitation was complete, the solution was digested, allowed to settle overnight, filtered, washed with 0.05 M HCl until free of $Ba^{2+}$, dried and ignited in a porcelain crucible at 800-900°C.

The "reverse precipitation" method in a 2-3 M HCl medium is reported to minimize interference by +3 valent cations (164).

### 4.6.5. Selenium

The selenium content of europium monoselenide samples was analyzed by the gravimetric sulfur dioxide method (164,165). Samples of EuSe were dissolved in aqua regia in a closed system to form selenious acid. The clear solution was evaporated 3X to fumes with $H_2SO_4$ to remove all nitric acid. Addition of a few milligrams of solid sulfamic acid at this stage ensured destruction of any remaining nitrate ion. After extraction with 50 ml 8-9 M HCl, the solution was cooled to 15-20°C and a concentrated solution of sodium metabisulfite was added to precipitate elemental selenium. After digestion at this temperature, 1-2 ml of a 20 w/v percent hydroxylamine hydrochloride was also added and the precipitate allowed to settle overnight. It was then filtered on a weighed Pyrex sintered glass crucible, washed with 9 M HCl and then sequentially with cold water and hot water to convert the red amorphous Se to the black granular form, and finally with alcohol. The selenium was dried at 105°C and weighed.

Attempts to analyze EuSe samples by direct dissolution in conc. HCl or in an $H_2SO_4$-$HNO_3$ acid mixture in open containers were unsuccessful; appreciable amounts of selenium were lost as $H_2Se$ during dissolution. Use of aqua regia substantially mitigated loss of $H_2Se$, and dissolution in a closed vessel ensured recovery of even those traces that did escape.

## 4.7. Mass Spectrometry

A Bendix Model 12-107 time-of-flight mass spectrometer equipped with a high temperature Knudsen source was used to obtain the mass spectra and identify the vapor species in equilibrium with $EuI_2(l)$, EuS(s) and EuSe(s). Non-symmetric effusion cells with channeled orifices of the design described by Pilato (166) were heated by radiation and electron bombardment. The spectrometer was operated in the pulsed ionization mode and ionizing energies of 25-30 eV were employed while spectra of the various parent and fragmentation species were monitored. Temperatures of the effusion channels were measured with an optical pyrometer by directly sighting the hot cavity through the spectrometer window and an external glass prism. Absorption corrections for the optical elements were applied to all of the temperature readings.

Ion intensities at the various mass values were considered as the total height of the peak over the clearly defined background spectra. Thus the intensities were only of comparative value.

Appearance potentials of the species $EuI_2^+/EuI_2$, $EuI^+/EuI_2$, $Eu^+/EuI_2$, $Eu^+/EuS$ and $Eu^+/EuSe$ were determined; Hg, $N_2$ and $H_2O$ served as references. The shutterability of the several peaks from each material was checked mainly at the lowest and highest temperatures.

## 4.8.  Target Collection Equipments and Procedures

### 4.8.1.  Target Collection Apparatus

The general design of the target collection apparatus used in the high temperature vaporization experiments was similar to that described by Ackermann et al. (125) and Kent (167).  However, three different apparatus were utilized during the course of this work:

(a)  An all-Vycor apparatus pumped with a 5 cm mercury diffusion pump and capable of $< 10^{-6}$ torr.  The target magazine was cooled with liquid nitrogen.  This equipment was used for the vaporization of EuS.

(b)  A design basically similar to (a), but with the introduction of a demountable Pyrex section between the main water-cooled Vycor heating chamber and the liquid nitrogen-cooled target magazine.  This apparatus was used for the $EuCl_2$ and $EuI_2$ studies.

(c)  An all-metal target collection apparatus designed by Seiver (168) was utilized for the vaporization of EuSe.  This equipment was pumped directly with a 10 cm oil diffusion pump and could be evacuated to $\sim 10^{-8}$ torr.  The water-cooled target magazine, of circular design, carried eleven targets and a sight hole and was moved mechanically through a Wilson-type "O"-ring rotary seal.

### 4.8.2.  Effusion Cells

The effusion cells used in the target collection experiments were of the symmetric design with knife-edge orifices described by Haschke (155). These were fabricated from high density graphite, tungsten and molybdenum. The 45° beveled effusion orifices varied from 0.4 to 1.0 mm diameter, while the similar blackbody hole was maintained $\sim 1.0$ mm in diameter.

The cells had L/D $\sim$ 1 (L is the length and D the diameter of the main body of the sample cavity). Orifice areas were determined from enlarged photomicrographs (X80,X100 and X200; Bausch and Lomb Dynazoom Metallograph) by measuring the area with a compensating polar planimeter (Keuffel and Esser Co.). The effusion cells were outgassed for $\sim$ 8 hours in $10^{-6}$ torr at temperatures which were at least 200°C above those in the subsequent vaporization experiments. The effusion and blackbody holes were then reamed before the cell assembly was used in an experiment.

### 4.8.3. Targets

Targets for vapor deposition were fabricated from stock copper and were 2.70 cm in diameter and 0.46 cm thick with a 2.08 X 0.19 cm cylindrical recession on the collection side. The targets were degreased with 1.1.1. trichloroethane, washed with conc. HCl, polished with fine steel wool, washed with distilled water and acetone, and oven-dried at 110°C before use.

### 4.8.4. Target to Cell Distance

The vertical distance between the target and the effusion orifice was measured with a precision cathetometer (Gaertner Scientific Co., readability 0.005 cm) only after the experimental assembly had been pumped down to $\sim$ $10^{-6}$ torr with liquid nitrogen in the target magazine dewar. A set of three cathetometer readings of the target end and cell surface were made alternately. To the mean measured distance was added the target recess (0.190 cm) to obtain the orifice to target surface distance. When the cell was enclosed in the oven (sec. 4.8.5), the cell surface could not be sighted directly. A well-defined mark on the overn surface was sighted instead, and a correction was obtained for

the cell surface to the oven mark.  This distance was measured with a precision vernier calipers (readability 0.005 cm) at the end of the experiment.

### 4.8.5.  Effusion Cell Heating

The Knudsen effusion cells were heated to the experimental temperatures by two different techniques with a push-pull type 250-kHz 20-kva Thermonic high frequency induction generator.  The metallic effusion cells coupled directly with the 14-turn induction coil positioned symmetrically to the cell.  The graphite effusion cells were heated by radiation from an inductively heated tungsten-molybdenum oven.  The design and configuration of the latter assembly is depicted in Figure 3. A 0.47 cm diameter hole in the oven cover offered no resistance to the beam which effused from the well-aligned effusion cell.  The suitability of such a system in the determination of vapor pressures and derived thermochemical values was confirmed by a redetermination of the vapor pressure of silver in the temperature range 1242-1570 K (Appendix 1).

### 4.8.6.  Temperature Measurements

Temperatures were measured by sighting the blackbody hole in the effusion cells with National Bureau of Standards-calibrated disappearing filament optical pyrometers (serial numbers:  1524388, 1572579, Leeds and Northrup).  These instruments were also intercompared with another NBS-calibrated instrument (serial number:  16404444; 1948 IPTS).  Wien's law correction factors for absorption by the window and prism were determined from pyrometer readings of a tungsten filament lamp at the strip V with and without the optical elements.  The average $\Delta$ (equation 3—17) ranged around - $1.30000 \cdot 10^{-5}$ $K^{-1}$ during the course of this work in which a total of 8 calibrations were made.
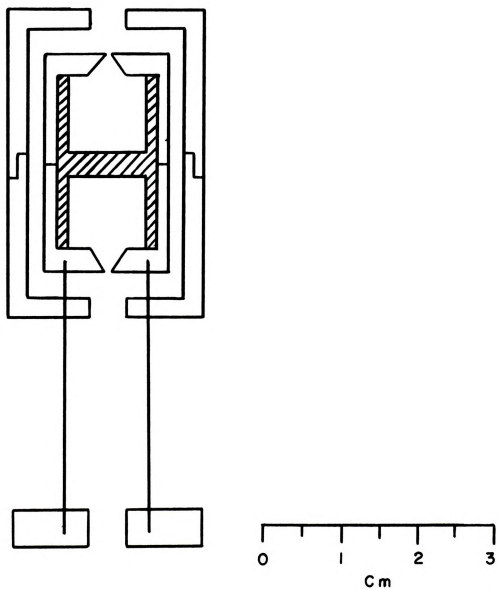
Figure 3.  Graphite Knudsen Cell in Oven Arrangement

Additionally, the temperatures of the orifice and blackbody hole were frequently compared to ensure that the induction coil was located properly with respect to the metallic cells and the oven so that no measurable temperature gradient occurred along the cell or oven assembly.

### 4.8.7. Typical Target Collection Procedure

The general target collection procedure used in this laboratory has been described by Kent (167) and Haschke (155). Normally 0.15-0.25 g samples were used in each vaporization experiment and approximately 20-25% of this material vaporized. Hygroscopic samples of $EuCl_2$ and $EuI_2$ were loaded into the effusion cell in the argon-atmosphere glove box and were protected at the cell sides and orifice with drops of sodium-dried paraffin oil. The cell was then located symmetrically in the oven. The entire assembly on a boron nitride table was brought out of the glove box in a ground-glass covered weighing bottle and assembled quickly in the vaporization apparatus. The whole operation to the start of evacuation normally took less than a minute. At the conclusion of the experiment, the system was brought to atmospheric pressure with cylinder argon and the cell assembly returned immediately to the glove box using the weighing bottle. Samples of EuS and EuSe were loaded into the cells in the glove box, but the subsequent handling in the vaporization apparatus did not prove to be critical.

The ten targets in each experiment provided data at increasing and decreasing temperatures. Each time the temperature was changed, 10-15 min were allowed for cell equilibrium to be achieved. Temperatures remained within 2°C during exposures of up to 2 hrs, but drifts of as much as 5°C were common during exposure times of 4-6 hrs. When drastic

temperature excursions occurred during target exposure, that target was omitted from the data collection.

Orifice areas remained almost constant in every vaporization experiment. An average value of the effusion orifice area, obtained from measurements of the orifice before and after the experiment, was utilized in the calculations.

Target exposure times which were measured with a laboratory timer were adjusted to provide $\sim$ 4-10 micrograms of europium on each target. They were assayed for europium by X-ray fluorescence immediately at the conclusion of the vaporization experiment.

## 4.9. X-Ray Fluorescence Analysis

The calibration technique and analytical procedure utilized in X-ray fluorescence have been amply discussed by Haschke (155) and Work (120). Only a few pertinent details will be discussed here.

Targets from the EuS vaporization experiments were analyzed on a Siemens Goniometer with a 4b spectrometer attachment. The X-radiation source was a broad focus tungsten tube powered by a Siemens Kristalloflex IV generator. The Eu L$\beta$1 radiation ($\lambda$ = 1.920 $\overset{\circ}{A}$) was analyzed with a LiF crystal at the peak maximum of $2\theta$ = 56.94° and a water-cooled NaI(Tl) scintillation counter. The spectrometer was optimized for microgram quantities of europium on copper targets according to the criteria of Neff (169). The pulse height was set at 5.5 v and the channel width at 10 v for a 20 min counting.

Targets from the vaporization of $EuCl_2$, $EuI_2$ and EuSe were analyzed on a 4-position Norelco Universal Vacuum spectrograph. A Norelco XRG-5000 X-ray generator powered the broad focus tungsten tube. The Eu L$\alpha$1 radiation ($\lambda$ = 2.120 $\overset{\circ}{A}$) was analyzed with a graphite crystal at

the peak maximum of $2\theta = 36.84°$ with a NaI(Tl) scintillation counter.
A pulse height of 1.9 v and channel width of 5.0 v was utilized for a
1 min counting.

Additionally, the I L$\alpha$1 ($\lambda = 3.148$ Å) was also optimized with an
EDDT crystal in conjunction with a flow proportional counter that used
Ar/10% CH$_4$ (P-10) gas. The optimum setting for the peak maximum,
$2\theta = 41.88°$, utilized a pulse height of 1.8 v and channel width of 2.7 v
for a 100 sec counting. The target material, as in all the europium
analyses, was copper.

The selected spectral peaks for europium and iodine were free from
background interferences and were routinely reproducible. At the
beginning of a calibration or analysis schedule, the required spectral
peak was scanned within a 3° region of its $2\theta$ value three times with
amounts of the element comparable to those expected on the targets, and
the spectrometer was locked in the peak maximum position.

Standard solutions for europium calibration were prepared by
volumetrically diluting a stock solution (conc. 5.0 mg Eu/ml in dilute
hydrochloric acid) to the desired concentration ranges of 2 to 12 µg
Eu/50 µl. A set of 7 to 10 different dilute solutions were used. Aliquots
measuring 50 µl of these solutions along with the pipet washings
(3 X 25 µl dilute HCl) were delivered carefully and uniformly onto
precounted targets within an area of 2 cm$^2$. To provide reasonably
uniform deposits on the defined target area it was necessary to deliver
very small droplet volumes and evaporate immediately under an infrared
lamp. By careful practice it became possible to distribute the volume
of the standard solution over the target surface.

To insure maximum counting precision a normalized procedure was followed throughout the course of this work. Sets of five blank targets were initially counted between the counting of a control blank target. Similarly the calibration or exposed targets were counted in sets of five between the counting of the control blank and a control standard target. The latter contained $\sim$ 8 µg Eu and was prepared by volumetric transfer. Each target was counted three times; the count rate was reproducible to within one standard deviation. This counting procedure permitted all experimental targets to be corrected to a net standard europium count rate, thus affording a correction factor for the day-to-day drift of the equipment that was inevitable. The count rate for typical calibration targets was within +5% for the range of 2 to 12 µg Eu. An occasionally abnormal count rate could be traced to non-uniform deposition on the target; data from such targets were omitted. The calibration was linear in the above-mentioned range.

During the course of this study the scintillation detector decayed steadily. It was therefore necessary to calibrate the europium count rate frequently, and this procedure interposed sets of vaporization experiments to realize the corresponding calibration number.

In all the calibration and vaporization targets the area exposed to the X-ray beam was defined precisely and reproducibly to 2.0 cm$^2$ with a circular 45° beveled copper insert. The targets were also rotated while counting to offset any non-uniformity in the beam or deposit.

## 4.10. Sticking Coefficient Experiment

The sticking coefficients of gaseous Eu and EuBr$_2$ on liquid nitrogen-chilled copper targets have been shown to be $\sim$ 1 (155). However, as was mentioned in Section 4.8.1, vaporization experiments with EuSe

utilized water-cooled copper targets. A 2 hr vaporization at 2075 K of a sample of EuSe confined in a molybdenum cell (orifice $9.641 \cdot 10^{-3}$ $cm^2$) was performed to determine the sticking coefficient of Eu(g) on such targets. The effusing beam was defined with a 0.994 $cm^2$ collimator that was 1.11 cm away from the main water-cooled copper target. A separate 0.125 mm thick copper annulus, 2.08 cm o.d. and 1.23 cm i.d. (1.188 $cm^2$), rested over the collimator assembly and was cooled by conduction from the walls of the equipment. Europium that did not condense/stick on the main copper target would be scattered in measurable fraction onto the annulus. At the conclusion of the vaporization the precounted annulus was removed carefully from the collimator assembly and assayed for europium by X-ray fluorescence.

CHAPTER 5

RESULTS AND DATA REDUCTION


5.1. Preparative

   5.1.1. $EuCl_2$

Preparations in the flow apparatus yielded white melted chunks

of pure anhydrous europium(II) chloride. Crystals of distilled $EuCl_2$

exhibited a faint reddish brown tinge, but the powder was white. The

intensities of the powder diffraction lines were compared with those

generated by the program ANIFAC from the lattice and positional

parameters of orthorhombic $EuCl_2$ (32,170). The agreement was good.

   5.1.2. $EuI_2$

The preparation of europium(II) iodide by the method of Taylor and

Carter (5) was more difficult than anticipated. During evaporation of

the hydrated $EuI_3$ and excess $NH_4I$ over a hot plate copious amounts of

free iodine were liberated. There was evidence of the formation of

europium(III) oxide iodide even at temperatures below 150°C in air.

After two unsuccessful attempts to prepare the hydrated $EuI_3-NH_4I$

matrix in this manner, it was decided to dry the wet material over

conc. $H_2SO_4$ in a vacuum dessicator. The dried cake was utilized in the

two preparations that yielded pure $EuI_2$. During the initial heating of

the matrix in dry helium, appreciable amounts of free iodine were liberated

at < 150°C, an indication of the instability of $EuI_3$. The final product,

$EuI_2$, melted in the vitreous carbon boat into a greenish mass. Distilled $EuI_2$ had a yellow coloration; the powder was also light yellow. The powder diffraction intensities and lattice parameters compared favorably with those reported for monoclinic $EuI_2$ (171).

### 5.1.3. EuS

The two different preparations of europium(II) monosulfide yielded dark brownish-black samples which appeared insensitive to the laboratory atmosphere.

### 5.1.4. EuSe

The single preparation of europium(II) monoselenide gave a pure dark khakhi-colored sample. It was also air insensitive at room temperature.

## 5.2. Analytical

The results of the wet chemical and X-ray diffraction analyses of $EuCl_2$, $EuI_2$, EuS and EuSe are given in Tables 4 and 5. Analyses of the pure samples were always performed in duplicate. X-Ray diffraction patterns of the residues from each vaporization were only compared with the master film for positions and intensities of the diffraction lines.

## 5.3. Weight-Loss Experiments

Total weight-loss of materials from typical Knudsen effusion cells are carried out to establish two important aspects: (a) the nature of the vaporization process - congruent or incongruent, and (b) the extent, if any, of the interaction of the sample at high temperatures with the cell material.

Table 4.  **Chemical Analytical Results**

| Material | Calculated (%) | | Found (%) | |
|---|---|---|---|---|
| $EuCl_2$ | Eu: | 68.18 | Eu: | $68.1_1 \pm 0.2_1$ |
| | Cl: | 31.82 | Cl: | $31.8_0 \pm 0.0_2$ |
| $EuI_2$ | Eu: | 37.46 | Eu: | $37.5_2 \pm 0.2_0$ |
| | I: | 62.54 | I: | $62.3_7 \pm 0.0_6$ |
| EuS | Eu: | 82.58 | Eu: | $82.1_9 \pm 0.4_3$ |
| | S: | 17.42 | S: | $17.4_0 \pm 0.1_2$ |
| EuSe | Eu: | 65.81 | Eu: | $66.0_3 \pm 0.2_4$ |
| | Se: | 34.19 | Se: | $34.1_5 \pm 0.2_0$ * |

* Estimated error in a single determination.

Table 5.  <u>X-Ray Diffraction Results</u>

(a)  $EuCl_2$:  Orthorhombic $PbCl_2$ Structure, Space Group Pbnm.

$$a = 8.957 \pm 0.009 \overset{\circ}{A}$$

$$b = 7.526 \pm 0.006 \overset{\circ}{A}$$

$$c = 4.501 \pm 0.006 \overset{\circ}{A}$$

(b)  $EuI_2$:  Monoclinic, Space Group P $2_1/c$.

$$a = 7.632 \pm 0.009 \overset{\circ}{A}$$

$$b = 8.251 \pm 0.006 \overset{\circ}{A}$$

$$c = 7.907 \pm 0.007 \overset{\circ}{A}$$

$$\beta = 98.09 \pm 0.07°$$

(c)  EuS:  Face centered cubic NaCl Type, Space Group Fm3m.

$$a = 5.963 \pm 0.001 \overset{\circ}{A}$$

(d)  EuSe:  Face centered cubic NaCl Type, Space Group Fm3m.

$$a = 6.196 \pm 0.001 \overset{\circ}{A}$$

<u>Note</u>:  Indicated uncertainties are calculated standard errors in the

least squares fit.

### 5.3.1. $EuCl_2$

In view of the information (65) that graphite is an inert and impervious container for $EuCl_2(l)$ and that the vaporization of the dichloride is congruent, no independent weight-loss experiment was performed.

### 5.3.2. $EuI_2$

An experiment specifically designed to check for weight-loss of $EuI_2(l)$ from graphite effusion cells was not performed. However a sample of $EuI_2$ confined in a graphite cell was vaporized to total depletion during collection of the mass spectrometric data. The final weight of the cell confirmed the absence of interaction between $EuI_2(l)$ and graphite.

### 5.3.3. EuS

Two samples of EuS were vaporized _in toto_ at 1823 K and 1998 K from a molybdenum effusion cell. No interaction was observed between the sample and the molybdenum or the tungsten effusion cells used subsequently for the vaporization experiments.

### 5.3.4. EuSe

Total weight-loss of EuSe contained in a tungsten effusion cell at 1973 K and partial evaporation from molybdenum cells used in subsequent vaporization experiments indicated no interaction of EuSe with these cell materials.

## 5.4. Mass Spectrometric Results

### 5.4.1. $EuCl_2$

No mass spectrometric investigation of the vapor species over $EuCl_2(l)$ was carried out in this work. However, Hastie et al. (65) reported congruent vaporization of $EuCl_2(l)$ and only the ions $EuCl_2^+$, $EuCl^+$ and $Eu^+$ appear in the mass spectrum at an ionizing electron energy of 50 eV. There was no evidence of either gaseous $EuCl_3$ or dimeric $Eu_2Cl_6$ species in the temperature range 1143-1291 K. They report the following relative ratios, $EuCl_2^+:EuCl^+:Eu^+ \sim 12:100:46$ at 1218 K and 50 eV and appearance potentials, $EuCl_2^+/EuCl_2 = 10.5 \pm 0.5$ eV; $EuCl^+/EuCl_2 = 10.3 \pm 0.5$ eV, and $Eu^+/EuCl_2 = 15.0 \pm 0.5$ eV. Their data indicate that all three ions derive from the common molecular precursor, $EuCl_2$, and all have an enthalpy of vaporization of $\sim 61 \pm 1$ kcal $gfw^{-1}$.

### 5.4.2. $EuI_2$

Mass spectrometric data for the vapor species over $EuI_2(l)$ indicated the parent molecular vapor to be entirely $EuI_2(g)$, which then fragmented to $EuI^+$ and $Eu^+$. No gaseous $EuI_3$ was observed. The relative intensities of the ions in the temperature range 1237-1345 K were $EuI_2^+:EuI^+:Eu^+ \sim 34:100:81$ at 30 eV electron energy. The appearance potentials were determined as $EuI_2^+/EuI_2 = 8.8_5 \pm 0.2_0$ eV; $EuI^+/EuI_2 = 9.9_0 \pm 0.2_0$ eV, and $Eu^+/EuI_2 = 12.4_5 \pm 0.2_0$ eV. The ion intensity-temperature data indicated all three ions were derived from the common molecular precursor, $EuI_2(g)$, with an enthalpy of vaporization of $\sim 66$ kcal $gfw^{-1}$ at 1291 K.

### 5.4.3. EuS

Mass spectrometric analysis of the vapor species in equilibrium with condensed EuS(s) was carried out in the temperature range 1998-2273 K.

Only shutterable peaks assignable to $Eu^+$, $S^+$ and $S_2^+$ were detected at a 25 eV ionizing electron energy over the entire temperature range. Mass peaks assignable to $EuS^+$ were not detected even when the ionizing energy was varied from a minimum of 4 to a maximum of 30 eV. The appearance potential of $Eu^+/EuS$ was determined to be $5.9_0 \pm 0.2_0$ eV, a value that corresponds very well to the first ionization potential of europium ($5.66_4 \pm 0.00_8$ eV; Ref. 172) and indicates that the primary vapor species is $Eu(g)$. A plot of $\ln I^+_{Eu}T$ vs $1/T$ (one Mo and one W cell; 24 data points) yielded an average enthalpy of $102._5 \pm 6._0$ kcal $gfw^{-1}$. The intensities of $S^+$ and $S_2^+$ ions were not determined as a function of temperature due to the generally high background in these mass regions.

### 5.4.4. EuSe

A mass spectrometric investigation of the vapor species in equilibrium with condensed EuSe(s) was carried out in the temperature range 1914-2118 K. Here again only shutterable masses assignable to $Eu^+$, $Se^+$ and $Se_2^+$ were detected at 25-30 eV ionizing electron energies. Peaks attributable to $EuSe^+$ were not observed in the mass spectrum in the entire temperature range with 4-30 eV ionizing energies. The appearance potential of $Eu^+/EuSe$ was determined as $5.8_5 \pm 0.2_5$ eV, an indication that $Eu^+$ is the primary species as in the case of EuS. The $\ln I^+_{Eu}T$ vs $1/T$ plot (one W cell; 16 data points) gave an average enthalpy of $98._2 \pm 4._6$ kcal $gfw^{-1}$. The intensities of $Se^+$ and $Se_2^+$ were not determined.

### 5.5. Sticking Coefficient of Europium on Water-Cooled Copper Targets

The 0.125 mm thick annulus from the sticking coefficient experiment (sec. 4.10) contained $0.1_1$ µg eu. The total amount of europium that struck the main water-cooled copper target was computed as $70.4_6$ µg Eu.

On the assumption that the effusate not condensed on the main target will be reemitted according to the cosine distribution through the collimator, the fraction that strikes the 0.125 mm annulus is calculated as $0.1_0$ (118). These data indicate better than 98.5% for the collection efficiency of the primary water-cooled copper target, or a sticking coefficient of $\sim 1$. This result is in good correspondence with the earlier documented data on the sticking coefficient of Eu(g) and $EuBr_2$(g) on liquid nitrogen-chilled copper (64,155).

## 5.6. Vaporization Results and Data Treatments

In the following sections the experimental vaporization results are presented, followed by a thermodynamic treatment of the data. Details of the calculations and sources of auxiliary thermochemical data are included as appropriate. The general pattern of estimating the composite of errors in the second- and third-law treatment of the experimental data has been discussed under section 3.10. Nominal uncertainties of $\pm 1._0$ eu for the standard entropy, $S°_{298}$, of the condensed phases and $\pm 1._0$ kcal $gfw^{-1}$ for the enthalpy of fusion have been uniformly ascribed to their estimates. Appropriate error estimates for the heat capacities and derived thermal functions for the condensed and vapor phases were also considered in the overall data reduction.

### 5.6.1. Europium(II) Chloride

The X-ray diffraction analysis of the residues from the vaporization experiments always indicated only the orthorhombic $EuCl_2$. This observation and the mass spectral data (sec. 5.4.1) established congruent vaporization according to

$$EuCl_2(l) = EuCl_2(g). \tag{5-1}$$

Graphite, which has been used successfully as a container material in the high temperature vaporization of $EuBr_2$ (64) and $SrCl_2$ (173), proved to be impervious and non-reactive to liquid $EuCl_2$.

Five independent vaporization experiments (1135-1569 K; 49 data points) were performed and the pertinent details are presented in Table 6.

Table 6. $EuCl_2$ Vaporization Experiments

| Expt No | Effusion Orifice $(X10^3)$ | Temp Range |
|---------|----------------------------|------------|
| 1 | 5.54 $cm^2$ | 1288-1436 K |
| 2 | 5.54 | 1244-1375 |
| 3 | 7.28 | 1135-1256 |
| 4 | 1.17 | 1409-1563 |
| 5 | 1.17 | 1412-1569 |

The vapor pressure-temperature data are tabulated in Appendix 2-A and represented graphically in Figure 4 by a plot of log $P_{EuCl_2(g) \text{ atm}}$ $\underline{vs}$ $1/T$. An unweighted linear least squares treatment yielded equation (5-2) with its associated standard deviations,

$$\ln P_{EuCl_2(g)atm} = -(354_{22} \pm 1_{50})/T + 15.9_1 \pm 0.1_1. \tag{5-2}$$

At the median temperature, 1352 K, $\Delta H° = 70.3_9 \pm 0.3_0$ kcal $gfw^{-1}$ and $\Delta S° = 31.6_2 \pm 0.2_2$ eu.

Thermodynamic functions for $EuCl_2$ were derived as follows. From published heat capacities of $Sr(\alpha)$, $Ba(\alpha)$, $Eu(s)$ and isostructural $SrCl_2(s)$ and $BaCl_2(s)$ (35,174-176), the heat capacity of $EuCl_2(s)$ at 298.15 K was estimated as $18.1_3 \pm 0.1_5$ eu. At the melting point of $EuCl_2$ (1000 K) the heat capacity is estimated as $21.7_5$ eu (sec. 3.8.1.1). On the assumption that the variation of $C°_p$ is linear in this temperature range, the heat
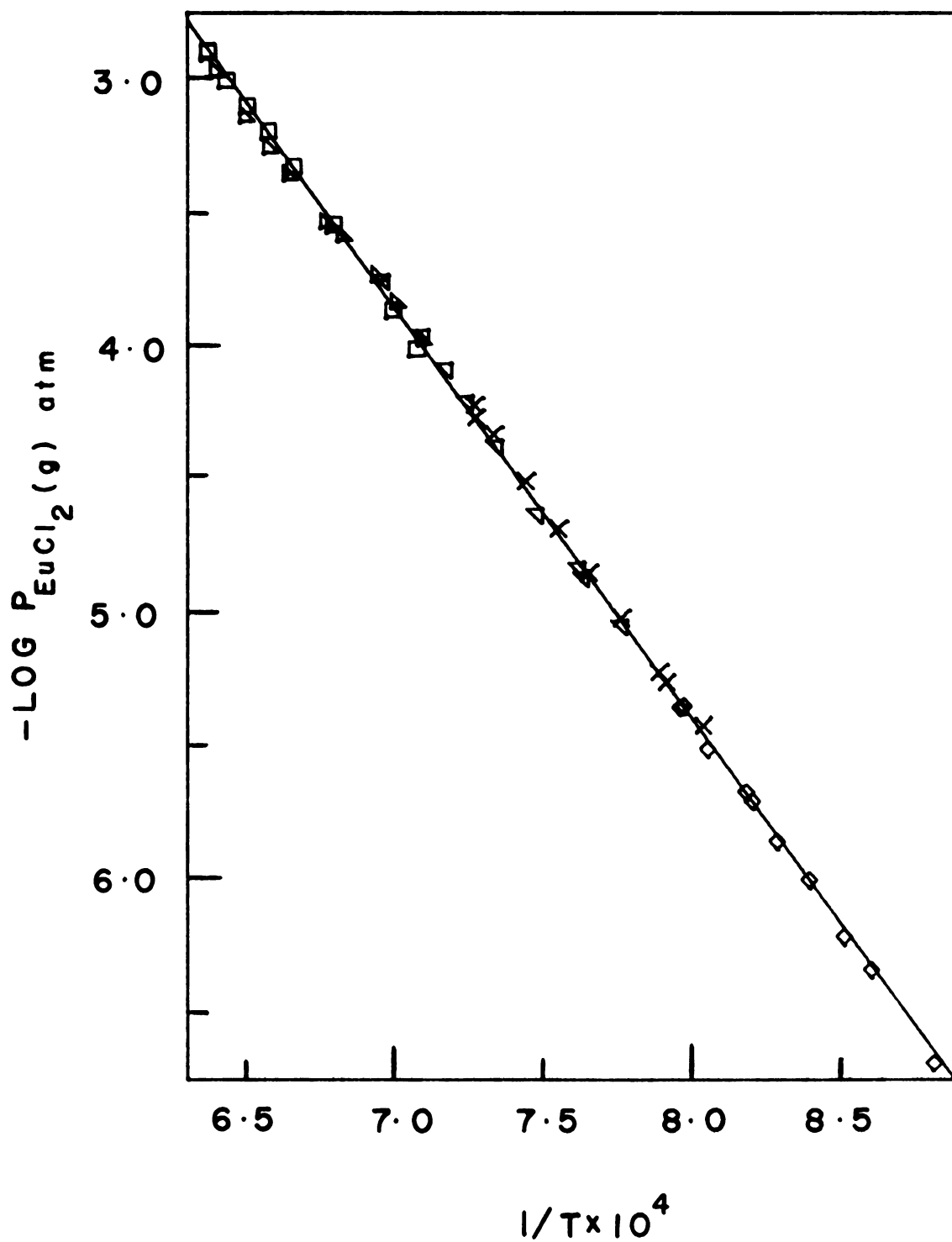
Figure 4. Logarithm of the Pressure of $EuCl_2(g)$ in Equilibrium with $EuCl_2(l)$ versus Reciprocal Temperature. Runs 1 ($\triangledown$), 2 ($X$), 3 ($\diamondsuit$), 4 ($\triangle$) and 5 ($\boxdot$).

capacity of $EuCl_2(s)$ may be represented by

$$C^\circ_p[EuCl_2(s)] = (16.5_9 \pm 0.1_5) + 5.1_6 \times 10^{-3} \text{ T} \qquad (5\text{-}3)$$

$$(298\text{-}1000 \text{ K}).$$

For $EuCl_2(1)$ a heat capacity of $25.6 \pm 0.7$ eu has been estimated by analogy with the published data for $BaCl_2(1)$ (42,177), and was assumed constant over the entire liquid range. For the solid-liquid transformation, $\Delta H^\circ_{fus} = 6._0 \pm 1._0$ kcal $gfw^{-1}$ and $\Delta S^\circ_{fus} = 6._0 \pm 1._0$ eu at 1000 K are estimated (38). A standard entropy, $S^\circ_{298}[EuCl_2(s)] = 34._5 \pm 1._0$ eu, was estimated (156) from additive contributions of 14.1 eu for Eu(II), 8.1 eu for $Cl^-$ associated with a divalent cation, and 4.2 eu for the magnetic entropy of Eu(II) (158). The derived thermodynamic functions for $EuCl_2(1)$ are given in Table 7. An uncertainty of $\pm 1._4$ eu, which originates primarily from uncertainties in the standard entropy and $\Delta S^\circ_{fus}$, is calculated in the free energy functions for $EuCl_2(1)$.

The molecular constants obtained by Hastie, Hauge and Margrave (88) were used for the derivation of the thermal functions of $EuCl_2(g)$. These values are: $Cl\text{-}Eu\text{-}Cl = 135 \pm 10^\circ$; $Eu\text{-}Cl = 2.6_7 \pm 0.0_5$ Å; $\omega_1 = 280 \pm 5$ $cm^{-1}$; $\omega_2 = 64 \pm 10$ $cm^{-1}$ and $\omega_3 = 290 \pm 5$ $cm^{-1}$. A statistical weight of 16 for the ground state electronic partition function is also included (sec. 2.5). The derived thermal functions are presented in Table 8. On the assumption that the statistical weight may be in error by a factor of 2, the uncertainty in the free energy functions is estimated as $\pm 1._5$ eu.

Reduction of the second-law data with the thermal functions listed in Tables 7 and 8 give for the sublimation reaction (5-4):

$$EuCl_2(s) = EuCl_2(g), \qquad (5\text{-}4)$$

Table 7. Thermodynamic Functions for $EuCl_2(\ell)$

| T | $C^\circ_p$ | $S^\circ_T$ | $H^\circ_T - H^\circ_{298}$ | $- FEF$ |
|---|---|---|---|---|
| 298.15 K | 18.13 eu | 40.50 eu | 0.0 cal gfw$^{-1}$ | 40.50 eu |
| 1000 | 25.60 | 64.20 | 13994.4 | 50.20 |
| 1200 | 25.60 | 68.87 | 19114.4 | 52.94 |
| 1400 | 25.60 | 72.81 | 24234.4 | 55.50 |
| 1600 | 25.60 | 76.23 | 29354.4 | 57.88 |

Table 8. Thermodynamic Functions for $EuCl_2(g)$

| T | $C^\circ_p$ | $S^\circ_T$ | $H^\circ_T - H^\circ_{298}$ | $- FEF$ |
|---|---|---|---|---|
| 298.15 K | 13.32 eu | 81.24 eu | 0.0 cal gfw$^{-1}$ | 81.24 eu |
| 1000 | 13.85 | 97.80 | 9634.4 | 88.16 |
| 1200 | 13.87 | 100.32 | 12407.1 | 89.99 |
| 1400 | 13.88 | 102.46 | 15182.5 | 91.62 |
| 1600 | 13.89 | 104.32 | 17959.6 | 93.09 |

$$H^\circ_{298} - H^\circ_0 = 3427.1 \text{ cal gfw}^{-1}$$

$\Delta H^\circ_{298} = 84._9 \pm 1._1$ kcal gfw$^{-1}$ and $\Delta S^\circ_{298} = 48._3 \pm 1._8$ eu. Average $\Delta C^\circ_p$ values for the sublimation (5-4) and vaporization (5-1) reactions are computed as $-(6.3_5 \pm 0.1_6)$ eu and $-(11.7_0 \pm 0.7_1)$ eu, respectively. The free energy change for the vaporization reaction (5-1) is represented by

$$\Delta G^\circ_T = (862_{08} \pm 8_{11}) - (127.6_7 \pm 0.8_6)T + (11.7_0 \pm 0.7_1)T \ \ell n \ T$$

$$(1000 \ K - bp). \qquad\qquad (5-5)$$

At the extrapolated boiling point of $2335 \pm 35$ K, $\Delta H^\circ_v = 58._9 \pm 1._8$ kcal gfw$^{-1}$ and $\Delta S^\circ_v = 25.2 \pm 0.7$ eu.

The free energy functions (Tables 7 and 8) were combined with the experimental pressure-temperature values to give the third-law data for reaction (5-1): $\Delta H^\circ_{298} = 76._7 \pm 2._5$ kcal gfw$^{-1}$; $\Delta S^\circ_{298} = 40._7 \pm 1._8$ eu, and for reaction (5-4): $\Delta H^\circ_{298} = 82._7 \pm 2._7$ kcal gfw$^{-1}$; $\Delta S^\circ_{298} = 46._7 \pm 2._1$ eu, with no observable temperature trend in the enthalpy values (Appendix 2-A).

The standard entropy, $S^\circ_{298}[EuCl_2(s)]$, computed from the second-law entropy change for reaction (5-4) and $S^\circ_{298}[EuCl_2(g)]$, is $32._9 \pm 2._4$ eu (cf. estimated: $34._5 \pm 1._0$ eu).

The vaporization enthalpy values were combined with the published data for the enthalpy of formation of $EuCl_2(s)$ (45), enthalpy of sublimation of Eu(s) (178), and the dissociation energy of chlorine (179) to give $D^\circ_0[EuCl_2(g)] = 209._8 \pm 1._5$ kcal gfw$^{-1}$ ($D^\circ_{298} = 210._8 \pm 1._5$ kcal) and $D^\circ_0[EuCl_2(g)] = 212._0 \pm 2._8$ kcal gfw$^{-1}$ ($D^\circ_{298} = 213._0 \pm 2._8$ kcal), respectively, by use of the second- and third-law derived enthalpies of sublimation of $EuCl_2(s)$.

## 5.6.2. Europium(II) Iodide

The invariant nature of the X-ray diffraction patterns of the vaporization residues, total vaporization of a typical sample from a graphite effusion cell, and the mass spectral data (sec. 5.4.2.) indicate congruency of vaporization according to

$$EuI_2(l) = EuI_2(g). \tag{5-6}$$

As with $EuCl_2$, graphite was a suitable container material for liquid $EuI_2$.

Four independent vaporization experiments (1086-1395 K; 40 data points) were performed with $EuI_2$ and are detailed in Table 9. The vapor pressure-temperature data (Appendix 2-B) give the unweighted linear least squares equation (5-7) with the associated standard deviations:

$$\ln P_{EuI_2(g)atm} = -(315_{52} \pm 1_{69})/T + 16.0_2 \pm 0.1_4. \tag{5-7}$$

In Figure 5 is depicted the log $P_{EuI2(g)atm}$ $\underline{vs}$ 1/T plot of the data. At the median temperature, 1241 K, $\Delta H° = 62.7_0 \pm 0.3_4$ kcal gfw$^{-1}$ and $\Delta S° = 31.8_3 \pm 0.2_7$ eu.

Table 9. $EuI_2$ Vaporization Experiments

| Expt No | Effusion Orifice ($X10^3$) | Temp Range |
|---------|------------------------------|------------|
| 1 | 4.45 cm$^2$ | 1203-1310 K |
| 2 | 1.07 | 1286-1395 |
| 3 | 5.85 | 1086-1197 |
| 4 | 4.45 | 1194-1277 |

Thermodynamic functions for $EuI_2$ were derived in the following manner. From published data for the heat capacities of $Sr(\alpha)$, $Eu(s)$ and $SrI_2(s)$ (35,175), the heat capacity of $EuI_2(s)$ at 298.15 K is estimated as
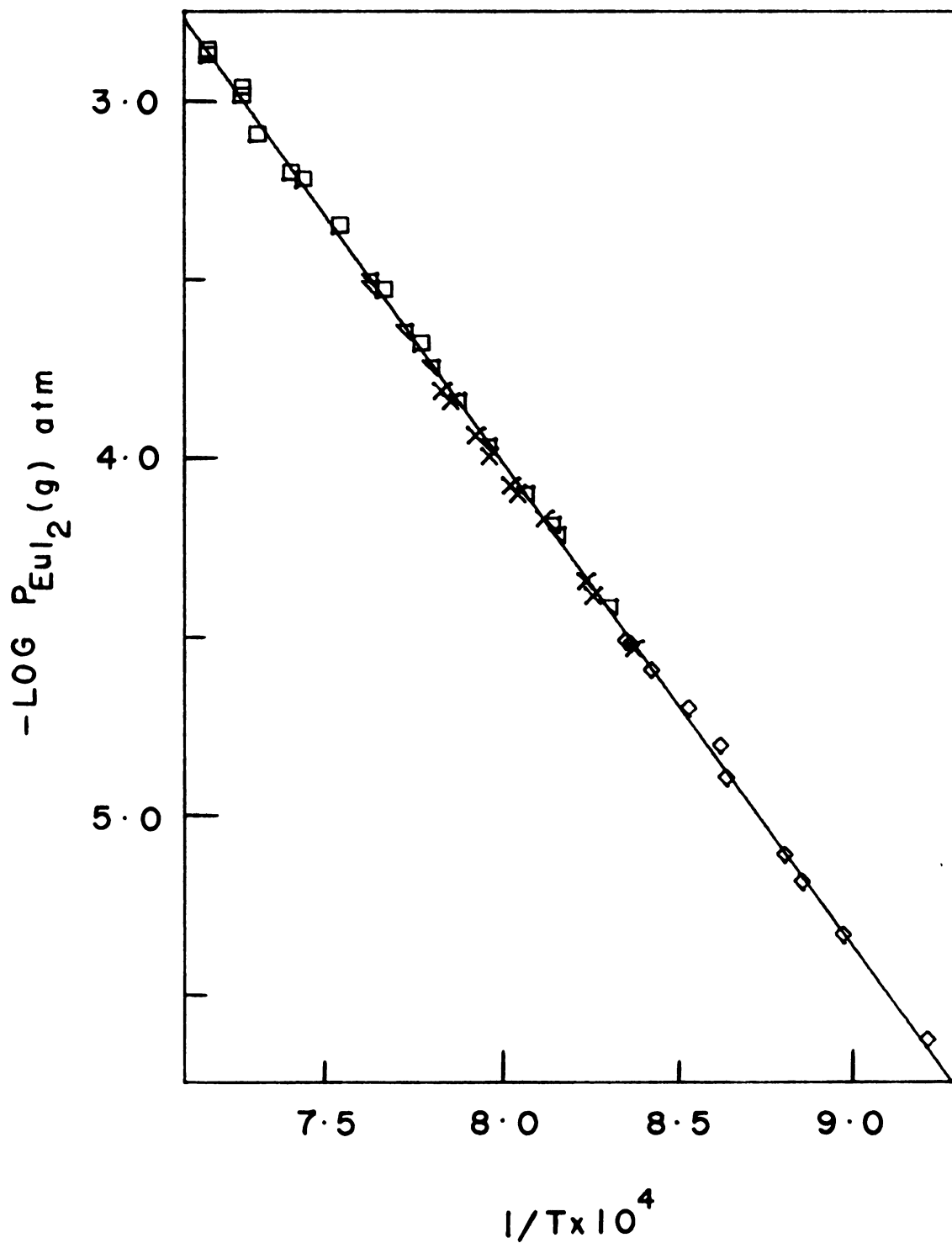
Figure 5. Logarithm of the Pressure of $EuI_2(g)$ in Equilibrium with
$EuI_2(l)$ versus Reciprocal Temperature. Runs 1 ($\triangledown$), 2 ($\boxdot$),
3 ($\diamondsuit$) and 4 ($\times$).

$19.8_2 \pm 1._0$ eu. Together with a value of $21.7_5$ eu at the melting point (853 K) (sec. 3.8.1.1), the linear equation (5-8) is derived for the heat capacity of $EuI_2(s)$.

$$C^\circ_p[EuI_2(s)] = (18.7_8 \pm 0.1_0) + 3.4_8 \times 10^{-3} \; T$$

$$(298-853 \; K) \hspace{3cm} (5-8)$$

For $EuI_2(l)$ a heat capacity of $26.3 \pm 0.7$ eu has been estimated by analogy with published data for $SrI_2(l)$ and $BaI_2(l)$ (42), and was assumed constant over the entire liquid range. For the solid-liquid transformation at 853 K, $\Delta H^\circ_{fus} = 5._0 \pm 1._0$ kcal gfw$^{-1}$ and $\Delta S^\circ_{fus} = 5._9 \pm 1._2$ eu are estimated (38). The standard entropy, $S^\circ_{298}[EuI_2(s)]$, was computed in two ways by (a) combining the values for the Eu(II) ion, its magnetic contribution and $I^-$ associated with a divalent cation (12.2 eu; Kelley in Ref. 153), $S^\circ_{298} = 42._7 \pm 1._0$ eu, and by (b) using the estimated and derived values for the standard entropy of $EuCl_2(s)$ in equation (3-44), $S^\circ_{298} = 41._2 \pm 2._2$ eu. A weighted average of these estimates, $41._6 \pm 1._0$ eu, was used in the calculations. The free energy functions derived for $EuI_2(l)$ are presented in Table 10. An overall uncertainty of $\pm 1._6$ eu is estimated in these values.

Molecular constants for $EuI_2(g)$ were derived as follows. By analogy with the geometry of $SrI_2(g)$ (180,181), $EuI_2(g)$ is believed to be a linear molecule. The Eu-I bond distance is estimated as $3.0_0 \pm 0.0_5$ Å, which is $0.2_8$ Å less than the sum of the cation and anion crystal radii. The vibrational frequencies were evaluated by the valence force field approximation with estimated stretching and bending force constants for $EuI_2$. In this procedure the triatomic stretching force constant, $k_1$, was assumed equal to the diatomic force constant, $k_e$. In addition, the

bending force constant, $k\delta/l^2$, was considered as 1% $k_1$, in accordance with those used for $CaI_2$, $SrI_2$ and $BaI_2$ (182). The vibrational frequency and the force constant for EuI were interpolated from a linear least squares fit of $\omega_e^2$ (diatomic) versus the inverse of the reduced mass of CaI, SrI and BaI (183): $\omega_e(EuI) = 145$ $cm^{-1}$; $k_e(EuI) = 0.857$ $md/\overset{\circ}{A}$. The derived values for the triatomic $EuI_2$ are: $\omega_1 = 107$ $cm^{-1}$; $\omega_2 = 25$ $cm^{-1}$ (doubly degenerate), and $\omega_3 = 175$ $cm^{-1}$. Individual error estimates for the vibrational frequencies were not made, but the overall errors in the estimated molecular constants are assumed to contribute an uncertainty of $\pm 1._0$ eu to the entropy of the gas. A statistical weight of 16 has also been assumed for the ground state electronic partition function. The derived thermodynamic functions are presented in Table 11. The uncertainty in the free energy functions are estimated as $\pm 1._7$ eu, the composite of the contributions from the errors in the molecular constants and the statistical weight.

Reduction of the second-law data with the thermodynamic functions listed in Tables 10 and 11 gave for sublimation reaction (5-9):

$$EuI_2(s) = EuI_2(g), \qquad (5-9)$$

$\Delta H°_{298} = 75._4 \pm 1._1$ kcal $gfw^{-1}$ and $\Delta S°_{298} = 48._1 \pm 1._9$ eu. Average $\Delta C°_p$ values for the solid-vapor (5-9) and liquid-vapor (5-6) transitions computed as $-(5.9_8 \pm 0.1_1)$ eu and $-(11.4_1 \pm 0.7_1)$ eu, respectively. The free energy change for the vaporization reaction (5-6) is represented by

$$\Delta G°_T = (768_{61} \pm 7_{45}) - (124.5_3 \pm 0.8_9)T + (11.4_1 \pm 0.7_1)T \ell n T$$
$$(853-bp). \qquad (5-10)$$

Table 10.  Thermodynamic Functions for $EuI_2(l)$

| T | $C^\circ_p$ | $S^\circ_T$ | $H^\circ_T - H^\circ_{298}$ | $-$ FEF |
|---|---|---|---|---|
| 298.15 K | 19.82 eu | $47._{50}$ eu | 0.0 cal gfw$^{-1}$ | $47._{50}$ eu |
| 853 | 26.30 | $69._{17}$ | 11531.5 | $55._{65}$ |
| 1000 | 26.30 | $73._{35}$ | 15397.6 | $57._{96}$ |
| 1200 | 26.30 | $78._{15}$ | 20657.6 | $60._{93}$ |
| 1400 | 26.30 | $82._{20}$ | 25917.6 | $63._{69}$ |

Table 11.  Thermodynamic Functions for $EuI_2(g)$

| T | $C^\circ_p$ | $S^\circ_T$ | $H^\circ_T - H^\circ_{298}$ | $-$ FEF |
|---|---|---|---|---|
| 298.15 K | 14.74 eu | $88._{46}$ eu | 0.0 cal gfw$^{-1}$ | $88._{46}$ eu |
| 853 | 14.88 | $104._{05}$ | 8237.8 | $94._{40}$ |
| 1000 | 14.89 | $106._{42}$ | 10426.2 | $95._{99}$ |
| 1200 | 14.89 | $109._{14}$ | 13404.6 | $97._{96}$ |
| 1400 | 14.90 | $111._{43}$ | 16383.8 | $99._{73}$ |

$$H^\circ_{298} - H^\circ_0 = 4018.5 \text{ cal gfw}^{-1}$$

At the extrapolated boiling point of $2048 \pm 25$ K, $\Delta H^\circ_v = 53._5 \pm 1._6$ kcal gfw$^{-1}$ and $\Delta S^\circ_v = 26.1 \pm 0.7$ eu.

The thermodynamic functions were combined with the experimental pressure-temperature data to give for reaction (5-6): $\Delta H^\circ_{298} = 68._9 \pm 2._9$ kcal gfw$^{-1}$; $\Delta S^\circ_{298} = 41._0 \pm 2._3$ eu, and for reaction (5-9): $\Delta H^\circ_{298} = 73._9 \pm 3._1$ kcal gfw$^{-1}$; $\Delta S^\circ_{298} = 46._9 \pm 2._6$ eu. No observable temperature dependency of the third-law enthalpy data is noticed (Appendix 2-B). The large error in the derived thermochemical values is a reflection of the uncertainties in the free energy functions of $EuI_2(l)$ and $EuI_2(g)$.

The standard entropy, $S^\circ_{298}[EuI_2(s)]$, calculated from the second-law entropy change for reaction (5-9) and $S^\circ_{298}[EuI_2(g)]$, is $40._4 \pm 2._6$ eu (cf. estimated: $41._6 \pm 1._0$ eu).

### 5.6.3. Europium(II) Monosulfide

Total weight-loss data, invariance of the X-ray diffraction patterns of partially evaporated samples and mass spectrometric results (sec. 5.4.3) indicate congruent vaporization of EuS according to

$$EuS(s) = Eu(g) + S(g). \tag{5-11}$$

On the assumption that the sensitivity of the mass spectrometer to $EuS^+$ is comparable to that of $Eu^+$, the absence of an $EuS^+$ species in the observed mass spectra implies that at 2000 K the partial pressure of the gaseous molecule is $< 3\%$ of that of $Eu(g)$. This upper limit (of 3%) was deduced from the minimum spectral peak that could be isolated from the background spectra in $EuS^+$ mass region.

Since the experimental vaporization targets were analyzed only for europium, an effective pressure, $P_E$, is defined by equation (5-12) which

is based on the effusion equation (3-10):

$$P_{E,atm} = 1/44.33 \ A_o tF \cdot T^{1/2} \cdot Z_{Eu} \cdot M_{Eu}^{1/2} \tag{5-12}$$

with $M_{Eu}$ the atomic weight and $Z_{Eu}$ the number of moles of europium. The steady state effusate from the Knudsen cell, however, consists of Eu(g), EuS(g), S(g) and $S_2$(g). The calculated effective pressure, $P_E$, may be related to the partial pressures of Eu(g) and EuS(g) according to

$$P_E = P_{Eu} + P_{EuS} \cdot (M_{Eu}/M_{EuS})^{1/2}. \tag{5-13}$$

Equation (5-13), where $M_{EuS}$ is the molecular weight of EuS, follows directly from (5-12) in view of the fact that the total number of moles of europium, $Z_{Eu}$, on each target could only be those from Eu and EuS. Because there was no definite evidence for molecular species in the vapor, $P_E$ was assumed equal to $P_{Eu}$ in the treatment of the experimental data. This approximation could introduce a maximum correction of no more than 2.65% to the computed $P_{Eu}$.

Seven independent vaporization experiments were performed from tungsten effusion cells. These are detailed in Table 12.

Table 12.  EuS Vaporization Experiments

| Expt No | Effusion Orifice (X10$^3$) | Temp Range |
|---|---|---|
| 1 | 4.86 cm$^2$ | 2068-2221 K |
| 2 | 4.86 | 1925-2067 |
| 3 | 4.89 | 1837-2035 |
| 4 | 4.85 | 2090-2222 |
| 5 | 4.84 | 1968-2083 |
| 6 | 8.58 | 1801-2044 |
| 7 | 1.80 | 2063-2212 |

An unweighted linear least squares treatment of the 67 vapor pressure-temperature data points (Appendix 2-C) yielded equation (5-14) with its associated standard deviations.

$$\ln P_{Eu(g)atm} = -(529_{90} \pm 4_{30})/T + 14.9_1 \pm 0.2_1 \qquad (5-14)$$

The pressure of EuS(g) to the maximum extent of 3% $P_{Eu}$ would contribute no more than an error of $-0.02_7$ in the intercept of equation (5-14).

Congruent vaporization of EuS(s) requires that the number of moles of Eu(g) effusing from the cell be equal to the number of moles of sulfur according to

$$Z_{Eu} = Z_S + 2Z_{S_2}. \qquad (5-15)$$

Hence the partial pressures of Eu(g), S(g) and $S_2$(g) inside the Knudsen cell will be related according to

$$P_{Eu(g)}/M_{Eu}^{1/2} = P_{S(g)}/M_S^{1/2} + 2\, P_{S_2(g)}/M_{S_2}^{1/2}. \qquad (5-16)$$

By introduction of the gas phase equilibrium constant, $K_S$, for the dissociation of sulfur according to

$$S_2(g) = 2\, S(g); \quad K_S = P^2_{S(g)}/P_{S_2(g)}, \qquad (5-17)$$

one obtains

$$P_{S(g)} = P_{Eu(g)} \cdot (M_S/M_{Eu})^{1/2} - 2\, P^2_{S(g)}/K_S \cdot (M_S/M_{S_2})^{1/2}. \qquad (5-18)$$

Knowing $K_S$ and a value of $P_{Eu(g)}$, one can compute $P_{S(g)}$ by solving the quadratic equation (5-18). The equilibrium constant, $K_S$, was computed from the free energy functions and enthalpies of formation of S(g) and

$S_2(g)$ $[\Delta H^\circ_{f,298}[S(g)] = 66.6_8 \pm 0.5_0$ kcal gfw$^{-1}$; $\Delta H^\circ_{f,298}[S_2(g)] =$
$30.8_4 \pm 0.2_0$ kcal gfw$^{-1}$, Ref. 179].

The linear least squares equation for $\ln P_{S(g)atm}$ derived from the
experimental $P_{Eu(g)}$ and temperature values is given by

$$\ln P_{S(g)atm} = -(529_{87} \pm 3_{26})/T + 13.7_4 \pm 0.1_6 \qquad (5-19)$$

Over the measured temperature range of 1801-2222 K, $P_{S(g)}$ averaged
$\sim 30.9\%$ of $P_{Eu(g)}$, while the pressure of the $S_2(g)$ species in the
equilibrium gas phase was $\sim 33-34\%$ of $P_{S(g)}$.

The combined least squares equation for the equilibrium constant, K,
for the congruent vaporization reaction (5-11) is given by

$$\ln K = -(1059_{77} \pm 5_{40})/T + 28.6_5 \pm 0.2_6, \qquad (5-20)$$

where the standard deviations include the uncertainties in the thermal
functions for S(g) and $S_2(g)$.

The experimental vapor pressure-temperature data are represented
graphically by the plot of log $P_{Eu(g)atm}$ vs 1/T in Figure 6. At the
median temperature (2011 K) the following thermodynamic values are
calculated for reaction (5-11) from equation (5-20): $\Delta H^\circ = 210._6 \pm$
$1._1$ kcal gfw$^{-1}$, $\Delta S^\circ = 56.9_4 \pm 0.5_3$ eu.

The second-law values were reduced to 298.15 K with thermal functions
reported for Eu(g) (184) and S(g) (179), and estimated for EuS(s) as
follows. From the component elements (35,179) $C^\circ_p$ for condensed EuS
was calculated as $11.9_9 \pm 0.0_6$ eu at 298.15 K. From the approximation
that the heat capacity is $7.2_5$ eu/g atom at the melting point (sec.
3.8.1.1) and an estimate of 2473 K for the latter (by comparison with
the melting points of other lanthanide monosulfides) the following heat
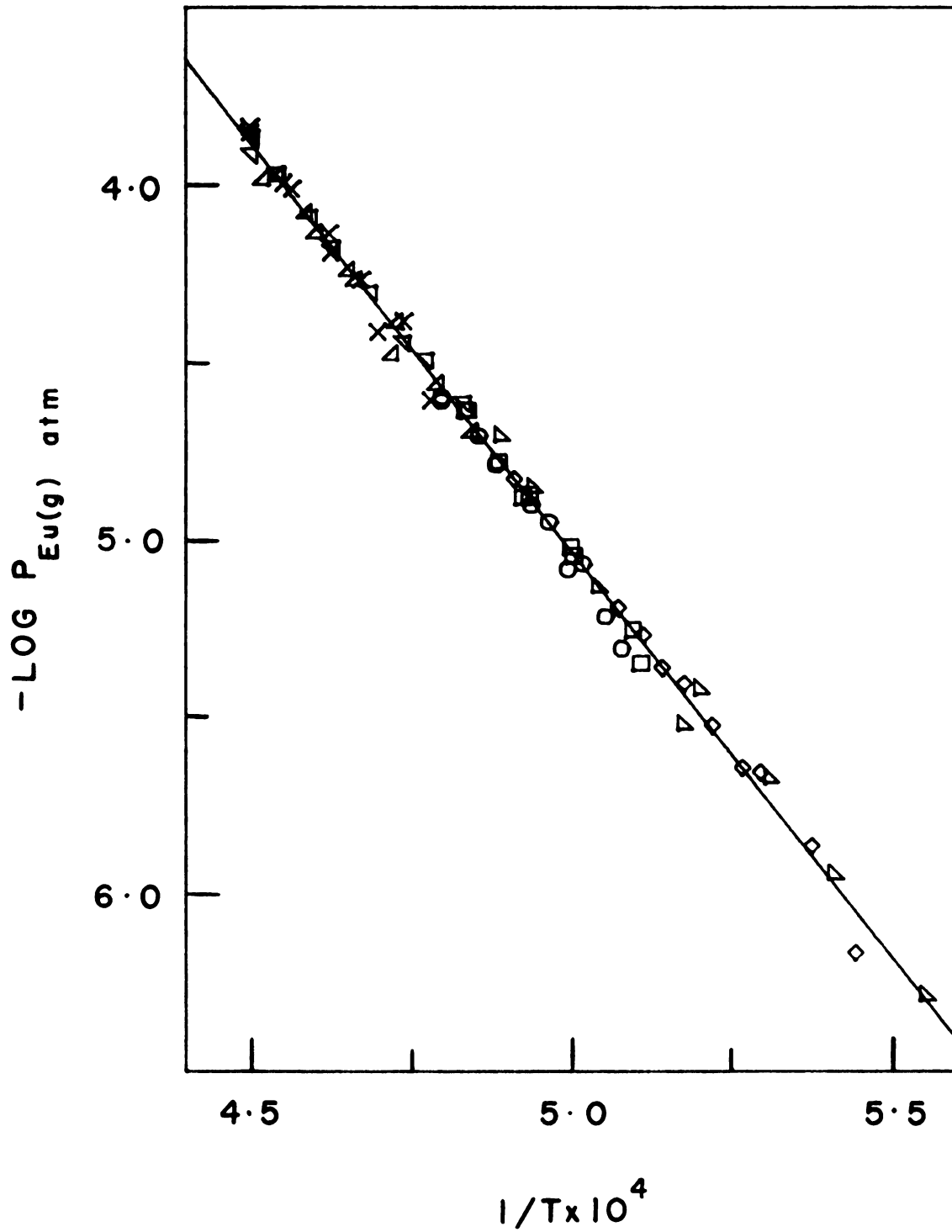
Figure 6. Logarithm of the Pressure of Eu(g) in Equilibrium with
EuS(s) versus Reciprocal Temperature. Runs 1 (▽),
2 (⊡), 3 (◇), 4 (✗), 5 (⊙), 6 (△) and 7 (◁).

capacity equation (5-21) was derived for EuS(s):

$$C^\circ_p \ EuS(s) \ = (11.6_5 \pm 0.0_6) + 1.1_5 \ X \ 10^{-3} \ T \qquad (5\text{-}21)$$

$$(298\text{-}2473 \ K).$$

The standard entropy was computed from the values for Eu(II), its magnetic contribution and $S^{2-}$ associated with a divalent cation ($5._0$ eu; Ref. 156) to give $S^\circ_{298}$ [EuS(s)] $= 23._3 \pm 1._0$ eu. The derived thermodynamic functions for EuS(s) are given in Table 13. An uncertainty of $\pm 1._2$ eu is estimated in the free energy functions.

The second-law thermodynamic values for reaction (5-11) together with the estimated error which results from the data reduction are: $\Delta H^\circ_{298} = 215._4 \pm 1._2$ kcal gfw$^{-1}$; $\Delta S^\circ_{298} = 61.6 \pm 0.9$ eu. These values were combined with the enthalpies and entropies of formation of Eu(g) (35,178,184) and S(g) (179) to yield for the formation of EuS(s), $\Delta H^\circ_{f,298} = -(106._7 \pm 1._3)$ kcal gfw$^{-1}$ and $\Delta S^\circ_{f,298} = -(2.8 \pm 0.9)$ eu.

The standard entropy, $S^\circ_{298}$[EuS(s)], calculated from the entropies of Eu(g) (184) and S(g) (179) and the second-law entropy change for reaction (5-11) is $23.6 \pm 0.9$ eu.

The experimental pressure-temperature data for reaction (5-11) were combined through the equilibrium constant with published values for the free energy functions of Eu(g) (184) and S(g) (179) and those derived for EuS(s) (Table 13) to give the third-law enthalpy, $\Delta H^\circ_{298} = 216._1 \pm 2._9$ kcal gfw$^{-1}$, with no temperature dependency in the individual values (Appendix 2-C).

### 5.6.4. Europium(II) Monoselenide

A congruent vaporization mode for EuSe(s) according to equation (5-22) is indicated from the weight-loss data, the invariant nature of the X-ray diffraction patterns of the residues from vaporizations, and the
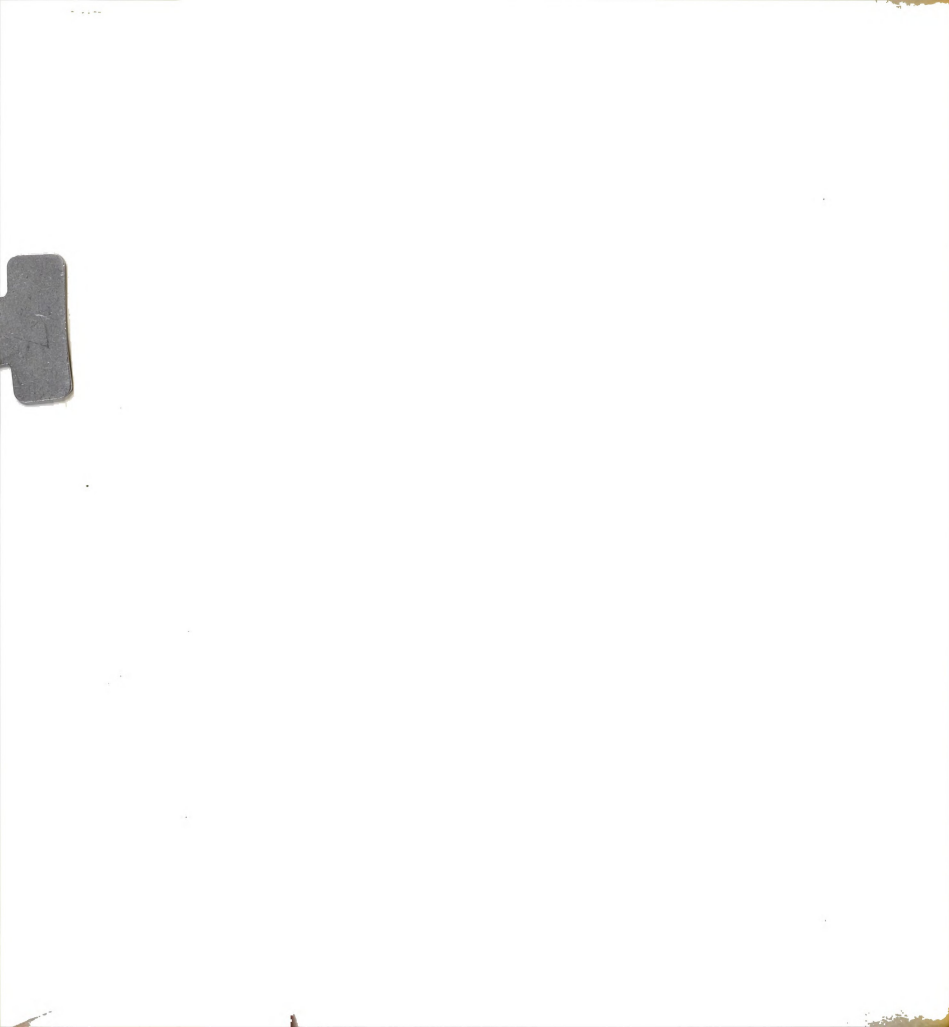
Table 13. <u>Thermodynamic Functions for EuS(s)</u>

| $T$ | $C^\circ_p$ | $S^\circ_T$ | $H^\circ_T - H^\circ_{298}$ | $-$ FEF |
|---|---|---|---|---|
| 298.15 K | 11.99 eu | $23._{30}$ eu | 0.0 cal gfw$^{-1}$ | $23._{30}$ eu |
| 1700 | 13.61 | $45._{19}$ | 17942.2 | $34._{64}$ |
| 1900 | 13.84 | $46._{72}$ | 20686.8 | $35._{83}$ |
| 2100 | 14.07 | $48._{11}$ | 23477.6 | $36._{93}$ |
| 2300 | 14.30 | $49._{40}$ | 26314.6 | $37._{96}$ |

mass spectral results (sec. 5.4.4).

$$EuSe(s) = Eu(g) + Se(g) \qquad (5-22)$$

Mass spectral peaks assignable to $EuSe^+$ were not detected in the temperature range 1914-2118 K. Subsequently, Gordienko et al. (82) reported a mass spectrometric study of the decomposition of EuSe(s) in the range 1665-1910 K and concluded that the intensity ratio, $I^+_{Eu}/I^+_{EuSe}$, was > 1000, in agreement with our observation. Therefore, no contribution of the molecular species was considered in the treatment of the experimental data.

Three independent vaporization experiments were performed from molybdenum effusion cells. These are detailed in Table 14.

Table 14. EuSe Vaporization Experiments

| Expt No | Effusion Orifice $(X10^3)$ | Temp Range |
|---------|----------------------------|------------|
| 1 | 9.64 $cm^2$ | 1808-1967 K |
| 2 | 4.35 | 1947-2067 |
| 3 | 4.36 | 2078-2131 |

An unweighted linear least squares analysis of the 30 experimental data points (Appendix 2-D) yielded equation (5-23) with its associated standard deviations.

$$\ell n \ P_{Eu(g)atm} = -(520_{13} \pm 4_{42})/T + 14.6_4 \pm 0.2_2 \qquad (5-23)$$

By use of methods analogous to those described for EuS (sec. 5.6.3), the partial pressure of Se(g) in equilibrium with Eu(g) and $Se_2(g)$ was computed. The dissociation equilibrium constant, $K_{Se}[Se_2(g) = 2 \ Se(g)]$,

was calculated from the free energy functions for Se(g) (185), $Se_2$(g)
(81) and the dissociation energy, $D^°_0[Se_2(g)] = 78.6_3 \pm 0.0_3$ kcal gfw$^{-1}$
($D^°_{298} = 79.3_1 \pm 0.0_3$ kcal). The latter value corresponds to the
highest of the three spectroscopic values suggested by Barrow et al.
(186) and confirmed by Berkowitz in photoelectron spectroscopic studies
(187). The least squares $\ln P_{Se(g)atm}$ vs 1/T equation derived from
the experimental $P_{Eu(g)}$ and computed $K_{Se}$ values is given by

$$\ln P_{Se(g)atm} = -(519_{47} \pm 4_{39})/T + 14.2_7 \pm 0.2_2. \qquad (5\text{-}24)$$

In the temperature range of study, $P_{Se(g)}$ averaged $\sim$ 69% of $P_{Eu(g)}$,
while the pressure of the $Se_2$(g) species in the equilibrium gas phase
was only 0.3-0.6% of $P_{Se(g)}$.

The combined least squares equation for the equilibrium constant, K,
for reaction (5-22) is given by

$$\ln K = -(1039_{59} \pm 6_{23})/T + 28.9_0 \pm 0.3_1, \qquad (5\text{-}25)$$

where the standard deviations include the uncertainties in the thermal
functions for Se(g) and $Se_2$(g).

The experimental log $P_{Eu(g)atm}$ vs 1/T data are presented graphically
in Figure 7. At the median temperature (1970 K), the following
thermodynamic values are calculated for reaction (5-22): $\Delta H^° =$
$206._6 \pm 1._2$ kcal gfw$^{-1}$ and $\Delta S^° = 57.4_4 \pm 0.6_2$ eu. These values are
reduced to 298.15 K with thermal functions reported for Eu(g) (184)
and Se(g) (185) and estimated for EuSe(s) as follows. The heat capacity
of condensed EuSe was estimated as $12.5_1 \pm 0.1_0$ eu at 298.15 K from
the component elements (35,175). From an estimated melting point of
2473 K and methods similar to those described previously (sec. 5.6.3),
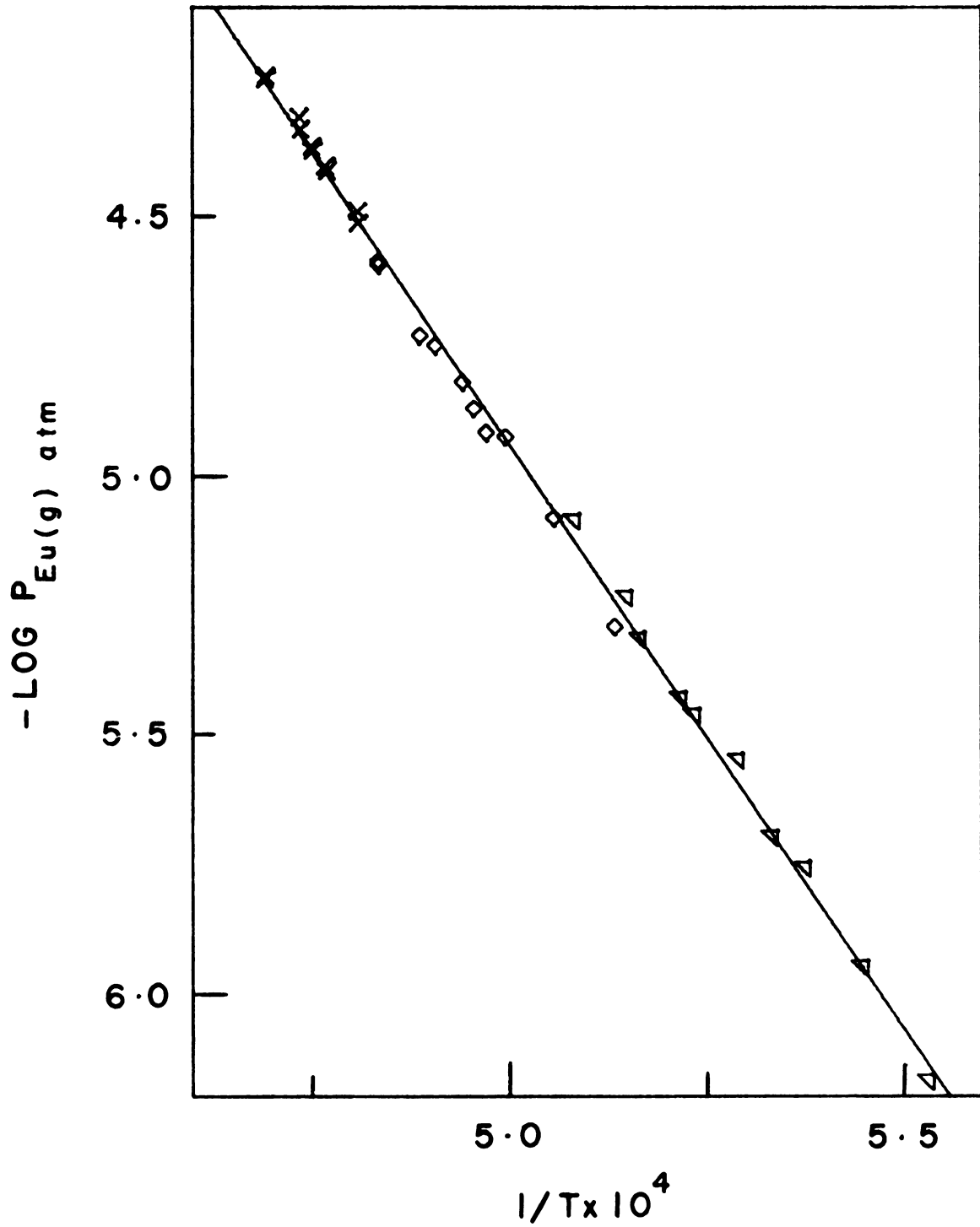
Figure 7. Logarithm of the Pressure of Eu(g) in Equilibrium with

EuSe(s) versus Reciprocal Temperature. Runs 1 (▽),

2 (◇) and 3 (✕).

a linear heat capacity equation (5-26) was derived for EuSe(s).

$$C^{\circ}_p \; EuSe(s) \;\; = \;\; (12.2_4 \pm 0.1_0) + 9.1_5 \times 10^{-4} \; T$$

$$(298-2473 \text{ K}) \hspace{4cm} (5-26)$$

The standard entropy was obtained from the additivity rule with a $7._0$ eu contribution for $Se^{2-}$ associated with a divalent cation (157):

$S^{\circ}_{298}[EuSe(s)] = 25._3 \pm 1._0$ eu. The derived thermodynamic functions are given in Table 15. The uncertainty in the free energy functions is estimated as $\pm 1._0$ eu.

The second-law thermodynamic values for reaction (5-22), together with the error resulting from data reduction, are: $\Delta H^{\circ}_{298} = 211._3 \pm 1._3$ kcal gfw$^{-1}$; $\Delta S^{\circ}_{298} = 62.5 \pm 0.7$ eu. Combination of these values with available data on the enthalpies and entropies of formation of Eu(g) (35,178,184) and Se(g) (185,188) yield the formation values, $\Delta H^{\circ}_{f,298}[EuSe(s)] = -(112._8 \pm 1._3)$ kcal gfw$^{-1}$ and $\Delta S^{\circ}_{f,298}[EuSe(s)] = -(4.1 \pm 0.7)$ eu. It should be mentioned that the enthalpy of formation of Se(g) is computed here as $56.38 \pm 0.05$ kcal gfw$^{-1}$ from $\Delta H^{\circ}_{f,298}[Se_2(g)] = 34.12 \pm 0.04$ kcal gfw$^{-1}$ (188) and the dissociation energy of $Se_2(g)$, and is significantly different from the value given in Ref. 185.

The standard entropy, $S^{\circ}_{298}[EuSe(s)]$, computed from the entropies of Eu(g) (184), Se(g) (185) and the second-law entropy change for reaction (5-22) is $24.8 \pm 0.7$ eu.

The published free energy functions for Eu(g) (184) and Se(g) (185) were combined with those derived for EuSe(s) (Table 15) and the equilibrium constant-temperature data for reaction (5-22) to yield the third-law enthalpy, $\Delta H^{\circ}_{298} = 210._3 \pm 2._2$ kcal gfw$^{-1}$, with no temperature trend in the individual values (Appendix 2-D).

Table 15.  **Thermodynamic Functions for EuSe(s)**

| T | $C_p^\circ$ | $S_T^\circ$ | $H_T^\circ - H_{298}^\circ$ | $-$ FEF |
|---|---|---|---|---|
| 298.15 K | 12.51 eu | $25._{30}$ eu | 0.0 cal gfw$^{-1}$ | $23._{30}$ eu |
| 1700 | 13.80 | $47._{89}$ | 18440.2 | $37._{04}$ |
| 1800 | 13.89 | $48._{68}$ | 19824.3 | $37._{67}$ |
| 1900 | 13.98 | $49._{43}$ | 21217.6 | $38._{27}$ |
| 2000 | 14.07 | $50._{15}$ | 22620.0 | $38._{84}$ |
| 2100 | 14.16 | $50._{84}$ | 24031.6 | $39._{40}$ |
| 2200 | 14.25 | $51._{50}$ | 25452.3 | $39._{93}$ |

# CHAPTER 6

## DISCUSSION

The purpose of any systematic series of investigations is to provide a body of information that establishes the trends and correlations among them. Although initially this investigator's curiosity may have been satisfied by the mere description of the composition and stabilities of the products of a vaporization or decomposition reaction, objectives beyond such mundane descriptions, those which permit extensions and utilization of the thermodynamic values became apparent. The importance of such studies in the final analysis of the nature and energetics of chemical bonding will be clear from consideration of the Born-Haber cycle for a typical compound, MX:
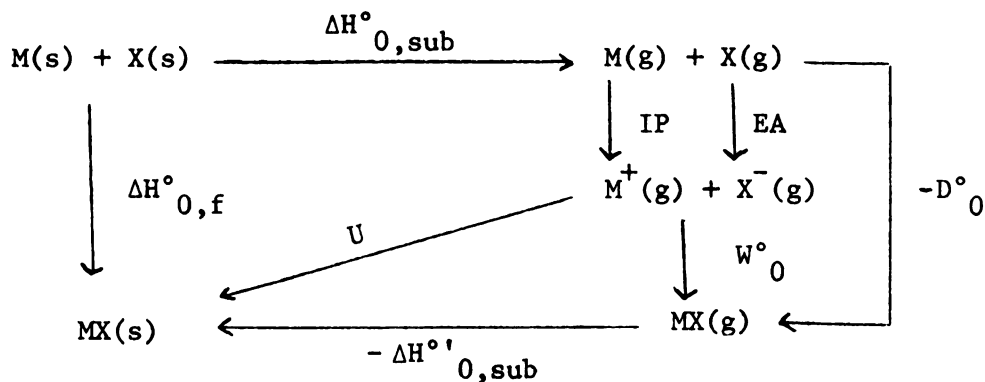


From this series of reactions the enthalpy of formation of MX(s), $\Delta H^{\circ}_{0,f}$ may be expressed by

$$\Delta H^{\circ}_{0,f}[MX(s)] = \Delta H^{\circ}_{0,sub}[M(s)] + \Delta H^{\circ}_{0,sub}[X(s)] + IP[M(g)] +$$
$$EA[X(g)] + W^{\circ}_{0}[MX(g)] - \Delta H^{\circ\prime}_{0,sub}[MX(s)]$$

(6-1)

in which IP is the ionization potential of the metal, EA the electron affinity of the non-metal, $W^{\circ}_0$ the binding energy of the system of cation and anion, and the enthalpy terms correspond to formation and sublimation. The term $W^{\circ}_0$ may be purely electrostatic, covalent or a mixture of the two, and together with $-\Delta H^{\circ}{}'_{0,sub}$ MX(s) is what is normally termed the lattice energy, U, of the system. Its value, derived indirectly from a Born-Haber thermochemical cycle or the dissociation energy $D^{\circ}_0[MX(g)]$, is of utmost importance in any theory of chemical bonding as it relates to these compounds. When applied to lanthanide compounds, such data would permit meaningful correlations with 4 f and 5 d orbital participations in bonding. However the study reported in this thesis has not been concerned with this aspect; the extensive thermodynamic data obtained, together with correlations in the series of europium(II) halides and chalcogenides will hopefully contribute towards a more meaningful theoretical analysis of bonding in the predominantly divalent lanthanides. Towards that end, the experimental vaporization data have been utilized to derive pertinent information for the system, normalize available thermodynamic quantities and evaluate missing data. These procedures and the trends observed in europium(II) compounds, together with a brief summary of the accuracy of the experimental methods, are considered in this chapter.

## 6.1. Evaluation of Experimental Procedures

### 6.1.1. Temperature Measurement

The importance of keeping the Knudsen cell at a uniform temperature and accurate measurement of that temperature cannot be over-emphasized. These aspects are particularly important in the second-law method of

data analysis as may be seen from

$$d_\Delta H^\circ(2)/\Delta H^\circ(2) = [(dT_1/T_1)^2 + (dT_2/T_2)^2 + (d\ln P/\ln P)^2 +$$

$$(d_\Delta T/T)^2]^{1/2}. \qquad (6\text{-}2)$$

where $T_1$ and $T_2$ are the two extremes of the experimental temperatures
and $\Delta T = (T_2 - T_1)$. The deltas refer to the composite of random and
systematic errors in the various defining quantities, and are assumed
independent of each other. Thus if only the error due to temperature is
considered, for a constant error $dT$ at both $T_1$ and $T_2$,

$$d_\Delta H^\circ(2)/\Delta H^\circ(2) \overset{\sim}{\sim} 2\ dT/T \qquad (6\text{-}3)$$

where $T$ is the median of $T_1$ and $T_2$. The fractional error in the second-
law derived enthalpy is only 2% at 1000 K or 1% at 2000 K for $dT = 10$ K.
However a corresponding uncertainty only at the extreme of temperature,
$T_2$, produces a fractional error of over 5% in the enthalpy for $\Delta T = 200$ K.
The third-law derived enthalpies do not suffer so drastically, as is
evident from equation (6-4),

$$d_\Delta H^\circ(3)/\Delta H^\circ(3) = [(T\ d_\Delta S^\circ/\Delta H^\circ)^2 + (RT\ d\ln P/\Delta H^\circ)^2 + (dT/T)^2]^{1/2}$$

$$= [\{d(\Delta S^\circ - R\ln P)/\Delta S^\circ - R\ln P\}^2 + (dT/T)^2]^{1/2} \qquad (6\text{-}4)$$

and the effect of an uncertainty of even 10 K at median temperatures of
1000 K or 2000 K contributes less than a percent to the uncertainties
in enthalpy values.

The effect of temperature gradients in Knudsen cells has been treated
in some detail by Storms (189). The consequence of even a slight
temperature gradient became evident during this research. When a graphite

Knudsen cell containing $EuCl_2$ was heated directly by induction the dichloride was transported either partially or completely to the effusion cell lid. The apparent temperatures of the blackbody and cell orifices were the same as those along the cell wall, and a temperature gradient could not be detected. Because of the low vapor pressure of $EuCl_2$ material transport of this magnitude could not have occurred by vaporization during the course of an experiment. From this observation it was concluded that temperature gradients existed in the sample cavity, that these caused liquid $EuCl_2$ to creep towards the cooler regions around the effusion orifice, and that a gradual decrease of the orifice area resulted. Enthalpy and entropy data derived from these preliminary and apparently non-equilibrium conditions were in general agreement with the values reported by Polyachenok and Novikov (8) and Hastie et al. (65). However, when the graphite cell was heated by radiation from the well-designed inductively heated oven surrounding it, material transport to the cell lid ceased; the residue consisted of a single button situated on the cell floor directly below the orifice. The good agreement of the vapor pressure of silver and the data derived therefrom with the NBS accepted values confirmed that reliable measurements could be made by this procedure (see Appendix 1).

Haschke (155) confirmed that accurate vapor pressure measurements could be made by the direct induction heating of metallic cells through a determination of the vapor pressure of gold.

It is difficult to assign an overall uncertainty in each experimental temperature measurement. These errors are believed to be of the same order of magnitude ($\pm$ 4-5°C) as those quoted in NBS calibration data for optical pyrometers.

## 6.1.2. X-Ray Fluorescence Analysis

X-Ray fluorescence proved to be a convenient technique for analysis of the microgram quantities of europium on the targets. The accuracy of the method as used in this research was limited solely by the manner in which the calibration standards were prepared. Volumetric transfer with in situ evaporation of the small droplets provided standard targets that were fairly uniform. However the method was not completely satisfactory. In retrospect I believe that it would have been rewarding to develop procedures for electrodeposition of europium (and other lanthanides) to prepare a set of standard targets that would have increased the reliability of the analytical procedure. Methods based on cathodic deposition of microgram quantities of hydrated oxides from alkaline, mildly acidic, and organic media are known to provide uniform and "weightless" sample mounts with the actinide elements. Such procedures should easily be extendable to the lanthanides.

Possible interference of the matrix materials, $Cl^-$, $I^-$, $S^{2-}$ and $Se^{2-}$, in the europium count rate was checked; none was found. A satisfactory calibration number could not be realized in the attempt to analyze the $EuI_2$ vaporization targets for iodide (sec. 4.9). The calibration value depended on the standard material ($NaI$, $NaIO_3$, $KI$, or $KIO_3$) and the substrate material (Cu or Pt) with no obvious correlation. The only inference that could be made from the extensive trials was that the intensity of the iodine $L\alpha_1$ seemed to be accentuated by the presence of europium, but that of the latter's $L\alpha_1$ was unaffected. The simultaneous analysis of $I^-$ in the vaporization targets was abandoned.

### 6.1.3. Equilibrium Vapor Pressures

Adherence to most of the criteria set forth under section 3.3.7 for Knudsen effusion, such as near ideal orifice, collimated collection geometry, and high temperatures, are believed to have contributed to reliable vapor pressure values. The invariance of the measured pressures both with either increasing or decreasing temperature and with different orifice areas substantiates that equilibrium conditions are realized very closely. Problems such as non-unity vaporization coefficients, kinetically controlled evaporation mechanisms and surface diffusion do not appear to have been experienced.

### 6.1.4. Knudsen Numbers

The upper pressure limit of the measured vapor pressures was limited to $10^{-3}$ atm. In Table 16 the ranges of Knudsen numbers (sec. 3.3.6.1) for the various vaporization reactions are given. The molecular diameters of $EuCl_2$ and $EuI_2$ have been estimated as $8.7_0$ and $10.0_7$ Å, respectively; the atomic radii of Eu ($1.8_5$ Å), S ($1.0_0$ Å) and Se ($1.1_5$ Å) are those given by Slater (190). With both the $EuCl_2$ and $EuI_2$ vaporization data three high temperature points have exceeded the high pressure limit set by Schulz and Searcy (K = 0.3; Ref. 129). However no significant change in either the least squares slope or intercept was noted when these data points were omitted; they have therefore been included. Otherwise the experimental pressures have all been well within the molecular flow region.

Table 16.  **Limits of Knudsen Numbers**

| Vapor | Diameter ($\sigma$) | $K = \lambda/2R_o$ |
|-------|---------------------|--------------------|
| $EuCl_2$ | $8.7_0$ Å | 211-0.13 |
| $EuI_2$ | $10.0_7$ | 17-0.08 |
| Eu/EuS | $3.7_0$ | 774-8 |
| S/EuS | $2.0_0$ | 8539-87 |
| Eu/EuSe | $3.7_0$ | 501-11 |
| Se/EuSe | $2.3_0$ | 1808-40 |

$\lambda$, mean free path in cm, $\lambda = kT/\sqrt{2}\pi P\sigma^2$

$R_o$, effusion orifice radius in cm.

## 6.2.  Thermochemical Properties of Europium(II) Compounds

Divalency is not a typical group property among the lanthanides and its occurrence is mainly limited to $f^7 s^2$ Eu and $f^{14} s^2$ Yb due to the extra stabilization of the half-filled and completely-filled f shells. At these electronic configurations one also observes remarkable changes in the properties of the metals and compounds from the general trend in the lanthanide series. Typically the density, transition points and enthalpy of vaporization are appreciably lower than those found among other lanthanide metals. Even other physical properties such as the tensile strength, modulus of elasticity, etc. evidence sharp variations for these elements. Interestingly, the properties of elemental europium correspond very closely to those of the alkaline earths and in particular to those of strontium. The crystallographic similarity between the compounds of these elements was observed first by Klemm et al. (2,31). Correspondence in the thermochemical properties of their compounds is a central theme in this discussion.

## 6.2.1.  Mass Spectrometric Results

### 6.2.1.1.  Europium(II) Halides

In Table 17 are compiled the information on the fragmentation patterns in the high temperature mass spectra of europium(II) halides. The mass spectra of inorganic halides do not always follow a consistent pattern (142).  However, the parent-minus one halogen ion seems fairly consistently to exhibit the highest intensity.  The actual fragmentation pattern would depend, among other things, on the geometry of $MX_2$ and $MX_2^+$, the origin of the ionized electron (i.e., if it is from a molecular orbital contributed predominantly by the metal or halogen), and the associated Franck-Condon factors.

Of relevance to this research is the similarity in the fragmentation patterns among the europium(II) halides and their close correspondence to those of the alkaline earth halides (191 and references therein). Factors that affect fragmentation are apparently similar in these compounds.  The measured ionization potentials of diatomic MF and MCl species in the alkaline earths (produced by high temperature reduction) of $MF_2$ and $MCl_2$ with the respective metals) are approximately 0.2-0.3 eV lower than those of the corresponding metals.  By extending this trend to the europium(II) halides, one estimates the ionization potentials of EuX species as 5.4 eV.  By use of the experimental data of the appearance potentials, $EuX^+/EuX_2$ and $Eu^+/EuX_2$, and the dissociation energies of the $EuX_2$ molecules the individual bond dissociation energies may be computed (sec. 3.5.4).  These are presented in Table 18.  Because of the large uncertainties ($\pm$ 0.5 eV) in measured appearance potentials, the table is intended only for a qualitative and order of magnitude comparison of the Eu-X bond strengths.

Table 17.  Mass Spectrometric Data on Eu(II) Halides

Relative Intensities of Ions

| Ion | $EuF_2$ | $EuCl_2$* | $EuBr_2$ | $EuI_2$ |
|-----|---------|-----------|----------|---------|
| $M^+$ | 33 | 46 | 50 | 81 |
| $MX^+$ | 100 | 100 | 100 | 100 |
| $MX_2^+$ | 24 | 12 | 15 | 34 |

*At 50 eV, Ref. 65.

All others at 25-30 eV, Ref. this work, 64,192.

Table 18.  Dissociation Energies* of Eu(II) Halides

from Mass Spectrometric Data

| Molecule | $D^{\circ}_0[MX_2(g)]$ | $D^{\circ}_0(XM-X)$ | $D^{\circ}_0(M-X)$ |
|----------|------------------------|---------------------|--------------------|
| $EuF_2$ | 11.4 | 7.1 | 4.3 |
| $EuCl_2$ | 9.1 | 4.9 | 4.2 |
| $EuBr_2$ | 8.1 | 5.0 | 3.1 |
| $EuI_2$ | 6.8 | 4.5 | 2.3 |

*In eV; accuracy $\pm$ 0.5 eV.

Table 17. <u>Mass Spectrometric Data on Eu(II) Halides</u>

<u>Relative Intensities of Ions</u>

| Ion | $EuF_2$ | $EuCl_2$* | $EuBr_2$ | $EuI_2$ |
|-----|------|--------|-------|------|
| $M^+$ | 33 | 46 | 50 | 81 |
| $MX^+$ | 100 | 100 | 100 | 100 |
| $MX_2^+$ | 24 | 12 | 15 | 34 |

*At 50 eV, Ref. 65.

All others at 25-30 eV, Ref. this work, 64,192.

Table 18. <u>Dissociation Energies* of Eu(II) Halides</u>

<u>from Mass Spectrometric Data</u>

| Molecule | $D^{\circ}_0[MX_2(g)]$ | $D^{\circ}_0(XM-X)$ | $D^{\circ}_0(M-X)$ |
|----------|---------------|-------------|------------|
| $EuF_2$ | 11.4 | 7.1 | 4.3 |
| $EuCl_2$ | 9.1 | 4.9 | 4.2 |
| $EuBr_2$ | 8.1 | 5.0 | 3.1 |
| $EuI_2$ | 6.8 | 4.5 | 2.3 |

*In eV; accuracy $\pm$ 0.5 eV.

## 6.2.1.2. Europium(II) Chalcogenides

The mass spectrometric data on the high temperature vaporization of europium(II) chalcogenides are similar; they vaporize almost entirely as the atomic species. Contrast this behavior to that of the corresponding monochalcogenides of the other lanthanides (except Yb). The gaseous molecule is the principal vapor species in the congruent vaporization of LaS and CeS (73,75), while for both PrS and GdS molecular and atomic species have been detected (76,77). Similarly, the main mode of vaporization of NdS and NdSe is with formation of gaseous molecular species (82). However the behavior of europium(II) chalcogenides is strikingly similar to that of strontium. The contribution of the molecular species is < 4% for SrS at 2100 K and $\sim$ 0.1% for SrSe at 1850 K (193-196).

The vaporization behavior of condensed EuO is different from that of SrO. Whereas the latter vaporizes congruently with < 0.3% SrO(g) (197), EuO vaporizes incongruently (155) according to

$$4 \text{ EuO}(s) = \text{Eu}_3\text{O}_4(s) + \text{Eu}(g). \tag{6-5}$$
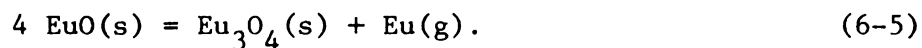
This vaporization mode is due to the stability of the +3 oxidation state of europium in the condensed oxide; this stability causes Eu(g) to be the only gaseous species in the EuO-Eu$_3$O$_4$ region.

## 6.2.2. EuF$_2$ Vaporization Data

During the course of this work Petzel and Greis (57) measured the sublimation pressure of EuF$_2$. The vapor pressure values were obtained by the Knudsen effusion weight-loss method from graphite cells in the temperature range 1412-1612 K. From heat capacities estimated for EuF$_2$(s) by analogy with isostructural BaF$_2$(s) and with methods similar

to those employed in this research together with the molecular data for

$EuF_2(g)$ (88), they derived the following values for the sublimation

reaction: $\Delta H^\circ_{298}$, second-law, $100._8 \pm 2._5$ kcal $gfw^{-1}$; $\Delta H^\circ_{298}$, third-law,

$98._3 \pm 2._0$ kcal $gfw^{-1}$; $\Delta S^\circ_{298}$, second-law, $48._9 \pm 2._5$ eu; $S^\circ_{298}[EuF_2(s)]$,

$27._1 \pm 1._0$ eu (estimated), and $25._5 \pm 2._7$ eu (derived). From the

dissociation energy, $D^\circ_{298}[EuF_2(g)] = 264._1 \pm 14._1$ kcal $gfw^{-1}$ ($D^\circ_0 =$

$262._6 \pm 14._1$ kcal), the authors calculated the enthalpy of formation,

$\Delta H^\circ_{f,298}[EuF_2(s)] = -(284 \pm 17)$ kcal $gfw^{-1}$.

I have extrapolated their sublimation data above the melting point

as follows. The data of Petzel and Greis correspond to a $\Delta C^\circ_p$ sublimation

of $-(5.9_0 \pm 0.1_5)$ eu. With an estimated melting point of $1676 \pm 5$ K,

$\Delta H^\circ_{fus}$ of $5._0 \pm 2._0$ kcal $gfw^{-1}$, $\Delta S^\circ_{fus}$ of $3._0 \pm 2._0$ eu and $\Delta C^\circ_p$ vaporization

of $-10$ eu, the following vaporization data were derived: boiling point,

$2505 \pm 35$ K; $\Delta H^\circ_v$, $79._3 \pm 2._0$ kcal $gfw^{-1}$; $\Delta S^\circ_v$, $31._7 \pm 1._0$ eu. The error

estimates are analogous to those of this work.

In Table 19 the thermochemical and molecular data on $EuF_2$ are

compared with those of the alkaline earth difluorides. The close

correspondence in the properties of $EuF_2$ and $SrF_2$ is particularly evident

in each individual quantity.

### 6.2.3. $EuCl_2$ Vaporization Data

The vaporization thermodynamics, molecular geometry and derived

thermochemical values for $EuCl_2$ are compared with those of alkaline

earth chlorides in Table 20. Again, as with the fluorides, the similarity

with $SrCl_2$ is remarkable.

An attempt was made prior to the availability of experimental data

on $EuCl_2(g)$ to estimate the molecular constants from the data of $CaCl_2$,

Table 19.   Summary Data on Alkaline Earth Difluorides and $EuF_2$

| | $CaF_2$ | $SrF_2$ | $BaF_2$ | $EuF_2$ |
|---|---|---|---|---|
| $-\Delta H°_{f,298}[MF_2(s)]$, kcal gfw$^{-1}$ | 289 ± 5 | 286 ± 5 | 283 ± 5 | 284 ± 5 |
| $\Delta H°_{298,sub}$, kcal gfw$^{-1}$ | 101 ± 2 | 100 ± 2 | 90 ± 2 | 101 ± 3 |
| $\Delta S°_{298,sub}$, eu | 46.9 ± 2.0 | 46.4 ± 2.0 | 45.8 ± 2.0 | 48.9 ± 2.5 |
| r (M-F) Å | 2.10 ± 0.03 | 2.20 ± 0.03 | 2.32 ± 0.03 | 2.20 ± 0.05 |
| F-M-F° | 140 | 108 | 100 | 110 ± 15 |
| $\nu_1$ cm$^{-1}$ | 494 | 462 | 389 | 464 ± 10 |
| $\nu_2$ cm$^{-1}$ | 167 | 85 | 64 | 114 ± 15 |
| $\nu_3$ cm$^{-1}$ | 563 | 462 | 414 | 487 ± 10 |
| $D°_0[MF_2(g)]$, kcal gfw$^{-1}$ | 266.5 | 261.5 | 271.5 | 262.6 ± 14.1 |
| $D°_0(FM-F)$, kcal gfw$^{-1}$ | 141 | 136 | 137 | (138 ± 10) |
| $D°_0(M-F)$, kcal gfw$^{-1}$ | 125.5 | 125.5 | 134.5 | 125 |

Enthalpy and entropy values:  second-law.

Dissociation energies:  third-law.

Ref. Alkaline earth fluorides, 198, 199, 200.

$EuF_2$, 55, 57, 88

Table 20. Summary Data on Alkaline Earth Dichlorides and $EuCl_2$

| | $CaCl_2$ | $SrCl_2$ | $BaCl_2$ | $EuCl_2$ |
|---|---|---|---|---|
| $-\Delta H^\circ_{f,298}[MCl_2(s)]$, kcal gfw$^{-1}$ | $191.4 \pm 1.0$ | $198.2 \pm 1.0$ | $205.4 \pm 0.6$ | $195.8 \pm 1.1$ |
| $\Delta H^\circ_{298,sub}$, kcal gfw$^{-1}$ | $75.6 \pm 2.0$ | $83.9 \pm 2.0$ | $84.8 \pm 2.0$ | $84.9 \pm 1.1$ |
| $\Delta S^\circ_{298,sub}$, eu | $45.2 \pm 2.0$ | $44.7 \pm 2.0$ | $47.2 \pm 2.0$ | $48.3 \pm 1.8$ |
| $r$ (M-Cl) Å | $2.51 \pm 0.03$ | $2.67 \pm 0.03$ | $2.82 \pm 0.03$ | $2.67 \pm 0.05$ |
| Cl-M-Cl° | 180 | $130 \pm 5$ | $120 \pm 10$ | $135 \pm 10$ |
| $\omega_1$ cm$^{-1}$ | 217 | $285 \pm 10$ | $279 \pm 10$ | $280 \pm 5$ |
| $\omega_2$ cm$^{-1}$ | 64 | $60 \pm 15$ | $60 \pm 10$ | $64 \pm 10$ |
| $\omega_3$ cm$^{-1}$ | 402 | $318 \pm 10$ | $285 \pm 10$ | $290 \pm 5$ |
| $D^\circ_0[MCl_2(g)]$, kcal gfw$^{-1}$ | $214.7 \pm 2.0$ | $211.0 \pm 2.0$ | $220.6 \pm 2.0$ | $212.0 \pm 2.8$ |
| $D^\circ_0(ClM-Cl)$, kcal gfw$^{-1}$ | $115.8 \pm 3.0$ | $112.5 \pm 3.0$ | $112.3 \pm 3.0$ | $113.0 \pm 5.0$ |
| $D^\circ_0(M-Cl)$, kcal gfw$^{-1}$ | $98.9 \pm 4.0$ | $98.5 \pm 4.0$ | $108.3 \pm 4.0$ | $99.0 \pm 6.0$ |

Enthalpy and entropy values: second-law

Dissociation energies: third-law

Ref. Alkaline earth chlorides, 147, 191,198,88

Molecular data $EuCl_2$, 88

$SrCl_2$ and $BaCl_2$ [quoted in Ref. 191]. The estimated values are:
Cl-Eu-Cl, 155°; Eu-Cl, $2.6_4 \pm 0.0_5$ Å; $\omega_1 = 221$ cm$^{-1}$; $\omega_2 = 40$ cm$^{-1}$;
$\omega_3 = 263$ cm$^{-1}$. Use of the thermal functions derived from these estimated
molecular constants gave for the sublimation of $EuCl_2(s)$: $\Delta H°_{298} =$
$84._8 \pm 2._5$ kcal gfw$^{-1}$; $\Delta S°_{298} = 48._2 \pm 1._8$ eu by the second-law and
$\Delta H°_{298} = 83._7 \pm 2._5$ kcal gfw$^{-1}$ by the third-law. The standard entropy,
$S°_{298}[EuCl_2(s)]$, was computed as $33._7 \pm 2._4$ eu. The estimated molecular
data for $EuCl_2(g)$ are slightly different from the experimental values
of Hastie et al. (88), just as the numbers obtained by White and
coworkers by matrix isolation infrared spectroscopy for $SrCl_2$ and $BaCl_2$
differ from those of Hastie et al. (88,191). The general agreement in
the derived thermodynamic data, however, indicate the consistency of the
europium dichloride molecular parameters with those of the alkaline earth
dichlorides.

### 6.2.4. EuI$_2$ Vaporization Data

The general vaporization pattern of $EuI_2$ and the derived thermo-
dynamic quantities are in line with the trends observed for $EuF_2$ and
$EuCl_2$. However, the largest uncertainty remains in the molecular data
for $EuI_2(g)$ since these are based totally on estimates. Even a meaningful
comparison to analogous $SrI_2$ is hampered by a lack of accurate experimental
data on the latter. At the same time the good agreement between the
standard entropy, $S°_{298}[EuI_2(s)]$, derived (from the second-law sublimation
data) $40._4 \pm 2._6$ eu, and estimated, $41._6 \pm 1._0$ eu, indicates the
reasonableness of the estimates.

The standard entropy estimate for condensed $EuI_2$ should be discussed.
Latimer suggests a 13.6 eu contribution for I$^-$ associated with a divalent
cation (156). However, a comparison of $S°_{298}$ values for a variety of

divalent metal iodides with those recommended by Kelley and King (176)

indicates that the standard entropies derived from estimates are

consistently 2-4 eu high. Kelley (in Ref. 153) suggests a value of 12.2 eu

for $I^-$ with a possible uncertainty of $\pm$ 1 eu; we have used this number.

From the mass spectrometric appearance potential of $Eu^+/EuI_2$ and

the first ionization potential for Eu, the dissociation energy of $EuI_2(g)$

is computed as $D^\circ_0 = 156._0 \pm 5._0$ kcal $gfw^{-1}$ (equation 3-20). Combination

of this value with the thermodynamic functions for $EuI_2(g)$ (this work),

Eu(g) (178), I(g) (148), the enthalpies of formation of Eu(g) (178) and

I(g) (148), and $\Delta H^\circ_{298,sub}[EuI_2(s)]$ (this work) gives the enthalpy of

formation, $\Delta H^\circ_{f,298}[EuI_2(s)] = -(138._9 \pm 5._0)$ kcal $gfw^{-1}$ and $-(137._3 \pm$

$5._6)$ kcal $gfw^{-1}$, respectively, by use of the second-law and third-law

sublimation values. These values are in good agreement with the enthalpy

of formation of $SrI_2(s)$ [$\Delta H^\circ_{f,298} = -(135._5 \pm 5._0)$ kcal $gfw^{-1}$; Ref. 147].

### 6.2.5. Entropy of Sublimation, $\Delta S^\circ_{298}$, of Europium(II) Halides

The single most important consistent quantity in the sublimation of

$EuF_2$, $EuCl_2$ and $EuI_2$ is the second-law entropy change for the reaction

at 298.15 K. This $\Delta S^\circ_{298,sub}$ value is remarkably constant at $48._0 \pm$

$2._0$ eu and is independent of uncertainties in all the estimated

thermodynamic functions. This behavior is expected because the pertinent

single factor in determining entropy changes in isothermal reactions is

the change in the number of gas molecules. Searcy (201) has considered

characteristic entropy changes in various classes of reactions which

involve gas phases and to his observations may be added the present one

of the constancy of the entropy of sublimation. Secondary effects may

produce systematic deviations from the broadly established values for

the entropy change, but within a class of compounds, such as the halides

of an element, this rule might serve as a general guide line of extreme usefulness.

### 6.2.6. Re-evaluation of EuBr$_2$ Vaporization Data

Haschke and Eick (64) studied the congruent vaporization of liquid EuBr$_2$ by the target collection Knudsen effusion method. I believe that the vapor pressure values they report are low as a consequence of an appreciable temperature gradient along the graphite containers and partial closure of the effusion orifice when the cells were heated directly by induction. In view of the consistency and trends observed in the vaporization behavior of EuF$_2$, EuCl$_2$ and EuI$_2$, it is possible to re-evaluate the pertinent thermochemical quantities for EuBr$_2$.

The significance of the entropy of sublimation, $\Delta S^{\circ}_{298}$, for europium(II) halides was pointed out in section 6.2.5. The value of $48._0 \pm 2._0$ eu may be assumed to hold for the sublimation of EuBr$_2$(s). The normal boiling point of EuBr$_2$(l) may be estimated as $2200 \pm 35$ K from the corresponding values for EuCl$_2$ and EuI$_2$ (see sec. 5.6.1 and 5.6.2). This value is 50 K higher than that estimated by Brewer et al. (37,38), as are the trends in the experimental values of the other europium(II) halides. With reasonable estimates for the heat capacities of EuBr$_2$(s), (l) and (g), all other thermochemical data for sublimation and vaporization may then be derived.

Thermodynamic functions for condensed EuBr$_2$ were estimated by methods similar to those used for EuCl$_2$ and EuI$_2$ from available data on isostructural SrBr$_2$ (42,175). The linear heat capacity equation for EuBr$_2$(s) may be represented by

$$C^\circ_p[\text{EuBr}_2(s)] = (18.2_5 \pm 0.1_0) + 3.6_6 \times 10^{-3} \, T$$

$$(298\text{--}956 \text{ K}). \hspace{3cm} (6\text{-}6)$$

For $\text{EuBr}_2(l)$ a constant heat capacity value of $26.7 \pm 0.7$ eu is estimated. The standard entropy, $S^\circ_{298}[\text{EuBr}_2(s)]$, is computed as $38._4 \pm 1._0$ eu by Latimer's method (with 10.5 eu for $\text{Br}^-$ associated with a divalent cation, Ref. 156) and from relationship (3-44) by utilization of the corresponding values for $\text{EuCl}_2$ and $\text{EuI}_2$. With an estimated $\Delta H^\circ_{fus} = 6._0 \pm 1._0$ kcal gfw$^{-1}$ and $\Delta S^\circ_{fus} = 6._3 \pm 1._1$ eu (38), free energy functions were derived for $\text{EuBr}_2(l)$ and are presented in Table 21. An uncertainty of $1._6$ eu is estimated in these functions.

Molecular constants for $\text{EuBr}_2(g)$ were derived by procedures identical to those used for $\text{EuI}_2(g)$ (sec. 5.6.2). These are: Eu-Br $2.8_0 \pm 0.0_5$ Å, Br-Eu-Br 180° (cf. $\text{SrBr}_2(g)$, Ref. 180,181), stretching force constant, $k_1 = 1.090$ md/Å $[= k_e$ diatomic EuBr; $\omega_e = 188$ cm$^{-1}]$, bending force constant, $k\delta/l^2 = 1\% \, k_1$, $\omega_1 = 152$ cm$^{-1}$, $\omega_2 = 31$ cm$^{-1}$ (doubly degenerate), $\omega_3 = 218$ cm$^{-1}$, and statistical weight 16. The derived thermodynamic functions for $\text{EuBr}_2(g)$ are presented in Table 22. An overall uncertainty of $\pm 1._7$ eu is estimated in the free energy functions.

By use of these thermodynamic functions average $\Delta C^\circ_p$ values have been computed for the sublimation and vaporization reactions: $-(5.7_9 \pm 0.1_5)$ eu and $-(11.8_2 \pm 0.7_1)$ eu, respectively, in good agreement with the corresponding values for $\text{EuF}_2$, $\text{EuCl}_2$ and $\text{EuI}_2$. The estimated $\Delta S^\circ_{298,sub}$ for $\text{EuBr}_2(s)$ is used with the derived $\Delta C^\circ_p$ values to calculate the entropy and enthalpy of vaporization at the normal boiling point. These are $\Delta H^\circ_v = 55._3 \pm 2._2$ kcal gfw$^{-1}$ and $\Delta S^\circ_v = 25._1 \pm 1._0$ eu. From the vaporization enthalpy the sublimation value of $\Delta H^\circ_{298} = 79._8 \pm 1._5$ kcal gfw$^{-1}$ is obtained.

Table 21.  Thermodynamic Functions for $EuBr_2(l)$

| $T$ | $C^\circ_p$ | $S^\circ_T$ | $H^\circ_T - H^\circ_{298}$ | $-$ FEF |
|---|---|---|---|---|
| 298.15 K | 19.34 eu | 45.38 eu | 0.0 cal gfw$^{-1}$ | 45.38 eu |
| 956 | 26.70 | 69.05 | 13515.6 | 54.91 |
| 1000 | 26.70 | 70.25 | 14690.4 | 55.56 |
| 1200 | 26.70 | 75.12 | 20030.4 | 58.43 |
| 1400 | 26.70 | 79.23 | 25370.4 | 61.11 |

Table 22.  Thermodynamic Functions for $EuBr_2(g)$

| $T$ | $C^\circ_p$ | $S^\circ_T$ | $H^\circ_T - H^\circ_{298}$ | $-$ FEF |
|---|---|---|---|---|
| 298.15 K | 14.64 eu | 84.55 eu | 0.0 cal gfw$^{-1}$ | 84.55 eu |
| 956 | 14.88 | 101.79 | 9748.7 | 91.59 |
| 1000 | 14.88 | 102.46 | 10403.4 | 92.05 |
| 1200 | 14.89 | 105.17 | 13380.1 | 94.02 |
| 1400 | 14.89 | 107.47 | 16358.1 | 95.78 |

$$H^\circ_T - H^\circ_{298} = 3908.4 \text{ cal gfw}^{-1}$$

The standard entropy, $S°_{298}[EuBr_2(s)]$, derived from the estimated $\Delta S°_{298,sub}$ and $S°_{298}[EuBr_2(g)]$ is $36._6 \pm 2._6$ eu (cf. estimated: $38._4 \pm 1._0$ eu).

All vapor pressure data (155) for $EuBr_2(l)$ in the temperature range 1185-1568 K were not used for individual third-law calculations, but three temperature-pressure data of Experiment 3B, obtained at the lowest temperature range (1185-1246 K), were treated. Since the temperatures were in the lower end of the experimental range, orifice clogging (see sec. 6.1.1) may not have occurred and "reasonably" accurate values of the vapor pressure of $EuBr_2(l)$ may have been realized. The results are presented in Table 23. The individual third-law enthalpy values are consistent and average to $73._2 \pm 3._0$ kcal gfw$^{-1}$ for vaporization and $79._2 \pm 3._0$ kcal gfw$^{-1}$ for sublimation. The excellent correspondence to the second-law derived value, $\Delta H°_{298} = 79._8 \pm 1._5$ kcal gfw$^{-1}$, lends credence to the assumptions and approximations made in the calculations of the vaporization thermodynamics of $EuBr_2$.

Table 23. Third-law Calculation for the Vaporization of $EuBr_2(l)$

| T | $- \ln P_{EuBr_2(g)}$ atm | $-\Delta FEF$ | $\Delta H°_{298}[l \rightarrow g]$ |
|---|---|---|---|
| 1185 K | 13.022 | $35._{66}$ eu | $72._{93}$ kcal gfw$^{-1}$ |
| 1228 | 12.262 | $35._{47}$ | $73._{48}$ |
| 1246 | 11.810 | $35._{38}$ | $73._{33}$ |

The vaporization enthalpy values were combined with the estimated enthalpy of formation of $EuBr_2(s)[-172._0 \pm 5._0$ kcal gfw$^{-1}$; cf. $SrBr_2(s)$: Ref. 147], enthalpy of sublimation of Eu (178) and dissociation energy of $Br_2$ (185) to derive $D°_0[EuBr_2(g)] = 187._9 \pm 5._0$ kcal gfw$^{-1}$ ($D°_{298} = 188._4 \pm 5._0$ kcal) from the third-law sublimation enthalpy.

## 6.2.7. Comparison of the Vaporization Thermodynamics of Europium(II) Halides

The pertinent thermodynamic and molecular data for the sublimation and vaporization of europium(II) halides are summarized concisely in Table 24. The trends in the values for the enthalpy of sublimation ($\Delta H^\circ_{298,sub}$), enthalpy of vaporization ($\Delta H^\circ_v$), and boiling point in the series $EuF_2$ to $EuI_2$ are in line with the corresponding data on other halides (147,182) and in particular with the alkaline earth dihalides. The entropy of vaporization at the boiling point, $\Delta S^\circ_v$, corresponds to the Trouton's rule value as modified by Gschneidner (159), for $EuCl_2$, $EuBr_2$ and $EuI_2$. The higher value generally observed for all fluorides, and in particular for $EuF_2$, is indicative of long range order in the molten fluorides even at temperatures close to the normal boiling point.

Hayes (181) invoked the necessity of including the d orbitals to explain the bent and linear geometries of alkaline earth halides. The lowering of the d in comparison to the p level as one goes from Ca to Sr to Ba and from the neutral metal atom to the positive ion, and while increasing the electronegativity of the halogen in changing from $I^-$ to $F^-$, provides a satisfactory explanation to the molecular shapes in this class of compounds. In any case a non-degenerate ground state with all the bonding orbitals completely filled is indicated for the alkaline earth halides. An explanation on similar lines is certainly appliacable to the molecular geometry of europium(II) halides that change from the bent $EuF_2$ and $EuCl_2$ to the (hopefully) linear $EuBr_2$ and $EuI_2$. However the extent of the importance of the 4 f orbitals in the proposed bonding scheme is difficult to envisage. In a purely ionic compound, especially with the added stability of the half-filled 4 f level in europium, the

Table 24.  Summary Data on Vaporization Thermodynamics of Europium(II) Halides

| | $EuF_2$ | $EuCl_2$ | $EuBr_2$* | $EuI_2$ |
|---|---|---|---|---|
| $\Delta H°_{298,sub}$, kcal gfw$^{-1}$ | $100.8 \pm 2.5$ | $84.9 \pm 1.1$ | $79.8 \pm 1.5$ | $75.4 \pm 1.1$ |
| $\Delta S°_{298,sub}$, eu | $48.9 \pm 2.5$ | $48.3 \pm 1.8$ | $48.0 \pm 2.0$ | $48.1 \pm 1.9$ |
| mp $EuX_2$(s), K | $1676 \pm 5$ | $1000 \pm 5$ | $956 \pm 5$ | $853 \pm 5$ |
| bp $EuX_2$(l), K | $2505 \pm 35$ | $2335 \pm 35$ | $2200 \pm 35$ | $2048 \pm 25$ |
| $\Delta H°_v$, kcal gfw$^{-1}$ | $79.3 \pm 2.0$ | $58.9 \pm 1.8$ | $55.3 \pm 2.2$ | $53.5 \pm 1.6$ |
| $\Delta S°_v$, eu | $31.7 \pm 1.0$ | $25.2 \pm 0.7$ | $25.1 \pm 1.0$ | $26.1 \pm 0.7$ |
| $D°_0[EuX_2(g)]$ kcal gfw$^{-1}$ | $262.6 \pm 14.1$ | $209.8 \pm 1.5$ | $187.3 \pm 5.0$ | $156.0 \pm 5.0$ |
| r (Eu-X), Å | $2.20 \pm 0.05$ | $2.67 \pm 0.05$ | $2.80 \pm 0.05$ | $3.00 \pm 0.05$ |
| X–Eu–X, ° | $110 \pm 15$ | $135 \pm 10$ | 180 | 180 |
| $\omega_1$ cm$^{-1}$ | $464 \pm 10$ | $280 \pm 5$ | 152 | 107 |
| $\omega_2$ cm$^{-1}$ | $114 \pm 15$ | $64 \pm 10$ | 31 | 25 |
| $\omega_3$ cm$^{-1}$ | $487 \pm 10$ | $290 \pm 5$ | 218 | 175 |

*estimated values

All enthalpy, entropy and dissociation energy values:  second-law

Molecular data $EuF_2$ and $EuCl_2$, Ref. 88

two s electrons may be treated exactly as those in the alkaline earths.
But in light of Gschneidner's arguments on the nature of 4 f bonding in
lanthanide metals and compounds (202), it does not seem unreasonable
that they be included in an overall molecular orbital scheme for the
bonding in the europium(II) compounds.

From a thermodynamic point of view, Hayes' bonding scheme results
in a more normal ground state of $^8S$ for $Eu^{2+}$ in the divalent europium
compounds, and thus with a statistical weight of 8. This is different
by a factor of two in the orbitally degenerate ground state (statistical
weight 16) assumed for europium(II) compounds in this work. Such a
choice was based on empirical correlations (see sec. 2.5 and Ref. 80)
and the present thermodynamic data are incapable of deciding the validity
of either choice, which from an entropy standpoint differ by only $1.3_8$ eu.
However, the good agreements in the standard entropies of condensed
europium(II) halides, derived from the second-law sublimation entropies
and $S^{\circ}_{298}$ values for the gases based on the degenerate ground state, with
the estimates based on ionic additivity rules justify the derived
thermochemical quantities to a great extent. In this connection it is
pertinent that Haschke's work on the vaporization thermodynamics of
EuO indicates that Westrum's estimate (158) for the magnetic entropy
of Eu(II) in europium(II) compounds (4.2 eu) may be in excess by $\sim$ 1.3 eu
(155). If this in fact is the case, the thermodynamic values obtained in
the present work would be the same with the assumption of the non-
degenerate ground state for $Eu^{2+}$ in the gaseous compounds.

The various thermodynamic approximations utilized in the reduction
of the experimental vaporization data for europium(II) halides seem
internally consistent (and thus hopefully valid). However, when

experimental heat capacity values and molecular data for $EuBr_2$ and $EuI_2$ become available, more accurate data reduction will be possible from the present compilation.

### 6.2.8. EuO Vaporization Data

From a mass spectrometric isomolecular exchange reaction (sec. 2.3.2.2), White et al. (71) derived the enthalpy of formation of EuO(g) as $\Delta H°_{f,0} = -(32._7 \pm 7._3)$ kcal gfw$^{-1}$ and the dissociation energy, $D°_0 [EuO(g)] = 133._7 \pm 7._5$ kcal gfw$^{-1}$. However, the third-law thermal functions utilized to derive these values employed vibrational frequencies of 830 cm$^{-1}$ for both SmO(g) and EuO(g). On the basis of recent spectroscopic studies (sec. 2.4.2) and the lower stability of EuO(g) than SmO(g), the use of identical vibrational frequencies is not justified. From trends in the alkaline earth monoxides and monochalcogenides, we estimate $\omega_e [EuO(g)] = 691$ cm$^{-1}$ (Eu-O $1.9_1 \pm 0.0_2$ Å). Recalculation of the original data of White et al. (71) with a more consistent set of free energy functions (statistical weight 16) results in $\Delta H°_{f,298} [EuO(g)] = -(13._8 \pm 7._3)$ kcal gfw$^{-1}$ and $D°_0 [EuO(g)] = 125._3 \pm 7._5$ kcal gfw$^{-1}$ ($D°_{298} = 126._2 \pm 7._5$ kcal). The enthalpy of formation of europium monoxide is computed as $\Delta H°_{f,298} [EuO(s)] = -(144._3 \pm 1._4)$ kcal gfw$^{-1}$ from the calorimetrically determined values (67,68). Thus the enthalpy change for the sublimation reaction

$$EuO(s) = EuO(g) \qquad (6-7)$$

is $\Delta H°_{298} = 130._5 \pm 7._6$ kcal gfw$^{-1}$ (cf. White et al. $110._8 \pm 7._6$ kcal) and for the vaporization reaction

$$EuO(s) = Eu(g) + O(g) \qquad (6-8)$$

is $\Delta H°_{298}$ = $256._7 \pm 10._0$ kcal gfw$^{-1}$ (cf. White et al. $243._9 \pm 10._0$ kcal).

The error values reflect both the uncertainties in the original data

of White et al. (71) and those in the present calculations.

### 6.2.9. EuS Vaporization Data

An upper limit of 3% was estimated for $P_{EuS(g)}/P_{Eu(g)}$ at 2011 K

(sec. 5.6.3) from the mass spectrometric data. A third-law calculation

with this estimate for the pressure of EuS(g) together with the thermo-

dynamic functions for EuS(g) [Smoes et al. Ref. 80; Eu-S $2.2_3$ Å,

$\omega_e$ = 410 cm$^{-1}$] and EuS(s) [this work, Table 13] provides for the reaction

$$EuS(s) = EuS(g), \qquad (6-9)$$

$\Delta H°_{298}$ = $135._4 \pm 3._1$ kcal gfw$^{-1}$. From this value and the third-law

enthalpy of vaporization [equation 5-11, $\Delta H°_{298}$ = $216._1 \pm 2._9$ kcal gfw$^{-1}$],

the dissociation energy of EuS(g) is computed as $D°_0$ = $79._8 \pm 4._2$

kcal gfw$^{-1}$ ($D°_{298}$ = $80._6 \pm 4._2$ kcal). As usual, the uncertainty reflects

the errors in the experimental and derived thermal functions. This

value may be compared with $D°_0[EuS(g)]$ = $85._9 \pm 3._5$ kcal gfw$^{-1}$ reported

by Smoes et al. (80) from the isomolecular exchange reaction

$$EuS(g) + Ti(g) = Eu(g) + TiS(g) \qquad (6-10)$$
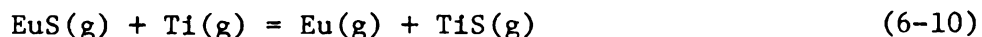
and $D°_0[TiS(g)]$ = $109._5 \pm 3._0$ kcal gfw$^{-1}$. However, the latter value is

now known to be in error (77) and the currently accepted value is

$D°_0[TiS(g)]$ = $101._8 \pm 1._8$ kcal gfw$^{-1}$. The revised dissociation energy

of EuS(g), $D°_0$ = $78._2 \pm 3._5$ kcal gfw$^{-1}$, is in excellent agreement with

the value calculated in this work.

## 6.2.10. EuSe Vaporization Data

At 1970 K the molecular EuSe species contributes no more than 0.1% $P_{Eu(g)}$ in the vaporization of the condensed material (sec. 5.6.4). With the thermodynamic functions derived by Bergman et al. (81) for EuSe(g) [Eu-Se $2.5_6$ Å, $\omega_e = 350$ cm$^{-1}$] and those obtained for EuSe(s) in this work (Table 15), the third-law enthalpy change for the sublimation reaction

$$EuSe(s) = EuSe(g) \qquad (6-11)$$

is calculated as $\Delta H°_{298} = 148._0 \pm 5._0$ kcal gfw$^{-1}$. By combining this value with the third-law vaporization enthalpy [equation 5-22, $\Delta H°_{298} = 210._3 \pm 2._2$ kcal gfw$^{-1}$], the dissociation energy, $D°_0[EuSe(g)]$, is computed as $61._6 \pm 5._5$ kcal gfw$^{-1}$ ($D°_{298} = 62._3 \pm 5._5$ kcal). Bergman et al. (81) from the mass spectrometric isomolecular exchange reaction

$$EuSe(g) + Se(g) = Eu(g) + Se_2(g) \qquad (6-12)$$
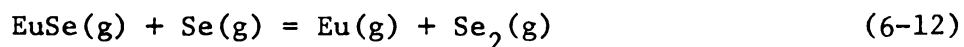
derived $D°_0[EuSe(g)] = 71._1 \pm 1._3$ kcal gfw$^{-1}$. The discrepancy will be discussed in the following section.

## 6.2.11. Comparison of the Vaporization Thermodynamics of Europium(II) Chalcogenides

The thermodynamic data for the vaporization reactions of europium(II) chalcogenides are collected in Table 25 along with the available data for the corresponding strontium compounds. The excellent consistency in each individual thermochemical quantity between the two series of compounds lends validity to the accuracy of the experimental data for europium compounds. The decreasing stabilities of the heteronuclear gaseous diatomic molecules from oxides to tellurides have been related (203)

Table 25.  Thermodynamic Data for the Oxides, Sulfides and Selenides of Europium and Strontium

| | EuO | SrO | EuS | SrS | EuSe | SrSe |
|---|---|---|---|---|---|---|
| $-\Delta H°_{f,298}[MX(s)]$, kcal gfw$^{-1}$ | $144.3 \pm 1.4$ | $141.5 \pm 1.0$ | $106.7 \pm 1.3$ | $108.3 \pm 4.0$ | $112.8 \pm 1.3$ | $92.2 \pm 4.0$ |
| $\Delta H°_{298}[MX(s) = MX(g)]$, kcal gfw$^{-1}$ | $130.5 \pm 7.6$ | $146 \pm 0.5$ | $135.4 \pm 3.1$ | $131.8 \pm 2.0$ | $148.0 \pm 5.0$ | — |
| $\Delta H°_{298}[MX(s) = M(g) + X(g)]$, kcal gfw$^{-1}$ | $256.7 \pm 10.0$ | $239.5 \pm 6.0$ | $216.1 \pm 2.9$ | $212.6 \pm 3.0$ | $210.3 \pm 2.2$ | — |
| $D°_0[MX(g)]$, kcal gfw$^{-1}$ | $125.3 \pm 7.5$ | $92.0 \pm 6.0$ | $79.8 \pm 4.2$ | $80.0 \pm 4.0$ | $61.6 \pm 5.5$ | $59.1 \pm 3.0$ |

Vaporization enthalpies derived from third-law

Strontium compounds, Ref. 195,196,204,205.

to a parameter $\alpha$ defined according to

$$\alpha = 0.5 \ \Delta H^{\circ}_{0}[\text{at.MX(s)}]/D^{\circ}_{0}[\text{MX(g)}], \qquad (6\text{-}13)$$

where $\Delta H^{\circ}_{0}[\text{at.MX(s)}]$ is the enthalpy change for the decomposition of

MX(s) to the component gaseous atoms and $D^{\circ}_{0}[\text{MX(g)}]$ is the dissociation

energy of the gaseous MX molecule. The tendency for $\alpha(> 1$, with the

exception of BaO) to increase from the oxides to the sulfides, indicative

of a decrease in thermal stability in that order, is observed for the

alkaline earth compounds. This behavior is amply satisfied in the

europium(II) compounds, for which $\alpha = 1.0_2$, $1.3_5$ and $1.7_1$ in the case of

EuO, EuS and EuSe, respectively.

Comprehensive thermochemical measurements on SrSe(s) are not

available and the enthalpy of formation, $\Delta H^{\circ}_{f,298}[\text{SrSe(s)}] =$

$-(92._2 \pm 4._0)$ kcal gfw$^{-1}$ is only a revised estimate (204) based on an

earlier solution calorimetric value $[-(78._7 \pm 4._0)$ kcal; Ref. 147]. The

enthalpy of formation of EuSe(s) is derived from the vaporization data

for reaction (5-22), $\Delta H^{\circ}_{298} = 210._3 \pm 2._2$ kcal gfw$^{-1}$, and this value is

in reasonable agreement with the mass spectrometric values of $202._0 \pm$

$3._0$ kcal (82) and $201._0 \pm 9._0$ kcal (this work).

Of particular interest are the dissociation energies of the europium

monoxide and monochalcogenides. The dissociation energies of the

lanthanide compounds have been related to the enthalpies of sublimation

of the respective metals (71,80,81). The double periodicity exhibited

by the trends in the sublimation enthalpies $(\Delta H^{\circ}_{0}[\text{Ln(s)} \rightarrow \text{Ln(g)}])$

corresponds to the $4 \ f^{n-1} \ d \rightarrow 4 \ f^{n}$ electronic transitions in going from

the condensed metal to free atomic states in the lanthanides. The

similar trends in the dissociation energies of the monoxides and

monochalcogenides were thus correlated to changes in the electronic structure of the metal ion in the bound state and the free metal gas. In particular, such behavior was presumed to indicate that the nature of bonding in these lanthanide compounds is similar to that in the condensed metals. The fairly consistent and systematic differences in the values of $\{D°_0[LnO(g)] - D°_0[LnS(g)]\}$, $\{D°_0[LnS(g)] - D°_0[LnSe(g)]\}$ and $\{D°_0[LnSe(g)] - D°_0[LnTe(g)]\}$ in the two halves (La-Eu and Gd-Yb) of the lanthanide series were also used to estimate dissociation energies of compounds that were not actually measured. However in all these correlations europium (and also ytterbium) compounds behave conspicuously differently from the other lanthanide compounds. It appears that a more reasonable correlation can be effected by comparing the quantities $\{D°_0[LnX(g)] - \Delta H°_{0,sub}\}$ for each series of compounds in the lanthanides. In Figure 8 we have plotted these quantities calculated from available and estimated sources (71,80,81) for all the lanthanide monoxides and monochalcogenides including those of europium obtained in the present work. The strikingly similar profile in the four series is essentially a comparison of the enthalpy change for the conversion, $Ln^{2+} \rightarrow Ln(s)$, in each series of compounds and it must remain reasonably constant. Estimations based on such correlations seem more consistent than those discussed previously. It is on this basis that we believe the dissociation energy of EuSe(g) derived in this work is more accurate than that of Bergman et al. (81). Extending the trend we estimate the dissociation energy of EuTe(g) as $36._0 \pm 5._0$ kcal gfw$^{-1}$.

### 6.2.12. Conclusions and Suggestions for Future Work

The thermodynamic data obtained in this research which led to this thesis form a comprehensive set of values for the europium(II) halides
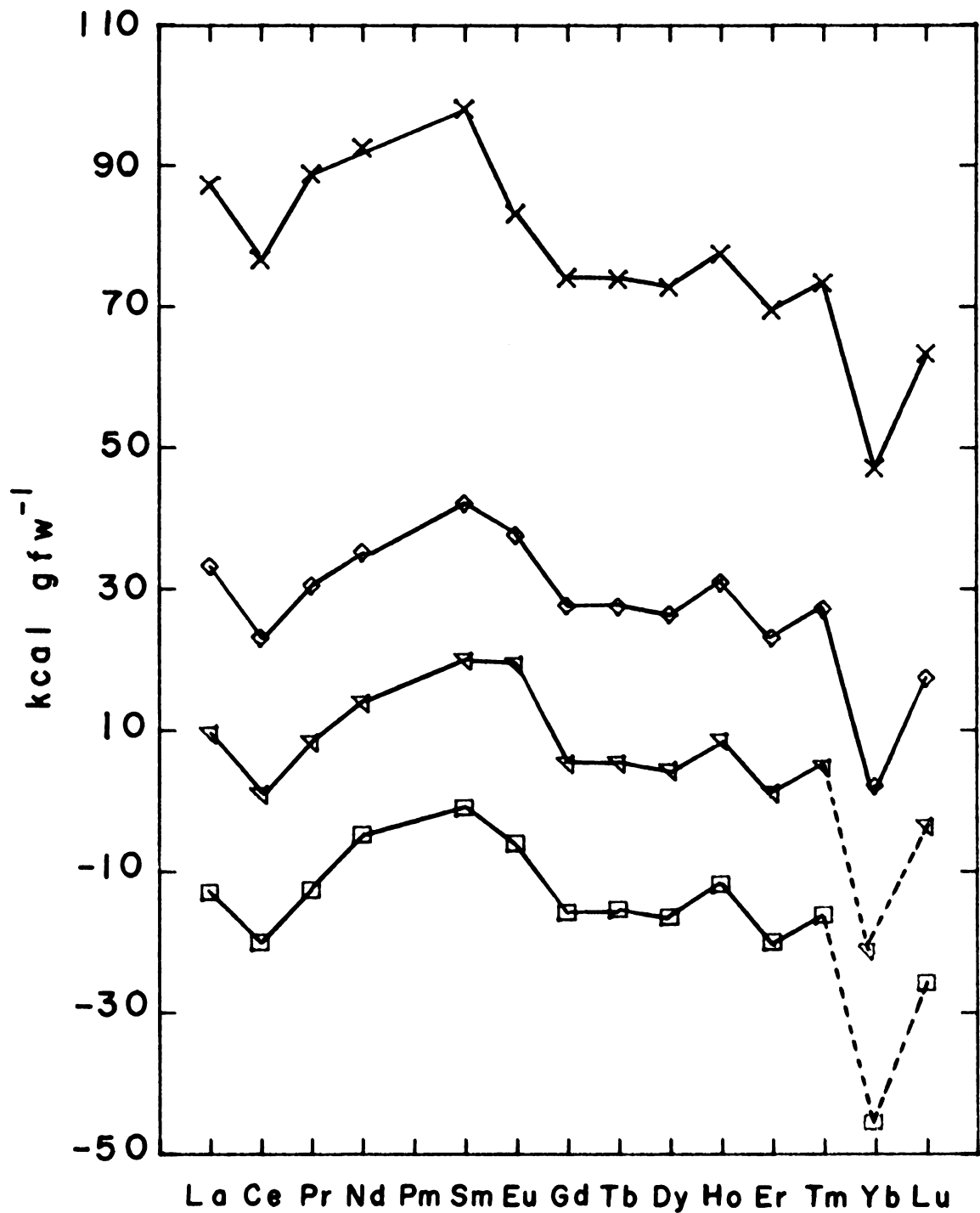
Figure 8.  Graph of the Difference Between the Dissociation Energies of the
Gaseous Lanthanide Monoxides and Monochalcogenides, and the
Enthalpies of Sublimation of the Elements versus Atomic Number

(X) $[D^{\circ}_0 \; LnO(g)-\Delta H^{\circ}_{0,sub}Ln(s)]$;  (◇) $[D^{\circ}_0 \; LnS(g)-\Delta H^{\circ}_{0,sub}Ln(s)]$

(▽) $[D^{\circ}_0 \; LnSe(g)-\Delta H^{\circ}_{0,sub}Ln(s)]$;  (□) $[D^{\circ}_0 \; LnTe(g)-\Delta H^{\circ}_{0,sub}Ln(s)]$

and monochalcogenides. An aspect that merits experimental investigation to complete the chalcogenide series is the vaporization thermodynamics of EuTe. Direct calorimetric enthalpies of formation of $EuF_2$, $EuBr_2$, $EuI_2$, EuS, EuSe and EuTe, heat capacity measurements in the series of compounds and molecular data on $EuBr_2$ and $EuI_2$ would help establish more accurate treatment of the experimental values than has been possible. More pertinent use of the present compilation is in establishing the thermodynamic properties of the halides and monochalcogenides of Yb(II) and Sm(II). A final analysis of the energetics and bonding in the predominantly divalent lanthanides can then be meaningfully attempted.

REFERENCES

## REFERENCES

1. G. Urbain and F. Bourion, <u>Compt. rend.</u>, 153, 1155 (1911).

2. W. Klemm and W. Döll, <u>Z. anorg. allg. Chem.</u>, 241, 233 (1939);

   W. Döll and W. Klemm, <u>ibid.</u>, 241, 239 (1939).

3. D. Brown, "Halides of the Lanthanides and Actinides", John Wiley

   and Sons, Ltd., London, 1968.

4. M. D. Taylor, <u>Chem. Rev.</u>, 62, 503 (1962).

5. M. D. Taylor and C. P. Carter, <u>J. Inorg. Nucl. Chem.</u>, 24, 387 (1962).

6. K. E. Johnson and J. R. Mackenzie, <u>ibid.</u>, 32, 43 (1970).

7. L. F. Drudig and J. D. Corbett, <u>J. Amer. Chem. Soc.</u>, 83, 2462 (1961).

8. O. G. Polyachenok and G. I. Novikov, <u>Russ. J. Inorg. Chem.</u>, 8,

   1378 (1963).

9. C. W. DeKock and D. D. Radtke, <u>J. Inorg. Nucl. Chem.</u>, 32, 3687 (1970).

10. J. K. Howell and L. L. Pytlewski, <u>J. Less-Common Metals</u>, 18, 437 (1969).

11. L. B. Asprey, F. H. Ellinger and E. Staritzky, Proc. Third Rare Earth

    Conf. (K. S. Vorres, ed.) p. 11, Gordon and Breach, New York, NY, 1964.

12. K. Lee, H. Muir and E. Catalano, <u>J. Phys. Chem. Solids</u>, 26, 523 (1965).

13. E. Catalano, R. G. Bedford, V. G. Silveira and H. H. Wickman, <u>ibid.</u>,

    30, 1613 (1969).

14. O. G. Polyachenok and G. I. Novikov, <u>Russ. J. Inorg. Chem.</u>, 9, 429 (1964).

15. J. M. Haschke and H. A. Eick, <u>J. Inorg. Nucl. Chem.</u>, 32, 2153 (1970).

16. K. Rossmanith, <u>Monatsh.</u>, 97, 87 (1966).

17. L. B. Asprey and F. H. Kruse, J. Inorg. Nucl. Chem., 13, 32 (1960); L. B. Asprey, T. K. Keenen and F. H. Kruse, Inorg. Chem., 3, 1137 (1964).

18. E. F. Westrum, Jr., "Progress in the Science and Technology of the Rare Earths" (L. Eyring, ed.), Vol. 1, p. 310, Pergamon Press, Long Island City, NY, 1964.

19. E. F. Westrum, Jr., ibid.,Vol. 2, p. 35, 1966.

20. E. F. Westrum, Jr., ibid.,Vol. 3, p. 459, 1968.

21. G. V. Samsonov, "High Temperature Compounds of Rare Earth Metals with Non-Metals", Consultants Bureau, New York, NY, 1965.

22. J. Flahaut and P. Laruelle, "Progress in the Science and Technology of the Rare Earths", op. cit., Vol. 3, p. 149, 1968.

23. A. Michel, (ed.), "Proprietes Thermodynamiques Physiques et Structurales Des Derives Semi-Metalliques", No. 157, Editions Du Centre National De la Recherche Scientifique, Paris, 1967.

24. H. A. Eick, N. Baenzinger and L. Eyring, J. Amer. Chem. Soc., 78, 5147 (1956).

25. H. Baernighausen, J. Prakt. Chem., 34, 1 (1966).

26. E. Kaldis, J. Crystal Growth.,3, 146 (1968).

27. C. J. Kershner, R. J. De Sando, R. F. Heidelberg and R. H. Steinmeyer, J. Inorg. Nucl. Chem., 28, 1581 (1966).

28. M. W. Shafer, U. S. Patent No. 3353907 (1967); Chem. Abstr., 68, 61076e (1968).

29. N. A. Fishel, J. M. Haschke and H. A. Eick, Inorg. Chem., 9, 413 (1970).

30. O. A. Sadovskaya, E. I. Yarembash and E. N. Naginaev, Izv. Akad. Nauk SSSR. Neorgan. Mat. (Engl. Trans).,7, 284 (1971).

31. W. Klemm and H. Senff, Z. anorg. allg. Chem., 241, 259 (1939).

32. H. Baernighausen, H. P. Beck and H. W. Grueninger, Proc. Ninth Rare Earth Research Conf., Blacksburg, Va, 1971.

33. J. J. Stezowski and H. A. Eick, _Inorg. Chem._, 9, 1102 (1970).

34. H. Baernighausen and N. Schultz, _Acta Cryst._, B25, 1104 (1969).

35. C. E. Holley, Jr., E. J. Huber, Jr. and F. B. Baker, "Progress in the Science and Technology of the Rare Earths", _op. cit._, Vol. 3, p. 343, 1968.

36. D. A. Johnson, _J. Chem. Soc. (A)_.,2578 (1969).

37. L. Brewer, L. A. Bromely, P. W. Gilles and N. L. Lofgren, "Chemistry and Metallurgy of Miscellaneous Materials:  Thermodynamics", Paper 6 (L. L. Quill, ed.), McGraw-Hill Publications, New York, NY, 1950.

38. L. Brewer, _ibid_.,Paper 7.

39. R. C. Feber, U. S. Atomic Energy Commission Report LA-3764, Los Alamos, NM, 1965.

40. G. I. Novikov and O. G. Polyachenok, _Russ. Chem. Rev._, 33, 342 (1964).

41. T. V. Charlu, A. K. Chaudhuri and J. L. Margrave, _High Temp. Sci._, 2, 1 (1970).

42. A. S. Dworkin and M. A. Bredig, _J. Phys. Chem._, 67, 697 (1963).

43. A. S. Dworkin and M. A. Bredig, _ibid._, 67, 2499 (1963).

44. A. S. Dworkin and M. A. Bredig, _High Temp. Sci._, 3, 81 (1971).

45. C. T. Stubblefield, J. L. Rutledge and R. Phillips, _J. Phys. Chem._, 69, 991 (1965).

46. G. R. Machlan, C. T. Stubblefield and L. Eyring, _J. Amer. Chem. Soc._, 77, 2975 (1955).

47. R. W. Mar and A. W. Searcy, _J. Phys. Chem._, 71, 888 (1967).

48. M. Lim and A. W. Searcy, _ibid._, 70, 1762 (1966).

49. H. B. Skinner and A. W. Searcy, _ibid._, 72, 3375 (1968).

50. R. A. Kent, K. F. Zmbov, A. S. Kanaan, G. Besenbruch, J. D. McDonald and J. L. Margrave, *J. Inorg. Nucl. Chem.*, 28, 1419 (1966).

51. K. F. Zmbov and J. L. Margrave, *J. Chem. Phys.*, 45, 3167 (1966).

52. G. Besenbruch, T. V. Charlu, K. F. Zmbov and J. L. Margrave, *J. Less-Common Metals.*, 12, 375 (1967).

53. K. F. Zmbov and J. L. Margrave, *ibid.*, 12, 494 (1967).

54. K. F. Zmbov and J. L. Margrave, Advances in Chemistry Series, No. 72, p. 267, American Chemical Society, Washington, D.C., 1968.

55. K. F. Zmbov and J. L. Margrave, *J. Inorg. Nucl. Chem.*, 29, 59 (1967).

56. H. B. Skinner and A. W. Searcy, *J. Phys. Chem.*, 75, 108 (1971).

57. T. Petzel and O. Greis, *Z. anorg. allg. Chem.*, 388, 137 (1972).

58. E. R. Harrison, *J. Appl. Chem.*, 2, 601 (1952).

59. V. Shimazaki and K. Niwa, *Z. anorg. allg. Chem.*, 314, 21 (1962).

60. J. L. Moriarty, *J. Chem. Eng. Data.*, 8, 422 (1963).

61. O. G. Polyachenok and G. I. Novikov, *Russ. J. Inorg. Chem.*, 8, 793 (1963).

62. F. Weigel and G. Trinkl, *Z. anorg. allg. Chem.*, 377, 228 (1970).

63. C. Hirayama and F. E. Camp, American Chemical Society Meeting, Washington, D.C., 1971.

64. J. M. Haschke and H. A. Eick, *J. Phys. Chem.*, 74, 1806 (1970).

65. J. W. Hastie, P. Ficalora and J. L. Margrave, *J. Less-Common Metals.*, 14, 83 (1968).

66. R. L. Montgomery, U. S. Bureau of Mines, Report of Investigations, No. 5468, U. S. Department of the Interior, Washington, D.C., 1959.

67. J. L. Burnett and B. B. Cunningham, U. S. Atomic Energy Commission Report UCRL-11126, University of California, Berkeley, CA, 1964.

68. E. J. Huber, Jr. and C. E. Holley, Jr., <u>J. Chem. Thermodynamics</u>, 1, 301 (1969); 2, 896 (1970).

69. J. M. Haschke and H. A. Eick, <u>J. Phys. Chem.</u>, 73, 374 (1969).

70. D. White, P. N. Walsh, L. L. Ames and H. W. Goldstein, "Thermodynamics of Nuclear Materials", p. 417, International Atomic Energy Agency, Vienna, 1962.

71. L. L. Ames, P. N. Walsh and D. White, <u>J. Phys. Chem.</u>, 71, 2707 (1967).

72. M. B. Panish, <u>J. Chem. Phys.</u>, 34, 1079, 2197 (1961).

73. E. D. Cater, T. E. Lee, E. W. Johnson, E. G. Rauh and H. A. Eick, <u>J. Phys. Chem.</u>, 69, 2684 (1965).

74. E. D. Cater and R. P. Steiger, <u>ibid.</u>, 72, 2231 (1968).

75. T. Petzel and P. W. Gilles, A Private Communication (1968) in Ref. 77.

76. E. D. Cater, B. A. Holler and J. A. Fries, U. S. Atomic Energy Commission Report, No. COO-1182-15, University of Iowa, Iowa City, IA, 1967.

77. R. L. Wu., Ph.D. Thesis, University of Kansas, Lawrence, KA, 1971.

78. R. P. Steiger and E. D. Cater, U. S. Atomic Energy Commission Report, No. COO-1182-23, University of Iowa, Iowa City, IA, 1968.

79. P. Coppens, S. Smoes and J. Drowart, <u>Trans. Faraday Soc.</u>, 63, 2140 (1967).

80. S. Smoes, P. Coppens, C. Bergman and J. Drowart, <u>ibid.</u>, 65, 682 (1969).

81. C. Bergman, P. Coppens, J. Drowart and S. Smoes, <u>ibid.</u>, 66, 800 (1970).

82. S. P. Gordienko, V. V. Fesenko, B. V. Fenochka and A. A. Lysenko, <u>Zh. Fiz. Khim.</u>, 45, 1932 (1971).

83. R. P. Steiger and J. C. Miles, <u>J. Inorg. Nucl. Chem.</u>, 32, 3469 (1970).

84. P. A. Akishin, N. G. Rambidi and V. P. Spiridinov, "The Characterization of High Temperature Vapors" (J. L. Margrave, ed.), p. 300, John Wiley and Sons, Inc., New York, NY, 1967.

85. R. H. Hauge, J. W. Hastie and J. L. Margrave, J. Less-Common Metals., 23, 359 (1971).

86. R. D. Wesley and C. W. DeKock, J. Chem. Phys., 55, 3866 (1971).

87. E. W. Kaiser, W. E. Falconer and W. Klemperer, ibid., 56, 5392 (1972).

88. J. W. Hastie, R. H. Hauge and J. L. Margrave, High Temp. Sci., 3, 56 (1971).

89. C. W. DeKock, R. D. Wesley and D. D. Radtke, ibid., 4, 41 (1972).

90. R. L. DeKock and W. Weltner, Jr., J. Phys. Chem., 75, 514 (1971).

91. M. Kaufman, J. Muenter and W. Klemperer, J. Chem. Phys., 47, 3365 (1967).

92. L. Brewer and G. M. Rosenblatt, Chem. Rev., 61, 257 (1961).

93. L. Brewer and D. F. Mastick, J. Chem. Phys., 19, 834 (1951).

94. W. Weltner, Jr., D. McLeod, Jr. and P. H. Kasai, ibid., 46, 3172 (1967); P. H. Kasai and W. Weltner, Jr., ibid., 43, 2553 (1965).

95. A. Adams, W. Klemperer and T. M. Dunn., Can. J. Phys., 46, 2213 (1968).

96. U. Uhler and L. Akerlind., Arkiv. Fysik., 19, 1 (1961).

97. R. A. Berg, L. Wharton, W. Klemperer, A. Buchler and J. L. Stauffer, J. Chem. Phys., 43, 2416 (1965).

98. D. W. Green, Can. J. Phys., 49, 2552 (1971).

99. N. S. McIntyre, K. C. Lin and W. Weltner, Jr., J. Chem. Phys., 56, 5576 (1972).

100. K. D. Carlson, E. Ludena and C. Moser, ibid., 43, 2408 (1965).

101. J. L. Margrave, "Physicochemical Measurements at High Temperatures" (J. O'M. Bockris, J. L. White and J. D. Mackenzie, eds.), Chapter 10, Butterworths Scientific Publications, London, 1959.

102. H. Hertz, *Ann. Physik.*, 17,177 (1882).

103. M. Knudsen, *ibid.*, 29, 179 (1909).

104. P. Clausing, *ibid.*, 12, 961 (1932).

105. W. C. DeMarcus, U. S. Atomic Energy Commission Report K-1302 (Parts 1-6), Oak Ridge, Tenn, 1957.

106. E. W. Balson, *J. Phys. Chem.*, 65, 1151 (1961).

107. R. P. Iczkowski, J. L. Margrave and S. M. Robinson, *ibid.*, 67, 229 (1963).

108. V. Ruth and J. P. Hirth, "Condensation and Evaporation of Solids" (E Rutner, R. Goldfinger and J. P. Hirth, eds.), p. 99, Gordon and Breach, New York, NY, 1964.

109. J. G. Edwards and P. W. Gilles, *J. Chem. Phys.*, 44, 4426 (1966).

110. R. D. Freeman and J. G. Edwards, "The Characterization of High Temperature Vapors", *op. cit.*, p. 508.

111. T. E. Dunham and J. P. Hirth, *J. Chem. Phys.*, 49, 4650 (1968).

112. W. L. Winterbottom and J. P. Hirth, *ibid.*, 37, 784 (1962).

113. W. L. Winterbottom, *ibid.*, 47, 3546 (1967).

114. W. L. Winterbottom, *ibid.*, 49, 106 (1968).

115. K. C. Wang and P. G. Wahlbeck, *ibid.*, 47, 4799 (1967).

116. C. I. Whitman, *ibid.*, 20, 161 (1952); M. G. Rossman and J. Yarwood, *ibid.*, 21, 1406 (1953); C. I. Whitman, *ibid.*, 21, 1407 (1953).

117. K. Motzfeldt, *J. Phys. Chem.*, 59, 139 (1955).

118. K. D. Carlson, P. W. Gilles and R. J. Thorn., *J. Chem. Phys.*, 38, 2064, 2725 (1963).

119. J. P. Hirth and G. M. Pound, *Prog. Mat. Sci.*, 11, 1 (1963).

120. D. E. Work, Ph.D. Thesis, Michigan State University, East Lansing, MI, 1972.

121. G. M. Pound, _J. Phys. Chem. Ref. Data._, 1, 135 (1972).

122. R. C. Paule and J. L. Margrave, "The Characterization of High Temperature Vapors", _op. cit._, p. 130.

123. M. Knudsen, _Ann. Physik._, 28, 999 (1909).

124. F. Knauer and O. Stern, _Z. Physik._, 39, 764 (1926).

125. R. J. Ackermann, P. W. Gilles and R. J. Thorn, _J. Chem. Phys._, 25, 1089 (1956).

126. P. G. Wahlbeck and T. E. Phipps, _ibid._, 49, 1603 (1968).

127. J. Q. Adams, T. E. Phipps and P. G. Wahlbeck, _ibid._, 49, 1609 (1968).

128. K. C. Wang and P. G. Wahlbeck, _ibid._, 49, 1617 (1968).

129. D. A. Schulz and A. W. Searcy, _J. Phys. Chem._, 67, 103 (1963).

130. J. W. Ward, R. N. R. Mulford and M. Kahn, _J. Chem. Phys._, 47, 1710 (1967).

131. J. W. Ward, R. N. R. Mulford and R. L. Bivins, _ibid._, 47, 1718 (1967).

132. J. L. Margrave, "Physicochemical Measurements at High Temperatures", _op. cit._, Chapter 2.

133. R. J. Corruccini, "Treatise on Analytical Chemistry" (I. M. Kolthoff, P. J. Elving and E. B. Sandell, eds.), Vol. 8, Part 1, Chapter 87, Interscience Publishers, New York, NY, 1968.

134. F. D. Rossini, _J. Chem. Thermodynamics._, 2, 447 (1970).

135. T. B. Douglas, _J. Res. Natl. Bur. Std._, 73A, 451 (1969).

136. J. Drowart and P. Goldfinger, _Angew. Chem. Internat. Edit._, 6, 581 (1967).

137. R. T. Grimeley, "The Characterization of High Temperature Vapors", _op. cit._, Chapter 8.

138. J. E. Collin, "Mass Spectrometry" (R. I. Reed, ed.), p. 183, Academic Press, New York, NY, 1965.

139. G. W. Otvos and D. P. Stevenson, _J. Amer. Chem. Soc._, 78, 546 (1956).

140. J. B. Mann, _J. Chem. Phys._, 46, 1646 (1967).

141. J. W. Hastie and J. L. Margrave, "Fluorine Chemistry Reviews" (P. Tarrant, ed.), Vol. 2, p. 77, Marcel Dekker, Inc., New York, NY, 1968.

142. J. W. Hastie and J. L. Margrave, _High Temp. Sci._, 1, 481 (1969).

143. R. Jenkins and J. L. De Vries, "Practical X-ray Spectrometry", Springer-Verlag, Inc., New York, NY, 1967.

144. L. S. Birks, "X-Ray Spectrochemical Analysis", Second Edition, Interscience Publishers, New York, NY, 1969.

145. J. R. McCreary and R. J. Thorn, _J. Chem. Phys._, 50, 3725 (1969).

146. W. S. Horton, _J. Res. Natl. Bur. Std._, 70A, 533 (1966).

147. O. Kubaschewski and E. Ll. Evans, "Metallurgical Thermochemistry", Pergamon Press, New York, NY, 1958.

148. G. N. Lewis and M. Randall, "Thermodynamics", revised by K. S. Pitzer and L. Brewer, Second Edition, McGraw-Hill Book Co., New York, NY, 1961.

149. D. Cubicciotti, _J. Phys. Chem._, 70, 2410 (1966).

150. J. R. McCreary and R. J. Thorn, _High Temp. Sci._, 3, 330 (1971).

151. R. J. Thorn, _ibid._, 3, 197 (1971).

152. E. R. Plante, A. B. Sessoms and K. R. Fitch, _J. Res. Natl. Bur. Std._, 74A, 647 (1970).

153. D. R. Stull and H. Prophet, "The Characterization of High Temperature Vapors", _op. cit._, Chapter 13.

154. H. H. Kellogg, "Application of Fundamental Thermodynamics to Metallurgical Problems" (G. R. Fitterer, ed.), p. 357, Gordon and Breach, New York, NY, 1967.

155. J. M. Haschke, Ph.D. Thesis, Michigan State University, East Lansing, MI, 1969.

156. W. M. Latimer, _J. Amer. Chem. Soc._, 73, 1480 (1951).

157. F. Gronvold and E. F. Westrum, Jr., _Inorg. Chem_, 1, 36 (1962).

158. E. F. Westrum, Jr., Advances in Chemistry Series, No. 71, p. 25, American Chemical Society, Washington, D.C., 1967.

159. K. A. Gschneidner, Jr., _Solid State Phys_, 16, 275 (1964).

160. T. L. Hill, "An Introduction to Statistical Thermodynamics", Addison-Wesley Publishing Co. Inc., Reading, MA, 1960.

161. J. J. Stezowski, Ph.D. Thesis, Michigan State University, East Lansing, MI, 1968.

162. J. M. Haschke and H. A. Eick, _J. Amer. Chem. Soc._, 92, 4550 (1970).

163. "Treatise on Analytical Chemistry", _op. cit_., Vol. 8, Part 2, 1963.

164. _ibid_., Vol. 7, Part 2, 1961.

165. "Standard Methods of Chemical Analysis" (N. H. Furman, ed.), Vol. 1, Sixth Edition, Van Nostrand Co. Inc., Princeton, NJ, 1962.

166. P. A. Pilato, Ph.D. Thesis, Michigan State University, East Lansing, MI, 1968.

167. R. A. Kent, Ph.D. Thesis, Michigan State University, East Lansing, MI, 1963.

168. R. L. Seiver, Ph.D. Thesis, Michigan State University, East Lansing, MI, 1971.

169. H. J. Neff, _Arch. Eisenhuettenw_., 34, 903 (1963); Siemens Pamphlet Eg 4/10e, August, 1964.

170. A. C. Larson, R. B. Roof and D. T. Cromer, U. S. Atomic Energy Commission Report LA-3335, Los Alamos, NM, 1965.

171. H. Baernighausen, _J. Prakt. Chem_., 14, 313 (1961).

172. A. C. Parr, <u>J. Chem. Phys.</u>, 54, 3161 (1971).

173. R. E. Toehman, R. A. Kent and J. L. Margrave, <u>J. Chem. Eng. Data.</u>, 10, 296 (1965).

174. A. S. Dworkin and M. A. Bredig, <u>ibid.</u>, 8, 416 (1963).

175. K. K. Kelley, "Contributions to the Data on Theoretical Metallurgy, XIII. High Temperature Heat Content, Heat Capacity and Entropy Data for the Elements and Inorganic Compounds", Bureau of Mines Bulletin, 584, U. S. Government Printing Office, Washington, D.C., 1960.

176. K. K. Kelley and E. G. King, "Contributions to the Data on Theoretical Metallurgy, XIV. Entropies of the Elements and Inorganic Compounds", Bureau of Mines Bulletin, 592, U. S. Government Printing Office, Washington, D.C., 1961.

177. G. J. Janz, F. J. Kelly and J. L. Perano, <u>Trans. Faraday Soc.</u>, 59, 2718 (1963).

178. C. E. Haaberman and A. H. Daane, <u>J. Chem. Phys.</u>, 41, 2818 (1964).

179. "Janaf Thermochemical Tables" (D. R. Stull, ed.), Dow Chemical Co., Midland, MI, 1965.

180. L. Wharton, R. A. Berg and W. Klemperer, <u>J. Chem. Phys.</u>, 39, 2023 (1963).

181. E. F. Hayes, <u>J. Phys. Chem.</u>, 70, 3740 (1966).

182. L. Brewer, G. R. Somayajulu and E. Brackett, <u>Chem. Rev.</u>, 63, 111 (1963).

183. G. Herzberg, "Molecular Spectra and Molecular Structure. Infrared Spectra of Diatomic Molecules", D. Van Nostrand and Co. Inc., Princeton, NJ, 1950.

184. R. C. Feber and C. C. Herrick, U. S. Atomic Energy Commission Report LA-3184, Los Alamos, NM, 1965.

185. D. R. Stull and G. C. Sinke, Advances in Chemistry Series, No. 18, American Chemical Society, Washington, D. C., 1956.

186. R. F. Barrow, G. G. Chandler and C. B. Meyer, Phil. Trans., 260A, 395 (1966).

187. J. Berkowitz, "Advances in High Temperature Chemistry" (L. Eyring, ed.), Vol. 3, p. 163, Academic Press, New York, NY, 1971.

188. R. E. Honig, "The Characterization of High Temperature Vapors", op. cit., p. 475.

189. E. Storms, High Temp. Sci., 1, 456 (1969).

190. J. C. Slater, J. Chem. Phys., 41, 3199 (1964).

191. D. L. Hildenbrand, ibid., 52, 5751 (1970), Int. J. Mass Spectrom. Ion. Phys., 4, 75 (1970).

192. S. L. Bacon, M.S. Thesis, Michigan State University, East Lansing, MI, 1971.

193. J. R. Marquart and J. Berkowitz, J. Chem. Phys., 39, 275, 283 (1963).

194. R. Colin, P. Goldfinger and M. Jeunnehomme, Trans. Faraday Soc., 60, 306 (1964).

195. E. D. Cater and E. W. Johnson, J. Chem. Phys., 47, 5353 (1967).

196. J. Berkowitz and W. A. Chupka, ibid., 45, 4289 (1966).

197. R. F. Porter, W. A. Chupka and M. G. Inghram, ibid., 23, 1347 (1955).

198. D. L. Hildenbrand, A Private Communication, 1971.

199. V. Calder, D. E. Mann, K. S. Seshadri, M. Allavena and D. White, J. Chem. Phys., 51, 2093 (1969).

200. D. L. Hildenbrand, "Advances in High Temperature Chemistry", op. cit., Vol. 1, p. 193, 1967.

201. A. W. Searcy, "Chemical and Mechanical Behavior of Inorganic Materials" (A. W. Searcy, D. V. Ragone and U. Colombo, eds.), p. 15, Wiley Interscience, New York, NY, 1970.

202. K. A. Gschneidner, Jr., _J. Less-Common Metals_ 25, 405 (1971).

203. R. Colin and P. Goldfinger, "Condensation and Evaporation of Solids", _op. cit._, p. 165.

204. V. B. Parker, D. D. Wagman and W. H. Evans, "Selected Values of Chemical Thermodynamic Properties", NBS Technical Note 270-6, U. S. Department of Commerce, Washington, D.C., 1971.

205. L. Brewer and G. M. Rosenblatt, "Advances in High Temperature Chemistry", op. cit., Vol. 2, p. 1, 1969.

206. National Bureau of Standards, special publication 260-21, U. S. Department of Commerce, Washington, D.C., 1971.

APPENDICES

# APPENDIX 1

## VAPOR PRESSURE OF SILVER

A redetermination of the vapor pressure of liquid silver was effected according to the procedure described in sec. 4.8.5 to establish the suitability of the experimental arrangement for reliable vapor pressure measurements. Three independent target collection Knudsen effusion experiments were performed with silver (Ag wire, 18 B & S gage, Analytical reagent grade; E. H. Sargent and Co., Chicago, IL) in the temperature range 1242-1570 K. Symmetric graphite effusion cells had knife-edge orifices with areas 1.18, 5.62 and 7.25 X $10^{-3}$ $cm^2$. Effusates which collected on liquid nitrogen cooled platinum targets were assayed by X-ray fluorescence. The Ag $L\alpha_1$ radiation ($\lambda$ = 4.154 Å) was determined at the peak maximum ($2\theta$ = 76.53°; graphite analyzing crystal) with the Norelco Universal Vacuum Spectrograph in conjunction with a flow proportional counter. A pulse height of 2.6 v and channel width of 2.3 v was utilized for a one minute counting. Calibration of the analytical procedure by use of standard silver nitrate solutions yielded a count rate of 1033 ± 15 counts per μg Ag.

The 29 vapor pressure-temperature data points yielded the unweighted linear least squares equation

$$\ln P_{Ag(g)atm} = -(329_{40} \pm 1_{70})/T + 14.3_3 \pm 0.1_2 \tag{A1-1}$$

At the median temperature (1406 K), $\Delta H^\circ = 65.4_6 \pm 0.3_4$ kcal gfw$^{-1}$ and

$\Delta S^\circ = 28.4_8 \pm 0.2_5$ eu. By use of the thermal functions for condensed

and monatomic gaseous silver (206) the median temperature data were

reduced to 298.15 K to give, for the sublimation of silver, the second-

law values, $\Delta H^\circ_{298} = 69.4_0 \pm 0.6_8$ kcal gfw$^{-1}$ and $\Delta S^\circ_{298} = 33.3_2 \pm 0.5_0$ eu.

A temperature-independent third-law sublimation enthalpy of $\Delta H^\circ_{298} =$

$67.3_1 \pm 0.2_3$ kcal gfw$^{-1}$ was also reduced.

The National Bureau of Standards has recently analyzed inter-

laboratory measurements of the vapor pressure of silver (206). The

pooled average sublimation enthalpy values are: second-law $\Delta H^\circ_{298} =$

$68.9_7 \pm 0.5_7$ kcal gfw$^{-1}$; third-law $\Delta H^\circ_{298} = 68.0_1 \pm 0.3_0$ kcal gfw$^{-1}$.

The good correspondence of the vapor pressure and enthalpy data of

silver obtained in the present work with the NBS-accepted values confirm

that accurate pressure measurements can be obtained by the procedure

followed in this research.

Table A-1. Silver Vaporization Data

| $T_K$ | $- \ln P$ (atm) | $\Delta H^\circ s,298$ (kcal/gfw) | $T_K$ | $- \ln P$ (atm) | $\Delta H^\circ s,298$ (kcal/gfw) |
|------|-----------------|-----------------------------------|-------|-----------------|-----------------------------------|
| 1291 | 11.1187 | 67.34 | 1530 | 7.1916 | 66.95 |
| 1304 | 10.9884 | 67.63 | 1540 | 7.0273 | 66.85 |
| 1349 | 10.0558 | 67.31 | 1570 | 6.7077 | 67.05 |
| 1363 | 9.8172 | 67.31 | 1569 | 6.6048 | 66.69 |
| 1370 | 9.7443 | 67.43 | 1531 | 7.2169 | 67.07 |
| 1375 | 9.6360 | 67.36 | 1274 | 11.5691 | 67.65 |
| 1419 | 8.9340 | 67.38 | 1280 | 11.4034 | 67.53 |
| 1419 | 8.8564 | 67.16 | 1293 | 11.2019 | 67.65 |
| 1403 | 9.1202 | 67.20 | 1311 | 10.9295 | 67.82 |
| 1372 | 9.6188 | 67.18 | 1314 | 10.6829 | 67.32 |
| 1395 | 9.3295 | 67.42 | 1285 | 11.2693 | 67.43 |
| 1418 | 8.9069 | 67.26 | 1263 | 11.7518 | 67.56 |
| 1454 | 8.2737 | 67.01 | 1250 | 12.0020 | 67.54 |
| 1481 | 7.9096 | 67.09 | 1242 | 12.1741 | 67.56 |
| 1502 | 7.6148 | 67.09 | | | |

## APPENDIX 2

### EQUILIBRIUM PRESSURE AND THIRD-LAW ENTHALPY DATA

Appendix 2-A.  Europium(II) Chloride Vaporization

| $T_K$ | $- \ln P$ (atm) | $\Delta H°_{v,298}$ (kcal/gfw) | $T_K$ | $- \ln P$ (atm) | $\Delta H°_{v,298}$ (kcal/gfw) |
|------|------|------|------|------|------|
| 1288 | 11.6224 | 76.94 | 1219 | 13.1328 | 76.86 |
| 1313 | 11.1230 | 76.97 | 1222 | 13.0546 | 76.85 |
| 1310 | 11.2079 | 77.04 | 1242 | 12.6868 | 77.08 |
| 1337 | 10.6590 | 77.00 | 1254 | 12.3134 | 76.83 |
| 1362 | 10.0691 | 76.69 | 1256 | 12.3271 | 76.97 |
| 1381 | 9.6837 | 76.58 | 1409 | 9.1468 | 76.45 |
| 1394 | 9.4033 | 76.44 | 1427 | 8.8292 | 76.40 |
| 1409 | 9.1135 | 76.35 | 1440 | 8.5994 | 76.36 |
| 1436 | 8.6385 | 76.28 | 1465 | 8.2488 | 76.49 |
| 1436 | 8.6378 | 76.28 | 1477 | 8.1382 | 76.71 |
| 1244 | 12.4889 | 76.70 | 1505 | 7.7247 | 76.74 |
| 1267 | 12.0237 | 76.82 | 1521 | 7.4937 | 76.75 |
| 1263 | 12.1119 | 76.82 | 1539 | 7.2255 | 76.71 |
| 1288 | 11.5582 | 76.77 | 1563 | 6.8400 | 76.54 |
| 1306 | 11.1683 | 76.72 | 1563 | 6.8341 | 76.52 |
| 1324 | 10.7869 | 76.67 | 1412 | 9.2306 | 76.82 |
| 1343 | 10.3783 | 76.56 | 1429 | 8.8929 | 76.68 |
| 1363 | 9.9708 | 76.47 | 1471 | 8.1539 | 76.49 |

Appendix 2-A (Cont.)

| $T_K$ | $- \ln P$ (atm) | $\Delta H^\circ_{v,298}$ (kcal/gfw) | $T_K$ | $- \ln P$ (atm) | $\Delta H^\circ_{v,298}$ (kcal/gfw) |
|-------|-----------------|-------------------------------------|-------|-----------------|-------------------------------------|
| 1375  | 9.7199          | 76.38                               | 1501  | 7.6557          | 76.36                               |
| 1374  | 9.8249          | 76.62                               | 1521  | 7.3498          | 76.31                               |
| 1135  | 15.3958         | 77.12                               | 1537  | 7.1332          | 76.34                               |
| 1163  | 14.5864         | 77.00                               | 1569  | 6.6720          | 76.26                               |
| 1175  | 14.3036         | 77.06                               | 1569  | 6.6594          | 76.22                               |
| 1191  | 13.8119         | 76.86                               | 1554  | 6.9132          | 76.38                               |
| 1207  | 13.4796         | 77.01                               |       |                 |                                     |

Appendix 2-B. Europium(II) Iodide Vaporization

| $T_K$ | $-\ln P$ (atm) | $\Delta H^\circ_{v,298}$ (kcal/gfw) | $T_K$ | $-\ln P$ (atm) | $\Delta H^\circ_{v,298}$ (kcal/gfw) |
|---|---|---|---|---|---|
| 1203 | 10.1630 | 68.83 | 1086 | 12.9611 | 68.81 |
| 1225 | 9.7005 | 68.82 | 1115 | 12.2814 | 68.98 |
| 1227 | 9.6343 | 68.76 | 1130 | 11.9396 | 69.05 |
| 1238 | 9.4354 | 68.82 | 1158 | 11.2719 | 69.06 |
| 1255 | 9.1258 | 68.89 | 1172 | 10.8236 | 68.77 |
| 1281 | 8.6160 | 68.85 | 1197 | 10.3904 | 69.06 |
| 1293 | 8.3896 | 68.84 | 1195 | 10.4101 | 69.00 |
| 1310 | 8.1059 | 68.89 | 1187 | 10.5801 | 68.99 |
| 1310 | 8.0579 | 68.77 | 1160 | 11.0646 | 68.69 |
| 1268 | 8.8359 | 68.79 | 1136 | 11.7683 | 69.00 |
| 1286 | 8.4682 | 68.71 | 1194 | 10.4429 | 69.03 |
| 1303 | 8.1233 | 68.62 | 1213 | 10.0128 | 68.97 |
| 1325 | 7.7088 | 68.54 | 1231 | 9.6078 | 68.90 |
| 1344 | 7.4115 | 68.60 | 1245 | 9.3920 | 69.06 |
| 1376 | 6.8212 | 68.40 | 1261 | 9.0705 | 69.04 |
| 1395 | 6.5807 | 68.55 | 1272 | 8.8480 | 69.01 |
| 1395 | 6.6121 | 68.64 | 1277 | 8.7808 | 69.08 |
| 1376 | 6.8741 | 68.55 | 1255 | 9.2033 | 69.08 |
| 1368 | 7.1244 | 68.88 | 1242 | 9.4471 | 69.05 |
| 1350 | 7.3686 | 68.75 | 1210 | 10.1055 | 69.05 |

Appendix 2-C.  Europium(II) Sulfide Vaporization

| $T_K$ | $-\ln P$ (atm) | $\Delta H^\circ_{v,298}$ (kcal/gfw) | $T_K$ | $-\ln P$ (atm) | $\Delta H^\circ_{v,298}$ (kcal/gfw) |
|---|---|---|---|---|---|
| 2068 | 10.6179 | 215.40 | 1898 | 12.9955 | 215.94 |
| 2093 | 10.3385 | 215.59 | 1955 | 12.1335 | 215.64 |
| 2109 | 10.2254 | 216.17 | 1860 | 13.5014 | 215.50 |
| 2132 | 9.8994 | 215.77 | 2035 | 11.1195 | 216.01 |
| 2159 | 9.6096 | 215.92 | 2109 | 10.0963 | 215.22 |
| 2176 | 9.4087 | 215.85 | 2139 | 9.8248 | 215.82 |
| 2200 | 9.1287 | 215.74 | 2162 | 9.5247 | 215.54 |
| 2201 | 9.1334 | 215.86 | 2190 | 9.2369 | 215.73 |
| 2220 | 8.8917 | 215.58 | 2222 | 8.8367 | 215.32 |
| 2221 | 9.0067 | 216.55 | 2222 | 8.8733 | 215.61 |
| 1956 | 12.3157 | 216.98 | 2196 | 9.1992 | 215.94 |
| 1961 | 12.0987 | 215.97 | 2161 | 9.6503 | 216.40 |
| 1999 | 11.5602 | 215.81 | 2127 | 10.1662 | 217.32 |
| 2025 | 11.2241 | 215.84 | 2090 | 10.6109 | 217.32 |
| 2045 | 11.0081 | 216.13 | 1968 | 12.2237 | 217.49 |
| 2065 | 10.6725 | 215.53 | 1992 | 11.6726 | 215.94 |
| 2067 | 10.6695 | 215.68 | 2013 | 11.4014 | 215.99 |
| 2029 | 11.2412 | 216.33 | 2047 | 11.0263 | 216.44 |
| 1997 | 11.6191 | 216.03 | 2083 | 10.5868 | 216.51 |
| 1837 | 14.1976 | 217.67 | 2083 | 10.6113 | 216.69 |
| 1888 | 13.0237 | 215.15 | 2058 | 10.8410 | 216.11 |
| 1915 | 12.7204 | 215.76 | 2024 | 11.2906 | 216.22 |
| 1944 | 12.3444 | 216.02 | 1978 | 12.0147 | 217.00 |

Appendix 2-C (Cont.)

| $T_K$ | $-\ln P$ (atm) | $\Delta H^\circ_{v,298}$ (kcal/gfw) | $T_K$ | $-\ln P$ (atm) | $\Delta H^\circ_{v,298}$ (kcal/gfw) |
|---|---|---|---|---|---|
| 1970 | 11.9551 | 215.83 | 2001 | 11.7079 | 217.02 |
| 1931 | 12.4489 | 215.49 | 1848 | 13.6864 | 215.49 |
| 1922 | 12.4821 | 214.85 | 2114 | 10.1037 | 215.71 |
| 1801 | 14.4745 | 215.72 | 2143 | 9.8305 | 216.20 |
| 1883 | 13.0613 | 214.91 | 2172 | 9.5238 | 216.38 |
| 1932 | 12.7121 | 217.36 | 2200 | 9.1501 | 215.90 |
| 2023 | 11.1741 | 215.31 | 2212 | 9.1735 | 217.09 |
| 2044 | 10.8381 | 214.83 | 2179 | 9.3934 | 215.99 |
| 1982 | 11.8237 | 216.05 | 2148 | 9.7665 | 216.16 |
| 2063 | 10.8197 | 216.41 | 2117 | 10.3122 | 217.52 |
| 2086 | 10.5059 | 216.19 | | | |

Appendix 2-D.  Europium(II) Selenide Vaporization

| $T_K$ | $-\ln P$ (atm) | $\Delta H^\circ_{v,298}$ (kcal/gfw) | $T_K$ | $-\ln P$ (atm) | $\Delta H^\circ_{v,298}$ (kcal/gfw) |
|------|-----------|-----------|------|-----------|-----------|
| 1808 | 14.2042 | 212.00 | 2067 | 10.5670 | 210.50 |
| 1836 | 13.6974 | 210.32 | 2045 | 10.8995 | 211.01 |
| 1875 | 13.1222 | 210.41 | 2017 | 11.2237 | 210.78 |
| 1910 | 12.5807 | 210.15 | 2000 | 11.3497 | 210.05 |
| 1942 | 12.0581 | 209.56 | 2023 | 11.1046 | 210.44 |
| 1967 | 11.7189 | 209.55 | 2078 | 10.4001 | 210.21 |
| 1935 | 12.2434 | 210.24 | 2078 | 10.3487 | 209.79 |
| 1890 | 12.7799 | 209.49 | 2104 | 10.0800 | 210.11 |
| 1860 | 13.2604 | 209.78 | 2104 | 10.0607 | 209.95 |
| 1916 | 12.5065 | 210.23 | 2131 | 9.7621 | 210.05 |
| 1947 | 12.1923 | 211.12 | 2130 | 9.7478 | 209.83 |
| 1976 | 11.7102 | 210.42 | 2111 | 9.9323 | 209.55 |
| 2010 | 11.3296 | 210.91 | 2110 | 9.9851 | 209.90 |
| 2037 | 10.9438 | 210.56 | 2096 | 10.1689 | 210.07 |
| 2067 | 10.5851 | 210.64 | 2097 | 10.1488 | 210.00 |